ABSTRACT

Title of Document: DEVELOPMENT AND TESTING OF A METABOLIC WORKLOAD MEASUREMENT SYSTEM FOR SPACE SUITS

Agnieszka Anna Kościelniak, M.S., 2007

Directed By: Associate Professor David Akin
Department of Aerospace Engineering

Real time knowledge of the metabolic workload of an astronaut during an Extra-Vehicular Activity (EVA) can be instrumental for space suit research, design, and operation. Three indirect calorimetry approaches were developed to determine the metabolic workload of a subject in an open-loop space suit analogue. A study was conducted to compare the data obtained from three sensors: oxygen, carbon dioxide, and heart rate. Subjects performed treadmill exercise in an enclosed helmet assembly, which simulated the contained environment of a space suit while retaining arm and leg mobility. These results were validated against a standard system used by exercise physiologists. The carbon dioxide sensor method was shown to be the most reliable and a calibrated version of it is recommended for implementation into the MX-2 neutral buoyancy space suit analogue.

DEVELOPMENT AND TESTING OF A METABOLIC WORKLOAD MEASUREMENT SYSTEM FOR SPACE SUITS

By

Agnieszka Anna Kościelniak

Thesis submitted to the Faculty of the Graduate School of the
University of Maryland, College Park, in partial fulfillment
of the requirements for the degree of
Master of Science
2007

Advisory Committee:
Associate Professor David Akin, Chair / Advisor
Assistant Professor Sean Humbert
Visiting Professor Mary Bowden

Acknowledgements

First of all, I would like to thank my subjects for taking time out of their busy lives and agreeing to don “the bubble” for the sake of science. There would be no data, and therefore no thesis, without them. I would especially like to acknowledge those who were asked to do the protocol multiple times because of treadmill malfunctions and to be “practice subjects” and did so without complaints.

None of this would have been possible without the guidance of my advisor, Dave Akin. He has created a lab with so many amazing opportunities that for many of us the greatest challenge was simply choosing one. I would also like to thank Mary Bowden and Sean Humbert for serving on my thesis committee.

Next, I would like to thank Sarah Witkowski and Mike Lockard of the Exercise Physiology Lab in the Kinesiology Department for trusting me with their expensive new equipment and taking the time to train me and supervise while I performed the control study.

I would like to express my appreciation to my treadmill moving crews. Due to a chain of unfortunate events, three different treadmills had to be brought to the NBRF and either carried up the stairs or craned up to the deck for this study. In particular, I would like to thank to John and Nick from England for lending their time and vehicles to transport treadmills from far away.

Life in the past two years would have been completely different without my fellow SSL graduate and undergraduate students. In this cooperative environment, many have generated great suggestions and advice when I got stuck or simply acted as

sounding boards for my numerous rants and complaints. I have made some great friends here and I will miss you all.

Last but not least I would like to thank my family for always supporting me, no matter what crazy new project I decide to undertake, my mom in particular for being my personal librarian at times, and Peter for being there for me and keeping me (relatively) sane throughout this process and always.

Table of Contents

List of Tables

List of Figures

List of Abbreviations

ACSM = American College of Sports Medicine
ATP = Adenosine Triphosphate
BMI = Body Mass Index
BMR = Basal Metabolic Rate
CCA = Communications Carrier Assembly
CE_{O_2} = Caloric Equivalent of Oxygen
ECG = Electrocardiogram
EMU = Extravehicular Mobility Unit
EPOC = Excess Post-exercise Oxygen Consumption
EVA = Extra-Vehicular Activity
HR = Heart Rate
HUT = Hard Upper Torso
IBG = Integral Ballast Garment
IR = Infrared
IRB = Institutional Review Board
ISS = International Space Station
LCG = Liquid Cooling Garment
LRV = Lunar Roving Vehicle
MARS = Maryland Advanced Research and Simulation
MDRS = Mars Desert Research Station
MET = Metabolic, a unit of energy expenditure
NDIR = Non-Dispersive Infrared Absorbance
PC = Phosphocreatine
PLSS = Portable Life Support System
$\dot{Q}$ = Cardiac Output
R = Pearson Correlation Coefficient
R^2 = Coefficient of Determination
RER = Respiratory Exchange Ratio
RH = Relative Humidity
RMR = Resting Metabolic Rate
RPE = Rating of Perceived Exertion
RQ = Respiratory Quotient
SI = International System of Units
SV = Stroke Volume
$\dot{V}CO_2$ = Rate of Carbon Dioxide Production
$\dot{V}O_2$ = Rate of Oxygen Consumption
$\dot{V}O_2$ max = Maximum Rate of Oxygen Consumption

Chapter 1 : INTRODUCTION

The primary goal of this chapter is to answer the "why?" question. The motivation behind this project and possible applications of this system are explained. This is followed by a statement of the actual problem addressed by this research. The general approach towards the solution is then given. Finally, the components of this thesis are outlined.

1.1 Motivation

As the completion of the International Space Station (ISS) draws near, NASA prepares to take the first steps towards building an outpost on the moon as a stepping stone to the long voyage to Mars. These goals of long duration space flight make the role of Extra-Vehicular Activities (EVA) even more critical. Astronauts will need to spend greater durations of time outside of the safety of their spacecraft and perform progressively more complex and demanding tasks. Preparation for these missions requires an intimate knowledge of the human response to EVA, particularly the metabolic workload while performing various tasks.

The metabolic workload, or the metabolic rate, is the amount of energy per unit time the human body is expending. It is directly proportional to the heat production by the body. Measurements of metabolic rate can provide useful insight into many aspects of EVA, including research, design, and operations.

The effects of an updated pressure suit design during an EVA task have historically been described qualitatively by astronauts. Improvements in pressure suit

joints continually lead to smaller torques required to move the space suit. Though these torques are measured in a laboratory, the proper system interaction with a human inside is the ultimate goal of these modifications. Human test sessions are often separated by significant time intervals for the replacement of suit hardware, which make ratings of perceived exertion less accurate, or are affected by fatigue from consecutive repetitions. The measurement of metabolic workload for a task performed with various space suit components could provide a quantitative assessment of the change.

Similarly, neutral buoyancy has been used as a training tool for EVA since the start of the space program. Though it is an excellent simulation of microgravity in some respects, large discrepancies between the two environments do exist. Notably, the presence of gravity and drag diminish the realism of neutral buoyancy as an analogue for space. Translation through the water requires significantly more force than through a vacuum. Through the suit and astronaut inside may be neutrally buoyant as a system, in a gravity field on earth the subject is still pulled down relative to the suit. Both of these phenomena alter the methods astronauts use to complete tasks to ones that may not be optimal on-orbit. Quantitative knowledge of the metabolic workload required for a certain task, both in a neutral buoyancy environment and the zero-gravity vacuum of space, can be a useful metric for the validation of neutral buoyancy simulation of EVA as a realistic training tool and for possible adjustments to training methods.

Human robotic interaction is currently a growing field of research and development. Robotic assistance during EVA could be used for applications such the completion of repetitive tasks, like tightening bolts with a wrench, or to fulfill a messenger function, such as fetching tools and hardware to limit the need for astronaut

translation in space. However, robotic assistance in the completion of these tasks is also likely to require some overhead tasks by the astronaut to initialize and control the robot. Measurements of metabolic rate could be used as an additional metric for quantification of how much assistance the robots are providing to the task overall.

Historic metabolic workload data is invaluable for requirement specification and design of next generation space suits. Current liquid cooling garments (LCGs) offer manual control of the water temperature. Astronauts can make corrective or anticipatory adjustments to the temperature for various EVA activities. Knowledge of the metabolic workloads for a specific activity in the past can remove some uncertainty from this adjustment process and improve astronaut comfort. This data is also used for overall LCG system sizing. Similarly, the amount of consumables, particularly oxygen, depends not only on the anticipated duration of the EVA, but also on the anticipated workload required to complete the scheduled tasks. Prior knowledge of metabolic workload can be used for sizing of oxygen supplies for EVA.

Historic metabolic workload data can also be used for mission planning and EVA task scheduling. The knowledge of the metabolic cost of certain activities is valuable for task distribution over multiple EVAs. To maintain astronaut comfort, taxing tasks can be interspersed with ones that require a lower level of exertion. Proper scheduling is instrumental to the maximization of the productivity of an astronaut without overexertion. Real time monitoring of metabolic workload can be utilized as part of health monitoring and can also be used to adjust task quantity and sequence during EVA as needed.

Finally, the metabolic data can be used on Mars to quantify some effects of deconditioning from long duration microgravity exposure on planetary EVA. Despite

regular cardiovascular and strength exercise, the multiple-month journey to Mars will have a profound effect on the exercise capacity of astronauts upon arrival. A reduction of the maximal capability of astronauts will increase the perceived exertion during EVA tasks because it will account for a greater percentage of maximal capacity. An absolute quantification of the metabolic workload can shed light on the amount of deconditioning encountered.

1.2 Problem Statement

The goal of this thesis is to design and test a metabolic workload measurement system for the MX-2 neutral buoyancy space suit analogue. The MX-2 is an open-loop system. Air is supplied from the surface, routed through the suit and back to the surface, and expelled into the ambient surroundings. This sets the MX-2 vastly apart from current operational space suits, which include a Portable Life Support System (PLSS). Suits outfitted with a PLSS circulate oxygen after removing carbon dioxide, water vapor, and particulates. This fundamental difference in breathing air systems alters the set of possible approaches to this problem from those used in the past or present.

The developed system must be able to measure the metabolic workload of a subject inside of the MX-2 unobtrusively and without impairing mobility or senses. The system must also be compatible with existing MX-2 hardware and software. Finally, the leakage rate of the MX-2 is unknown, but presumably substantial, and should not affect the output of the metabolic workload measurement system.

1.3 Approach

Three independent approaches were developed for measuring the metabolic workload of a subject inside MX-2. These methods include estimation of metabolic rate from measurements of oxygen consumption, carbon dioxide production, and heart rate. Each of these schemes involves a set of assumptions and is susceptible to a unique set of possible errors.

Testing was performed to determine which method is the most reliable for metabolic workload measurement, if any. An enclosed helmet assembly was constructed to simulate the sealed space suit environment and allow the subject full mobility below the neck. During the validation study, subjects performed treadmill exercise at various constant workloads twice, once in the experimental helmet assembly and once with a standard metabolic workload measurement system used by exercise physiologists. Metabolic rates were calculated via all three methods and a comparative analysis was performed to determine which system to implement on the MX-2 and its accuracy against the standard.

1.4 Thesis Structure

This thesis describes the development and testing of the metabolic workload measurement system for the MX-2 neutral buoyancy space suit analogue. Chapter 2 reviews some applicable exercise physiology and how it relates to EVA. It then lists some standard metabolic rate measurement methods and those implemented in past and present space suits. Chapter 3 explains the methods to be evaluated in this study and their implementation into the MX-2 system. Chapter 4 delves into the details of the

experimental hardware, protocol, and data processing. Chapter 5 presents and analyzes the results obtained during the validation study and discusses possible sources of error. Finally, Chapter 6 offers conclusions and some suggestions for possible future directions for this research.

Chapter 2 : BACKGROUND AND PREVIOUS WORK

The previous work pertaining to this research falls into two categories: exercise physiology and its application to EVA. This chapter describes the relevant concepts in exercise physiology and standard methods used for measuring metabolic workload. The discussion then turns to the effect of the EVA environment on the physiological response to exercise and the metabolic workload measurement methods that have been implemented in past and present space suits.

2.1 Exercise Physiology

Exercise physiology is a fundamental cornerstone of this thesis. This section describes a few topics germane to the subject of this research. The concepts described are the definition and components of energy metabolism, the varieties of muscle metabolism, the expected physiological response to exercise, the relationship between carbon dioxide production and oxygen consumption, and the idea of cardiac output.

2.1.1 Energy Expenditure

Energy expenditure is the amount of energy that an organism is using in a certain time period. It is measured in units of energy per time, such a Joules/second or Watts of the International System of Units (SI). However, when energy expenditure is discussed with reference to the human diet, in the context of weight loss for example, the large calorie is used. A calorie is the amount of energy required to raise the temperature of 1 gram of water by 1° Celsius. A kilocalorie, or large calorie, is the amount of energy

required to raise 1 kilogram of water by the same temperature difference. Throughout this thesis, energy expenditures will be given in kilocalories per hour. The terms energy expenditure, metabolic workload, metabolic rate, and caloric cost will be used interchangeably because all three appear commonly in literature.

Humans and other warm blooded animals expend energy in three distinct ways [1]. The basal metabolic rate (BMR) is the rate of energy expenditure under standardized conditions. These conditions include being immediately after waking while still in the supine position, after 12-18 hours of fasting, and in a thermoneutral environment. BMR is sufficient only to maintain the functioning of vital organs and accounts for about 60-75% of total energy expenditure. A typical value of BMR is 62.5 kcal/hr. Since standardized conditions are very difficult to maintain, lab measurements are often referred to as resting metabolic rate (RMR). This is usually higher than BMR due to the likely ongoing workload of food digestion, maintenance of body temperature, and recovering from recent exercise. [1]

BMR is proportional to body mass, specifically fat-free mass. It decreases by 2% per decade for women and 3% per decade for men after the age of twenty. The BMR of women is significantly lower at all ages because women have a lower fat-free mass. It has been shown that percent body fat does have a small impact on BMR. A 5% difference in body fat at the same weight translates into about 3 kcal/hr. There is also some variation in BMR as a result of genetic predisposition. The range of normal BMR values, within 3 standard deviations from the mean, is about +/- 21% of the average value. This explains why some individuals have less difficulty maintaining a constant body weight. Finally, the BMR is adjusted during periods of semi-starvation and periods of weight gain. During

periods of low caloric intake, the energy production in tissues adapts to reduce the rate of weight loss. Conversely, during periods of elevated caloric intake, BMR is increased because more energy is required to maintain weight gain rather than a constant body mass. [1]

The second component of energy expenditure is thermogenesis, or the creation of heat. The balance of heat production and heat loss maintains the core body temperature at 37° Celsius under normal circumstances. However, during cold conditions, involuntary muscle contractions, or shivering, are actuated. All of the energy required for shivering appears as heat applied to maintain the core body temperature. Some animals, including newborn humans, produce heat through non-shivering thermogenesis, or the use of brown adipose tissue. This type of adipose tissue increases heat production in response to norepinephrine. [1]

Thermogenesis also includes the thermic effect of feeding. This is the energy required to digest and assimilate food. It accounts for only about 10-15% of the energy expenditure. It is determined by monitoring RMR after a meal. This portion of metabolic workload is affected by genetic factors and is lower in obese individuals compared to lean individuals. However, because it accounts for such a small portion of metabolic workload, it is not a reliable predictor of subsequent obesity. [1]

Finally, energy wasteful systems are also a form of thermogenesis. These are natural responses to overfeeding as the body struggles to maintain constant weight. They occur through the appearance of additional brown adipose tissue or futile cycles, in which fructose-6-phosphate is converted to fructose-1 and 6-diphosphate and back. The responsiveness of these systems also depends on genetics. Individuals with a naturally

high BMR are more likely to maintain normal weight during a period of excess caloric intake. [1]

The third and final component of energy expenditure is physical exercise. This is the most variable factor of the three and can be between 5 and 40% of the daily energy expenditure. The great variation in physical exercise between individuals comes from differences in lifestyle. People with strenuous jobs or who participate in exercise activities in their leisure time expend significantly more energy this way. A link has been shown between physical exercise and appetite. This is a form of regulation of caloric intake relative to the caloric need. [1]

Since metabolic workload varies with body mass, it is sometimes convenient to express it in units relative to body mass. A MET (an abbreviation of metabolic) is the ratio of energy expended to the RMR [2]. A reasonable estimation of RMR is 1 kilocalorie per kilogram of body weight per hour. Alternatively, relative metabolic workload is sometimes given in units of kilocalories per kilogram of body weight per hour and this does not require the estimation of RMR.

2.1.2 Muscle Metabolism

Adenosine triphosphate (ATP) is a high-energy phosphate compound that serves as the immediate source of energy for muscle contractions. There are three methods of ATP production [1], which together satisfy the body's needs. First, ATP can be formed via the breakdown of phosphocreatine (PC). This is a simple reaction that only requires one enzyme (creatine kinase), but is limited by the quick depletion of stored PC. It can provide energy to the muscles for only a few seconds. ATP can then be created by glycolysis or the degradation of glucose or glycogen into pyruvic acid or lactic acid.

Pyruvic acid is used to initiate the third method of ATP production while lactic acid builds up in the muscles to be removed later. Both of these methods are considered to be anaerobic because oxygen is not required for the formation of ATP.

The third method of ATP formation is oxidative phosphorylation [1]. It occurs in the mitochondria as a result of a complex interaction between the Krebs cycle and the electron transport chain. It is considered to be aerobic because it requires oxygen. The products generated are carbon dioxide and water.

In general, anaerobic metabolism is for short-duration high-intensity exercise. When exercise begins, the breakdown of PC is the predominant supplier of ATP for the first 2-20 seconds. At this time, glycolysis becomes the primary source of ATP until about 45 seconds into the exercise. The aerobic metabolism then begins the production of ATP and becomes the predominant energy supplying mechanism throughout the prolonged low to medium intensity exercise.

However, when exercise intensity increases to a certain point, the respiratory and circulatory systems cannot supply the muscles with sufficient oxygen and glycolysis becomes a significant supplier of ATP again. This point is called the anaerobic threshold. It is also sometimes referred to as the lactate threshold because it marks the workload at which lactate begins to accumulate in the blood. The anaerobic threshold occurs at about 50-60% of maximal workload in untrained subjects and at higher workloads of about 65-80% of the maximum in trained subjects.

2.1.3 Physiological Response to Exercise

The rate of oxygen consumption is indicative of the current aerobic metabolism [1]. Oxygen consumption is also referred to as oxygen uptake or oxygen utilization in

literature. The symbol used for it, $\dot{V}O_2$, represents the rate of change of volume of oxygen. At steady workloads below the anaerobic threshold, $\dot{V}O_2$ has been shown to be proportional to metabolic workload and is therefore a quantity of interest. The maximum oxygen uptake ($\dot{V}O_2 \max$) is the greatest rate of oxygen uptake by the body measured during heavy dynamic exercise [1]. It is determined using incremental exercise tests on an ergometer or treadmill. It corresponds to the maximum work capacity and is often used as a measurement of aerobic fitness. Trained individuals tend to have a higher $\dot{V}O_2 \max$.

Figure 2-1 illustrates the profile of $\dot{V}O_2$ throughout a period of steady state exercise. When the exercise is initiated, respiration and circulation are not yet elevated to provide additional oxygen to the muscles. Anaerobic metabolism is utilized to supply the muscles with ATP. As the heart rate and circulation increase, the $\dot{V}O_2$ reaches a steady state in 1-4 minutes. This lag in oxygen uptake is the oxygen deficit. It is the transition from anaerobic to aerobic metabolism. Trained individuals tend to reach the required level of oxygen consumption faster, thus have a lower oxygen deficit and less lactic acid build-up. These individuals have a better developed bioenergetic capacity and are able to produce ATP aerobically sooner.

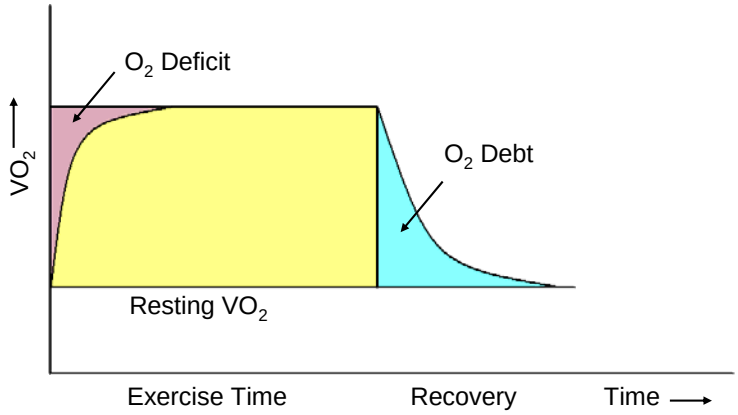

Figure 2-1: Oxygen consumption throughout exercise

At the completion of exercise, the oxygen consumption does not immediately return to resting levels. This utilization of oxygen above resting values following exercise is referred to as oxygen debt or excess post-exercise oxygen consumption (EPOC). There are multiple factors which contribute to EPOC. The additional oxygen at the beginning of recovery is mostly used to resynthesize the stores of PC in cells and replenish the oxygen levels in the blood and muscles. Throughout recovery, some of the elevated oxygen consumption goes to the elevated breathing and circulation, elevated body temperature, and higher levels of the hormones epinephrine and norepinephrine in the blood. Finally, a portion of the elevated oxygen uptake is used for gluconeogenesis or the conversion of lactic acid to glucose.

Higher exercise intensity results in increased oxygen deficit and EPOC. Oxygen deficit is elevated due to the higher difference between the resting $\dot{V}O_2$ and the level required to sustain aerobic exercise at this intensity. Additionally, it has been found that the settling time is longer at higher workloads [3]. During EPOC, greater amounts of PC need to be replenished due to the larger oxygen deficit at the onset of exercise.

Additionally, more lactic acid has accumulated in the blood and needs to be converted to glucose through gluconeogenesis. The body temperature is also more elevated after a period of intense exercise than after lower intensity exercise.

2.1.4 Respiratory Quotient and Respiratory Exchange Ratio

Respiratory quotient and respiratory exchange ratio are two very similar yet fundamentally different concepts. The respiratory exchange ratio (RER) is the rate of carbon dioxide exhaled ($\dot{V}CO_2$) divided by the $\dot{V}O_2$. This is what is being measured when respiratory gases are analyzed. The respiratory quotient (RQ) is the ratio of the rate of carbon dioxide produced to $\dot{V}O_2$. The difference between RER and RQ then lies in the difference between carbon dioxide exhaled and produced [4].

RQ refers to cellular metabolism and varies depending on what is being metabolized. Carbohydrates, fats and proteins are all metabolized differently and require various amounts of oxygen to complete the reaction. The RQ values for carbohydrates, fats, and proteins are about 1.00, 0.70, and 0.82, respectively [4]. Protein is typically not utilized to fuel muscles when there are abundant supplies of carbohydrates and fats. When RQ is not known, 0.8 is a reasonable approximation for a regular diet.

The RER is not only a function of cellular respiration. When anaerobic metabolism takes place at the beginning of exercise or during prolonged strenuous exercise, lactic acid accumulates in the blood, reducing the pH. This shift in acidity results in a higher amount of carbon dioxide exhaled than is generated through ATP production [4]. During heavy exercise, RER can increase to a value greater than 1.0.

2.1.5 Cardiac Output

The cardiac output ($\dot{Q}$) is the volume of blood pumped by the heart per unit time [5]. It is the product of stroke volume and heart rate. The stroke volume (SV) is the volume of blood pumped with each beat and the heart rate (HR) is the number of heart beats per unit time. The cardiac output is indicative of the oxygen carrying capability of the blood. When more oxygen is required by the muscles during exercise, the cardiac output increases by a slight increase in stroke volume and a significant increase in heart rate [4].

Throughout constant exercise, which requires a constant cardiac output, the heart rate may vary. Progressive dehydration decreases the stroke volume, therefore increases the heart rate. Increased body temperature has the same effect. In an effort to remove some heat from the body, vasodilation occurs and some blood pools near the surface of the skin. This reduces the stroke volume and therefore increases the heart rate.

2.2 Standard Methods for Measuring the Metabolic Workload

Multiple methods for measuring the metabolic workload exist. Each requires a different set of assumptions and produces results with varying degrees of reliability. The following sections describe direct and indirect calorimetry, the method of doubly labeled water, the relationship of heart rate to energy expenditure, and a few less common techniques.

2.2.1 Direct Calorimetry

Direct calorimetry, or the calculation body's metabolic rate by direct measurement of the amount of heat produced [2], is the most intuitive method of

measuring the energy expended by the body. However, the implementation of this method is not very practical. Room calorimeters have been used for this purpose. These are large chambers which circulate water through pipes running inside the insulated walls. Temperature is monitored frequently and accurately at the inlet and outlet.

There are many drawbacks to this method. The size and cost of the equipment make it prohibitive for many research applications. Not all exercise protocols can be carried out inside the restricted space of the calorimeter. There are also several sources of error in the implementation of this technique. There is some loss of calorimeter chamber integrity due to the need for carbon dioxide and water vapor removal and oxygen replacement for human respiration. Additionally, mechanical and electrical exercise equipment inside the chamber also produces heat, which must be distinguished from the human heat production. [1]

2.2.2 Indirect Calorimetry

Indirect calorimetry is the estimation of energy expenditure from oxygen consumption and carbon dioxide production [2]. Modern techniques have made this a reasonably practical and highly accurate method of assessing the metabolic workload. The open-circuit method of indirect calorimetry is used most often. It has two possible variants.

One is the flow-through technique in which a large volume of air flows through a hood worn by the subject [2]. The subject breathes normally and a fraction of the stream of air passes through the lungs where gas exchange occurs. The flow rate and percent of oxygen and carbon dioxide are used to calculate the $\dot{V}O_2$ and energy expenditure. One of the early implementations of this method was in the intensive care unit at Columbia

Presbyterian Medical Center in New York City for noninvasive monitoring of patient metabolism for the determination of dietary needs [6]. A clear plastic canopy was designed to be placed over a bed-ridden subject's head and closed around a pillow. The neck interface was made of lightweight plastic for comfort and an airtight seal. The system included two "scratch ports" or plastic bags attached to side openings in the canopy to allow the subjects to scratch their nose or adjust their glasses. The canopy was ventilated with 40 L/min (1.4 scfm) of air, which entered above the head and exited behind it. Air that left the system was routed to a gas analyzer, which included a paramagnetic oxygen analyzer and an infrared carbon dioxide analyzer. This system was used for multiple decades with thousands of patients without significant problems. Similar systems are commercially available today.

The second procedure for indirect calorimetry is the Douglas bag method [2]. This technique involved the collection of all exhaled gases over a known period of time in a bag. The volume and oxygen and carbon dioxide content of the collected gases were measured for the calculation of metabolic workload. Current versions of this method do not require an actual Douglas bag, but the operating principle remains the same. The parameters measured are the volume of air exhaled and the concentrations of oxygen and carbon dioxide in the exhaled air. The ventilation volume and the concentration of oxygen are used to calculate the $\dot{V}O_2$.

Descendants of the Douglas bag method are most commonly used today. High end open-circuit indirect calorimetry equipment, which often includes a mass spectrometer, tends to be the mounted on a cart for laboratory use only. Some portable systems exist, but come at a high price. However, the drawback to implementations of

this method is the need for an oronasal mask or a mouthpiece and a nose clip for exhaled gas collection.

Like the RQ, the caloric equivalent of oxygen used to convert $\dot{V}O_2$ to metabolic workload varies with the source of energy being metabolized. It has been found that 1 L of oxygen yields 5.06 kcal from carbohydrate alone, 4.68 kcal from fat alone, and 4.48 kcal from protein alone [2]. Equation 2-1 gives the caloric equivalent of oxygen (CE_{O_2}) in kcal/L.

$$CE_{O_2} = 3.9 + 1.1RQ \qquad \textbf{Equation 2-1}$$

The dependence of the caloric equivalent of oxygen on RQ is the reason for measuring the carbon dioxide concentration of exhaled air.

2.2.3 Doubly Labeled Water

The doubly labeled water method has become the gold standard in assessing the energy expenditure in non-laboratory situations. This technique begins with the administration of a dose of water with known elevated concentrations of naturally-occurring isotopes of hydrogen (^{2}H) and oxygen (^{18}O). Over the course of a few hours, these isotopes become evenly distributed throughout the body fluids. The labeled hydrogen leaves the body through water, including urine, perspiration, and respiration. The labeled oxygen leaves through water and exhaled carbon dioxide. The difference in elimination rates of these two isotopes, traced through the periodic sampling of blood, urine, or saliva, is used to accurately determine the $\dot{V}CO_2$, which is converted into $\dot{V}O_2$ [2].

There are a few disadvantages to this method. In a lot of applications it becomes prohibitively expensive and studies are limited to small numbers of subjects. The cost of ^{18}O is about $400-$600 per subject (1996) and a mass spectrometer is required to analyze the collected samples [2]. In field studies, additional error accrues due to the fact that carbon dioxide production is measured rather than oxygen uptake, and the RQ must be approximated in most cases.

The doubly labeled water technique is not very applicable to EVA. It is useful for the evaluation of long term averages of metabolic rate, but does not provide information about brief periods of energy expenditure. The knowledge of minute-by-minute changes in metabolic workload, when correlated with the tasks performed by an astronaut, is the information sought for during EVA.

2.2.4 Heart Rate

Heart rate can be used to calculate oxygen consumption indirectly. Laboratory tests have shown a linear relationship between heart rate and oxygen consumption, except at workloads close to resting values and those above the anaerobic threshold [2]. The most accurate results from this method can be obtained by developing a calibration curve for each subject under laboratory conditions, then applying it to heart rates measured in the field to obtain oxygen consumption. The relationship between these two physiological variables can also be determined using standardized equations [4], which are shown in Section 4.4.3. However, this approach is prone to higher errors.

Heart rate is relatively simple to measure in the field [2], as well as inside a space suit. Methods of measuring heart rate include the recording of the electrocardiogram (ECG) with chest electrodes or the weaker ECG in other parts of the body. The detection

of blood flow through a finger or ear lobe with an infrared (IR) sensor is also an option. However, heart rate is affected by psychological and environmental factors. As mentioned in the discussion of cardiac output in Section 2.1.5, heart rate can fluctuate at a steady workload as a result of dehydration or body temperature. Elevated heart rates have also been observed in situations of high stress or pressure to succeed such as athletic competitions [5]. It is preferable to measure oxygen consumption directly because of the limited accuracy of this method.

2.2.5 Additional Methods

Several other less common methods of metabolic workload measurement exist [2]. Core body temperature is closely related to energy expenditure. However, the time constant of the body's thermal system is very large. Exercise at a steady workload may have to be performed for 40-50 minutes before a steady state in body temperature is reached. This is not practical for EVA applications because the tasks performed on-orbit usually last significantly less time. The results from this method are also unpredictable for arm exercise and in hot and humid climates. Additionally, an inconvenient measurement of core body temperature, rather than skin temperature, is required.

Some correlation has been shown between systolic blood pressure and exercise intensity. However, portable blood pressure recorders do not perform well during strenuous exercise and the measurement is also affected by emotional factors. This is not a recommended method of energy expenditure measurement.

Measurements of ventilation have shown promising results for determination of metabolic workload. The extraction of oxygen from air is fairly constant over a large range of ventilations and the anticipated error from this method is only about 10%.

However, measuring the volume of expired air is as cumbersome as measuring oxygen uptake and almost as expensive. Oxygen uptake measurements are recommended over this method.

Electromyography, or the measurement of electrical discharge from muscles, is another possible option. Theoretically, it should give a good indication of muscle exertion. Unfortunately, this method is not very practical. It is very sensitive to sensor placement and numerous sensors are necessary to monitor multiple muscle groups. This method has not been implemented successfully.

2.3 Exercise Physiology of EVA

The environment of spaceflight has an effect on some distinct aspects of the physiological response to exercise. The influence of upper body exercise, an upwards fluid shift, cardiovascular deconditioning and variations in the thermoregulation process on the measurement of metabolic workload, as discussed by Cowell [7], are explained in the following sections.

2.3.1 Upper Body Exercise

A distinct characteristic of the tasks performed on-orbit by suited astronauts is that the majority of the work is carried out by the upper body muscles. An astronaut is typically firmly attached to foot restraints and performs tasks with arms and hands. The majority of this upper body aerobic work is at a relatively low intensity but long duration. Additionally, the upper body performs some static work to counteract the stiffness of the suit when the position that needs to be maintained is one other than neutral. The lower

body work is mostly isometric work against the foot restraints, which counteracts the torques produced by the upper body's interaction with hardware.

Very little reliable data exists on the metabolic workload of astronauts during on-orbit aerobic exercise in near laboratory conditions. There have been very few subjects in these studies and protocols across programs were not standardized. There is virtually no useful in-flight data on the metabolic workload of arm exercise. The Skylab bicycle ergometer had the capability of being used as an arm crank; however, only the commander of the Skylab 2 mission chose to use it as such. The majority of what is known about the effect of spaceflight on the energy expenditure during upper body exercise is from pre- and post-flight data. However, all existing data points to a reduction in the work capacity for EVA during extended missions.

The focus is then shifted to data from ground-based research on the metabolic workload of arm exercise. The muscle efficiency has been found to be lower for arm exercise compared to leg exercise. However, this is partially due to the fact that when exercise is being performed by the upper body, the lower body muscles are also working to stabilize the upper body. This is reflected in the workload measured via indirect calorimetry but not in the output power.

The rating of perceived exertion (RPE) has been found to be higher for arm exercise than leg exercise at the same absolute $\dot{V}O_2$. This is likely because the workload at this rate of oxygen uptake represented a larger percentage of the maximum. Some studies have even reported a difference in RPE at the same fraction of $\dot{V}O_2$ max.

Finally, it has been shown that the heart rate at a similar $\dot{V}O_2$ is higher for upper body exercise than for lower body exercise. This has some serious implications for

measuring metabolic workload by recording the heart rate. The subject laboratory calibration curves determined on an ergometer or treadmill are no longer valid for arm exercise.

2.3.2 Upwards Fluid Shift and Deconditioning

The human circulatory system is designed to counteract the earth's gravity and return blood from the lower extremities to the heart over an elevation change of several feet. This capability is not necessary in microgravity and results in an upwards body fluid shift. This phenomenon has been simulated on the ground with supine arm exercise. It causes increased venous return, which leads to a larger stroke volume and lower heart rate than sitting arm exercise.

Long term bed rest simulations reproduce the upwards fluid shift as well as other deconditioning responses. The 6° head-down position is commonly used for creating a headward fluid shift, rather than just pooling blood at the back. These studies have shown a general decrease in strength and power, which is in agreement with data from astronauts after spaceflight. An increase in the time to reach a $\dot{V}O_2$ equilibrium was also observed. This means the oxygen deficit for a given workload is elevated and a greater build-up of lactic acid in the blood can be expected. No change was found in the $\dot{V}O_2$ for cycling at an absolute workload, but the oxygen consumption represents a greater percent of the maximum because $\dot{V}O_2$ max has reduced. Finally, some studies have found a decrease in stroke volume during bed rest. This is counterintuitive to the result obtained from supine exercise to simulate a fluid shift and is therefore attributed to the

cardiovascular deconditioning. However, it also invalidates ground calibration curves for $\dot{V}O_2$ and heart rate.

2.3.3 Thermoregulation

Microgravity also effects the human body's thermoregulation. As mentioned in Section 2.2.5, core body temperature increases during prolonged exercise. In the body's effort to remove excess heat, vasodilation occurs and results in the blood pooling near the surface. The volume of blood is also reduced due to sweating and expired water vapor. Both of these factors reduce the stroke volume and therefore increase the heart rate for a given workload.

Deconditioning has been shown to lead to an excessive rise in core body temperature, making the increase in heart rate even more significant. There are two reasons for this rise in temperature. Deconditioning leads to a decrease in blood volume due to the reduction in plasma volume, total hemoglobin, and erythrocyte volume and mass. Less circulating blood reduces the core to periphery heat conduction. The fluid shift also leads to changes in thermoreceptor sensitivity in the brain, further destabilizing the core body temperature.

This reduction in stroke volume and therefore rise in heart rate affects measurements of metabolic workload as measured from heart rate. The elevated heart rate can lead to an overestimate in energy expenditure.

2.4 Measuring Metabolic Workload During EVA

Attempts have been made at measuring the metabolic workload of astronauts during EVA since the start of human sorties into space. Multiple methods have been

implemented into past and present space suits. Some were shown to be fairly effective and others did not yield any reliable data. The following sections discuss the metabolic workload measuring methods of many operational and simulation space suits throughout the past four decades.

2.4.1 Gemini

No attempt was made at measuring the metabolic rates during EVA throughout the Gemini program. However, heart rate was measured during all 5 EVAs. The energy expenditure was known to be above the capacity of the life support thermal control system. The heat removal capability was limited to 225 kcal/hr during the Gemini IV EVA, and was later increased to 250 kcal/hr with the addition of a gas cooling system. Nevertheless, astronauts continued to report overheating, therefore their metabolic workloads were above these values. [8]

2.4.2 Apollo

The Apollo era brought the aspect of gravity into EVA operations, requiring portability and reduced suit weight for long duration surface activity. Based on experience gained from the short Gemini EVAs, the Apollo space suits were greatly improved. The first American LCGs were implemented during Apollo. They were capable of suppressing sweating at work rates of up to 400 kcal/hr and allowed sustained operations of up to 500 kcal/hr without thermal stress [8]. The need for real-time metabolic data became apparent. However, the standard open-circuit oxygen consumption method was not an option within the confines of the life support system.

A variety of data was available for estimation of metabolic rates, including voice data, ECG data, oxygen bottle pressure, LCG inlet and outlet temperatures, suit gas entry temperature, and post-EVA total sublimator usage. Three methods for estimating metabolic rates were developed for Apollo planetary EVAs [9]. They included the analysis of oxygen usage, LCG heat removal, and heart rate measurements.

The analysis of oxygen bottle pressure decrement over time was a method of measuring oxygen consumption akin to indirect calorimetry. A pre-determined pressure suit leakage rate was taken into account. However, the maximum leak rate allowed by the specifications translates to 50 kcal/hr so it is a potentially significant source of error. Additionally, the telemetered data was found to be noisy, which made it difficult to obtain reliable oxygen consumption rates for time periods of less than 30 minutes, especially at low work rates. Nevertheless, this proved to be a satisfactory method of energy expenditure measurement.

Measurements of heat removal by the LCG were a method of metabolic rate determination congruous to direct calorimetry. The inlet and outlet water temperatures and the assumed flow rate were used to calculate the heat removed by the LCG. There was a lag time in the appearance of heat lost via perspiration due to the delayed evaporation of sweat; however, this error was accounted for in long duration averages. This method assumes the astronaut was maintaining a comfortable temperature with the manually controlled LCG. Barer [10] reports that this was not always the case and some crew members did not use the thermal controls during critical operations despite thermal discomfort. An estimated correction was included for the heat exchange with the

environment. This method was verified with test data from step exercises during altitude chamber training [11]. It was determined to be the most accurate of the three.

Heart rate was also recorded during Apollo EVAs and a metabolic rate was determined based on preflight bicycle ergometer correlations between heart rate and oxygen consumption. Due to environmental, psychological, and deconditioning effects, the pre-flight calibrations did not yield reliable data, especially at lower heart rates. However, the time constant of heart rate is only about 30 seconds [5], so the heart rate data was used to estimate the minute-by-minute cost of specific activities when related to the total energy expenditure determined using the other two methods.

In general, the best estimate of metabolic workload was obtained by averaging the LCG heat removal and the oxygen usage methods [9]. The average metabolic rate of Apollo EVAs of 234 kcal/hr was lower than originally predicted. Peak rates of 350-450 kcal/hr were measured during uphill walking traverses and overhead activities such as egress, ingress, loading and unloading of cargo. Lowest rates where measured during Lunar Rover Vehicle (LRV) operations.

An effort was made to find a correlation between the metabolic workload and walking speeds [9]. Data was collected during the Apollo 14 mission, which included some of the most extensive walks of the program. It was found that walking at a certain speed during a lunar EVA consumed more energy than walking in a shirt sleeve 1 G environment but less energy than walking in a space suit in a 1 G environment. However, a poor correlation was found between walking speed and energy expenditure, partially due to the varying terrain the astronauts had to cover.

The command module pilots of Apollo 15, 16, and 17 also performed short film retrieval EVAs in microgravity. Oxygen utilization data was not available during these EVAs because umbilical life support systems were used. No LCGs were used because of the brevity of this task. Therefore, only heart rate data was available. The heart rates were elevated due to psychogenic issues and were not useful for metabolic workload determination [9].

2.4.3 Skylab

The Skylab program followed Apollo. Although EVAs were performed in microgravity rather than lunar gravity, the space suit design remained very similar to Apollo. The most significant alteration was the replacement of the Portable Life Support System (PLSS) with an umbilical life support system. Since the astronauts no longer had personal oxygen supplies, oxygen usage was not a viable metabolic workload measurement method anymore. Data was only collected using the LCG heat removal and heart rate techniques described in Section 2.4.2. Real time data was only available while the station was in contact with a ground station. This allowed only partial real time analysis of metabolic rates. The complete data was acquired later [11]. The average metabolic rate of 230 kcal/hr was very similar to that of Apollo [8].

Skylab medical experiment M171 on metabolic activity was performed during the Skylab 3 mission. Its purpose was to determine whether a man's metabolic effectiveness during dynamic exercise was progressively affected by the exposure to space. The metabolic workload of crew members during rest and calibrated exercise at 25%, 50% and 75% of $\dot{V}O_2$ max was measured prior to the mission, every five or six days throughout the mission, and after the mission with indirect calorimetry. The experiment

showed that the strongest decrement in submaximal exercise response was immediately following the return from the mission due to the readjustment to gravity [12]. The data from this experiment was also utilized to obtain the heart rate and oxygen consumption calibration curves for each crew member. They were based on the most recent in-flight bicycle ergometer test. This is an improvement over the ground-based calibrations and eliminated some errors caused by deconditioning due to the lack of gravity [8].

2.4.4 Shuttle

Oxygen usage monitoring was selected as the sole method used to measure metabolic workload during EVAs on Shuttle flights. Lithium hydroxide carbon dioxide scrubbing canister data is used to verify metabolic rate averages as well, but is not used as a stand-alone method. During the first eleven Shuttle EVAs, oxygen bottle pressure data was only available periodically when the astronaut was asked to relay the oxygen gauge pressure to ground control. The lack of constantly updated data made it only possible to calculate mission averages of metabolic workload [13].

Starting with mission STS 61-B (1985), oxygen pressure data became available in two-minute intervals and the calculation of metabolic workload of specific short-duration tasks became possible. The average metabolic rate of Shuttle EVAs from the beginning of the program through STS-61 (1995) was 197 kcal/hr. This is significantly lower than Apollo and Skylab averages. A downward trend throughout the Shuttle program was also noted and attributed to gradual improvements in EVA equipment, training, and planning [13].

The Shuttle space suit, the Extravehicular Mobility Unit (EMU), was designed for similar metabolic workload capabilities as the Apollo space suits despite the difference in

gravity between the EVA environments [14]. This is due to the fact that during the early stages of Shuttle hardware design, the majority of successful U.S. EVA experience was performed on the moon and little microgravity EVA data was available. Unlike the Gemini program, it was found that the EMU heat removal capability is beyond that required by the Shuttle EVAs [13].

The doubly labeled water metabolic workload measuring technique was implemented during the 1996 life and microgravity sciences Shuttle mission to monitor the astronaut energy expenditure throughout the mission [15]. This experiment was controlled with a 6° head-down tilt bed rest study. It was found that the astronauts were in a severe negative energy balance throughout the mission. They were expending significantly more energy than they were consuming through food. This resulted in heightened oxidization of body fat rather than carbohydrates leading to a lower RQ than can typically be expected. If these findings are representative of other missions, indirect calorimetry methods of measuring metabolic workload, which rely on an approximation of RQ, may be inaccurate or in need of a correction factor.

2.4.5 Salyut 6, Salyut 7, and MIR

The metabolic workload was also measured during the EVAs performed on the Salyut 6, Salyut 7, and Mir space stations. During the lifetime of the Mir space station, 78 EVAs were conducted. The metabolic data collected included heart rate, breathing frequency, body temperature, oxygen bottle pressure, concentration of carbon dioxide inside the space suit, LCG inlet and outlet temperatures, level of gas ventilation, and verbal health reports. Three methods were used to estimate the energy expenditure [16].

The oxygen bottle pressure was monitored much like in the U.S. space program. Thermodynamic properties of oxygen at high pressure and the suit leak rate, as measured during the system check prior to each EVA, were taken into account. The caloric equivalent of oxygen assumed was 4.84 kilocalories per liter. It was derived during pre-mission experiments. This method was not found to be useful for time periods of less than 10 minutes because the sensitivity of the pressure gauge was too low. Additionally, this method was highly affected by the lowered pressure mode the Russian space suits had for additional mobility. [16]

The rate of production of carbon dioxide was computed in real time from the carbon dioxide concentration at the contamination control cartridge inlet and outlet and the gas flow rate through it. Corrections were made for suit volume and leak rate. The caloric equivalent of carbon dioxide used was 5.83 kilocalories per liter. This translates to an assumed RER of 0.83 and was also based on values from pre-flight experiments. A switch to the lowered pressure mode inside the space suit did not affect the results from this technique. This method was found to have only about 10% error and was considered the most effective of the three. [16]

LCG heat removal was also computed much like in the U.S. space program. However, the heat transfer between the suit and the space environment was not accounted for and a constant dew point of water at the heat exchanger was assumed. This method was found to have about 20% error. [16]

The carbon dioxide production method was the preferred one of these three. Heart rate was also measured. However, like in the U.S. space program, a poor correlation between heart rate and oxygen consumption was noted. The average metabolic rates on

the Salyut 6, Salyut 7, and Mir were 264 kcal/hr, 228 kcal/hr, and 222 kcal/hr, respectively [17]. As in the American space program, these average metabolic rates decreased over time as EVA equipment and knowledge improved. They were lower than the Apollo and Skylab metabolic workload measurements, but higher than those from the Shuttle program.

2.4.6 Mars Desert Research Station

The Mars Desert Research Station (MDRS) is a Mars analogue research habitat located in the Utah desert. Every winter crews of four to six volunteers perform Mars simulation research in two-week shifts. The goals of MDRS are to serve as an effective testbed for developing field tactics, test habitat and tool designs, assess crew selection protocols, and to generate public support for sending humans to Mars [18].

A study was performed at MDRS on the physiological demands of Mars analogue extravehicular activities [19]. Mars analogue suits were outfitted with a COSMED® K2b^4 portable gas exchange analyzer. Subjects were asked to perform two graded uphill runs to exhaustion to determine the $\dot{V}O_2$ max . Two simulated EVAs were then performed while collecting metabolic data with the COSMED® K2b^4. It was found that hill running was not an ideal method of $\dot{V}O_2$ max determination because the tests were likely terminated by the subject before maximal workload was reached. An unsuited laboratory ergometer would have been preferable.

The COSMED® K2b^4 portable gas analyzer is a commercially available product, which has been validated in numerous studies [20]. The transmitter weighs 475 g (17 oz) and measures 17.0 cm (6.7 in) by 5.5 cm (2.2 in) by 10.0 cm (3.9 in). Thus, it can be

easily integrated inside a space suit. However, it requires an oronasal mask for exhaled gas collection so it is not unobtrusive.

Chapter 3 : SYSTEM CONCEPT

The system presented in this thesis was developed specifically for the MX-2 neutral buoyancy space suit analogue. The first section of this chapter discusses the MX-2 design and operation. The second section outlines in detail the concept of the metabolic workload measurement system implemented.

3.1 MX-2 Neutral Buoyancy Space Suit Analogue

The following sections provide a system overview of the MX-2 and a detailed discussion of the life support system into which the metabolic workload measurement system will be integrated.

3.1.1 MX-2 System Overview

The MX-2 is the second generation Maryland Advanced Research and Simulation (MARS) suit. Its primary purpose is to replicate some aspects of a pressure suit to facilitate low-cost neutral buoyancy EVA research. The MX-2 has an outer mobility envelope and joint restrictions comparable to pressure suits and realistic audio and visual environments [21]. It is pictured during neutral buoyancy operations in Figure 3-1.

Figure 3-1: MX-2 during neutral buoyancy operations

The MX-2 is a rear-entry pressure suit with a hard upper torso (HUT) and a hemispherical helmet. The HUT is constructed of an epoxy resin fiberglass composite with built-in aluminum plates for hard attachment points. A backpack is integrated with the hatch and provides a pressurized environment for electronics, called the electronics box. It fits into the HUT like a plug, locks with a four-point latch system, and seals with an inflated Pneumaseal®. [21]

The arms and lower torso assembly are three-layer soft goods. The inside layer is a pressure bladder made of airtight urethane coated nylon. The second layer is the restraint layer, which is made of a nylon weave and is designed to carry the pressure loads. The outer layer is the integral ballast garment (IBG). It is made of a thicker nylon weave. Its purpose is to protect the inside layers and hold the ballast weight needed in integrated pockets. [21]

Modified ski boots are used as the MX-2 boots and serve as the restraint layer and IBG on the feet. They include a standard heal to lock into EVA foot restraints [21]. The gloves developed for the MX-2 include a pressure bladder and restraint layer with an integrated palm bar and an elastic restraint line system, which biases the metacarpophalangeal joint to a closed position [22].

Inside the suit, the subject wears an LCG made of flexible tubing woven through an elastic mesh suit. Cold water circulation is provided from the surface. The subject also wears a communications carrier assembly (CCA) for two-way communication with the surface control station and support divers. A harness and stirrup system is integrated into the suit for subject weight support. An in-suit drink bag is mounted inside the helmet and provides 1 L of drinking water to the subject. Lighter subjects also require additional ballast worn as a vest inside the MX-2. [22]

The pressurized electronics box contains a Macintosh Mini® computer for real time monitoring of suit systems. Onboard software logs pressure and other sensor data and sends it to the surface via Ethernet. Data is displayed and monitored on the surface. [22]

The MX-2 is connected to the surface via an umbilical at all times. The umbilical has multiple components. It includes the air inlet and outlet hoses for breathing air circulation. A cold water line provides LCG cooling. The LCG water exits into the surroundings and it is not collected. Finally, the Ethernet and communications cables are also routed through the umbilical.

3.1.2 MX-2 Life Support System

The MX-2 has an open-loop life support system. A schematic of this system is shown in Figure 3-2. Air is compressed by the Bauer Life Support Compressor for Breathing Air. It is certified for grade E air by Trace Analytics, Inc. Air can enter into the system from either or both of two sources. It can be supplied directly from the compressor while it is running. Alternatively, air can be used from a cascade of four large 24.8 MPa (3600 psi) cylinders. Typically, the cascade is filled prior to MX-2 operations and is used solely throughout the test while the compressor is reserved as a backup.

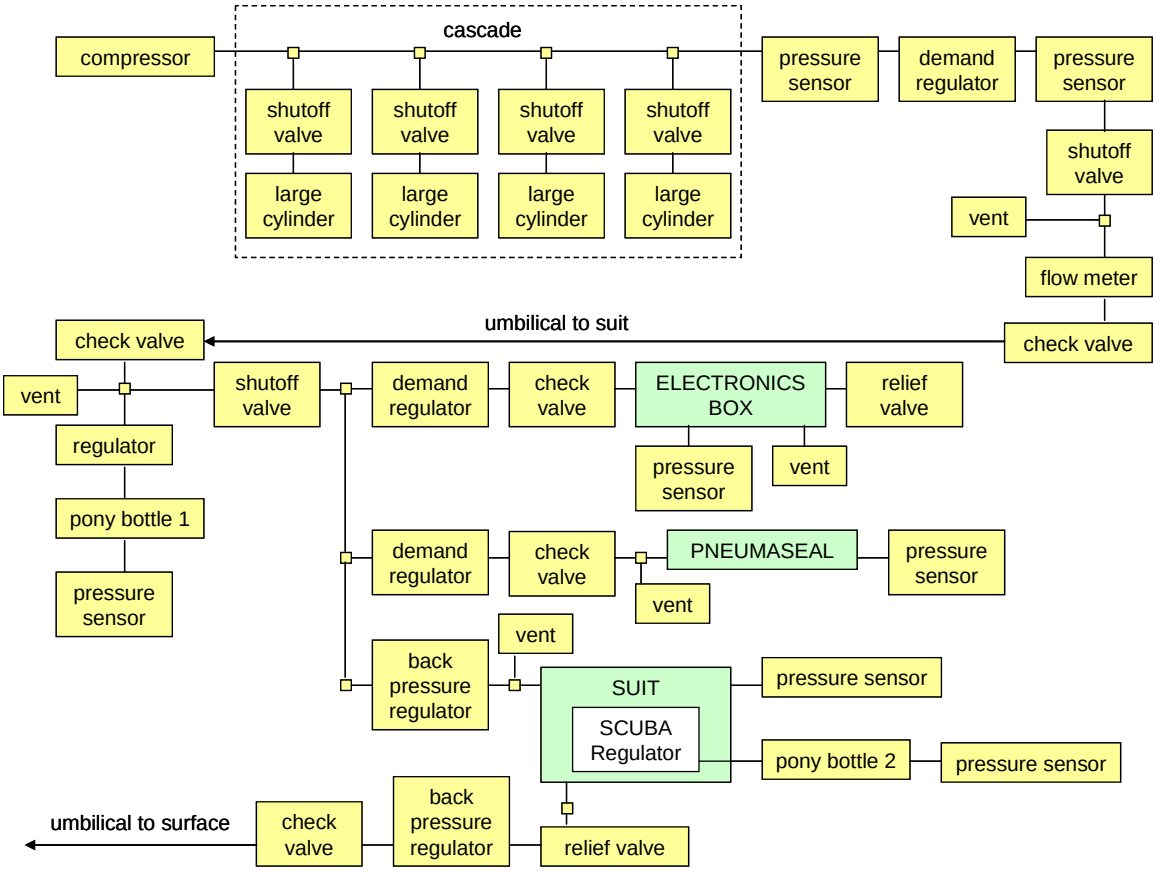

Figure 3-2: MX-2 air system schematic

From the high pressure source, air passes through a demand regulator which reduces the pressure to about 830 kPa (120 psi) before it enters the suit umbilical. The flow rate is also measured at this point.

At this juncture it is important to note the distinction between a demand regulator and a back pressure regulator. Both can be used to maintain the pressure of a pressure vessel supplied from a high pressure source. A demand regulator is placed between the source and the vessel. When the pressure in the vessel is below the set level, it “demands” more air from the regulator. However, when the pressure is at the desired level, no air passes through the demand regulator. A back pressure regulator is placed at the outlet of the pressure vessel. It allows all air to flow through it except for the air necessary to

maintain the set pressure in the vessel. Therefore, while the source is at a higher pressure than the vessel, a continuous flow of air will be maintained with a back pressure regulator. [23]

Upon entering the MX-2, the air travels to pressurize three distinct vessels. The electronics box is pressurized to about 35 kPa (5 psi) and is controlled by a demand regulator. The Pneumaseal® is also controlled by a demand regulator, which pressurizes it to about 414 kPa (60 psi). The electronics box and Pneumaseal® do not need a constant flow of air. However, the suit does require circulation of fresh air for the comfort and safety of the subject inside. Thus, it is controlled with a back pressure regulator, which maintains the pressure at 21 kPa (3 psi) above ambient pressure. A second back pressure regulator can be seen in Figure 3-2 before the air enters into the suit. This regulator maintains the pressure in the 100 ft long umbilical. Otherwise, pressure losses due to the Bernoulli effect would be too large and the Pneumaseal® would not be pressurized completely.

The MX-2 has triple redundancy in the air system. In the event of a primary air system failure, pony bottle 1 can pressurize the suit for 2-3 minutes. This is sufficient time to recognize a problem and begin suit extraction. Pony bottle 2 is connected to a SCUBA demand regulator inside the helmet. If pony bottle 1 is insufficient, pony bottle 2 can supply breathing air to the subject for 12-15 minutes. If all of these systems were no longer an option, the helmet can be removed by a safety diver and a reserve SCUBA regulator can be passed to the subject. [21]

3.2 Metabolic Workload Measurements in MX-2

An open-circuit flow through indirect calorimetry system was selected for the first generation of the MX-2 metabolic workload measurement system. The oxygen bottle pressure monitoring method used during Apollo, Shuttle, as well as the Russian Salyut 6, Salyut 7 and Mir space stations (described in Sections 2.4.2, 2.4.4, and 2.4.5, respectively) is not applicable to the MX-2 system. Oxygen usage cannot be measured directly because air is used in the system. Additionally, monitoring the depletion of the cascade air supply is not applicable to metabolic measurements because the back pressure regulator maintains a constant air flow rate through the suit independent of subject respiration. A portable metabolic analyzer, such as the COSMED® K4b^2 mentioned in Section 2.4.6, has an invasive oronasal mask not desired for MX-2 operations. It is also prohibitively expensive at about $30,000 to $37,000 (2006). Direct calorimetry measurements from the LCG inlet and outlet temperature difference are slated for future research and are discussed briefly in Section 6.2.2.

The MX-2 metabolic workload measurement system gathers data on three parameters: the rate of oxygen consumption, the rate of carbon dioxide production, and heart rate. Oxygen and carbon dioxide gas sensors are located inside the air outlet hose and monitor the percentage of these gases in the air departing the suit system. $\dot{V}O_2$ and $\dot{V}CO_2$ are calculated by multiplying the inlet gas flow rate by the change in percent of gas content. The change is measured between the system air outlet with and without a human in the loop.

Energy expenditure can be calculated in several ways from these three measurements. The method most similar to traditional metabolic measurement techniques

includes the calculation of RER from the $\dot{V}O_2$ and $\dot{V}CO_2$ to determine the caloric equivalent of oxygen to be used for calculating the metabolic rate from $\dot{V}O_2$. If the RER is assumed rather than measured, the oxygen sensor can be used independently of the carbon dioxide sensor. The assumed RER can also be used to calculate $\dot{V}O_2$ from $\dot{V}CO_2$ to obtain the metabolic rate without the oxygen sensor. The heart rate data collected can be utilized to calculate metabolic workload using personal calibration curves or less accurate standardized equations [4].

A significant advantage of this system over indirect calorimetry systems implemented in previous suits is that an estimate of the suit leak rate is not necessary. Air enters the MX-2 through a plenum at the forehead directed downward over the face and exits at the center of the back. Though there are multiple possible leak paths, they occur in sections of the suit other than the helmet. Therefore, with the assumption of evenly mixed gases beyond the helmet, the suit leak rate does not impact the results since the sensors measure the percentage of gases, not the absolute quantity. The flow rate is measured at the inlet and is the amount of air flowing over the face available for respiration.

Testing is required for validation of the MX-2 metabolic workload measurement system and the selection of the preferable calculation method. It is best to validate this system against a calibrated standard open-loop indirect calorimetry system. There are two possible approaches to this. One is to measure the metabolic workload of a subject performing exercise with a standard system and the MX-2 system simultaneously. This would require an expensive portable $\dot{V}O_2$ system to be used inside the suit helmet. Alternatively, subjects could perform the same exercise twice and the metabolic

workload can be measured separately with both methods. This requires a very controlled exercise protocol that can be accomplished with either metabolic workload measurement system.

Treadmill exercise at various speeds and inclines provides a workload that can be carefully controlled by the investigator. However, the MX-2 is designed for a neutral buoyancy environment and is too massive and cumbersome for walking or running in gravity. The breathing environment of the MX-2 is the only aspect applicable to this testing and can be replicated in an analogue. A sealed helmet assembly connected to the MX-2 air supply can provide the same respiratory conditions and allow full mobility below the neck for treadmill exercise.

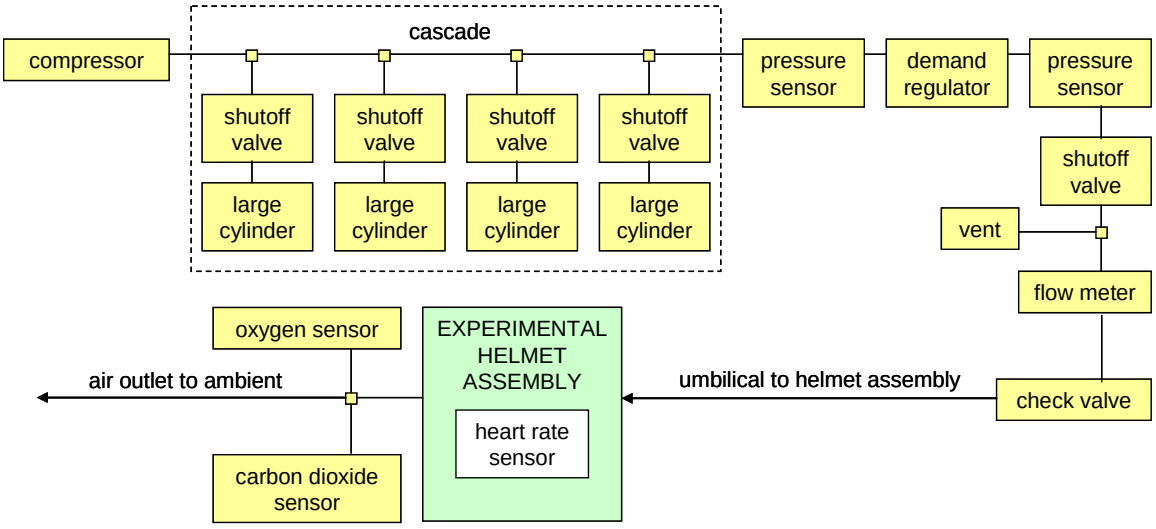

Figure 3-3: Experimental helmet assembly air system schematic

Figure 3-3 is a schematic of the experimental helmet assembly and its air supply. Air is supplied and regulated in the same manner as the MX-2. However, the experimental helmet assembly does not have a back pressure regulator for pressurization. The air outlet is open to the surrounding environment and the pressure inside of the

experimental helmet assembly is not elevated above ambient. A pressure differential between the interior of the experimental helmet assembly and the air surrounding the remainder of the body would be dangerous to the subject and could result in a lung overexpansion injury such as edema or pulmonary embolism.

In addition to the direct comparison of the experimental MX-2 system results to those from a standard metabolic workload measurement system, analysis can be performed with results from previous studies. Human energy expenditure during walking and running has been studied thoroughly in the past and prediction models for metabolic workload at various speeds and inclines for various subjects exist [34],[35],[36]. Though these models are not expected to be as precise as measuring the metabolic workload of a subject with a standard system, they can provide an estimate of the expected workload and be used as a guide for determination of possible causes of discrepancies found.

Chapter 4 : METHODS

The experimental concept of a metabolic workload measurement system described in Section 3.2 underwent a validation study against a standard indirect calorimetry system used by exercise physiologists. Human subjects participated in two identical exercise sessions, an experimental and a control session, in which they performed treadmill exercise at several velocities with the respective metabolic workload measurement system. The following sections provide a detailed description of the experimental and control session hardware, explain the protocol of the validation study, and the data processing methods.

4.1 Experimental Session Hardware

These sections reveal the hardware design and fabrication process and justify the component selection for the experimental helmet assembly, the sensors, and the data acquisition card.

4.1.1 Experimental Helmet Assembly

The apparatus the subjects were asked to wear during the experimental sessions, pictured in Figure 4-1, simulates the enclosed breathing environment of a space suit while allowing the subjects free mobility below the neck. It is a spherical helmet, 33.0 cm (13.0 in) in diameter, made of clear plastic with a 24.1 cm (9.5 in) diameter opening at the bottom. A modified adult bicycle helmet is glued inside the clear plastic helmet. The purpose of the bicycle helmet is to provide a firmly attached support for the larger helmet

on the subject's head and keep it stable throughout the exercise session. It is also adjustable for various head sizes. The colorful plastic covering was removed from the outside of the bicycle helmet. This allowed easy shaping of the helmet by cutting sections of polystyrene out. The bicycle helmet was shaped to fit the inside contour of the clear plastic helmet. The front section of the bicycle helmet was removed and a groove over the top of the head was cut out to allow space for the air inlet hose.

Figure 4-1: Experimental helmet assembly

A 3.8 cm (1.5 in) diameter blue hose is attached to the back of the clear plastic helmet at the base of the neck. This is the air outlet hose. It is attached by a bent hose clamp, which is glued to the lip of the clear plastic helmet on the outside, as pictured in Figure 4-2. The air inlet line is a 1.3 cm (0.5 in) clear vinyl hose which enters the helmet assembly next to the air outlet hose. It runs straight up and over the top of the head

through the groove in the bicycle helmet and ends in a plenum at the forehead. The plenum directs the fresh air down over the face and towards the air outlet hose for constant air circulation. The inlet and outlet hose diameters were selected to match those on the MX-2 for maximum commonality between the systems.

Figure 4-2: Air outlet hose attached to the clear plastic helmet

The clear plastic helmet is closed off at the neck with zero-porosity yellow nylon fabric, typically used in parachutes. It is sewn from six trapezoidal portions of fabric and tapers from the helmet interface to the neck, as illustrated in Figure 4-3. Anthropometric data was used to size this for neck circumferences ranging from 5th percentile U.S. women to 95th percentile Navy divers [24]. The Navy divers were chosen because their neck circumferences were the largest of the possible groups and U.S. men were not an option on the list. The maximum neck circumference to fit in the helmet assembly is 45.7 cm (18.0 in), which has an 8% margin over the 95th percentile Navy diver who has a 42 cm (16.6 in) neck. The fabric is attached around the subject's neck and the lip of the clear

plastic helmet with loose elastic and has a pass-through for the two air hoses and communications cables in the back. The purpose of this is to route the majority of the air leaving the helmet through the air outlet hose. However, it is not a complete seal and no pressure differential was measured across it.

Figure 4-3: Zero-porosity nylon interface between clear plastic helmet and subject necks

Though the helmet assembly is not sound proof, it would be difficult for the subject wearing it to hold a conversation with the researcher over the noise of the flowing air and the treadmill. To mitigate this, a two-way communication system between the subject and researcher is provided. A modified set of earbud headphones and a small microphone have been integrated into the helmet. The microphone is mounted inside of the clear plastic helmet in front of the subject's lips. Communication is enabled with a wireless intercom system. Through the use of belt pack transceivers, the researcher can maintain two-way communications with the subject at all times.

The inlet air is provided from compressed air cylinders at a flow rate of about 170 L/min (6 scfm). The Bauer Life Support Compressor for Breathing Air used is certified for grade E air by Trace Analytics, Inc. The compressed air is stored in a cascade of four

cylinders after exiting the compressor. In the unlikely event of a power failure, air will continue flowing for over an hour, which is much more than ample time to terminate the session.

The air outlet hose is 3.05 m (10 ft) long and terminates with a square fiberglass tube that has a 5.1 cm (2 in) square opening and is 38 cm (15 in) long. This serves as the mount for the oxygen and carbon dioxide sensors and is pictured in Figure 4-4. The interfaces between the square fiberglass tube and the air outlet hose and the sensor mounts are sealed with red RTV silicone gasket maker. The end of the air outlet hose opens to ambient air.

Figure 4-4: Oxygen and carbon dioxide sensors mounted in the air outlet

4.1.2 Treadmills

Three treadmills were used throughout the experimental sessions. The first treadmill (treadmill 1) is a Weslo® Cadence 865. It provides variable speed settings from

0 to 4.47 m/s (0-10 mph) in increments of 0.045 m/s (0.1 mph) and incline settings from 1-12% in increments of 1%. The motor is rated at 1492 watts (2 hp). This treadmill began to malfunction by self-terminating during exercise sessions. The second treadmill (treadmill 2) is a Weslo® Cadence 825. It can provide speeds of 0-2.68 m/s (0-6 mph) with manual control, has no power incline adjustability, and has a 933 watt (1.25 hp) motor. It was found to be too weak to maintain the fast walking speed and the belt was shorter than a comfortable stride length for some subjects during the fastest walking speed. This treadmill was not utilized for any official exercise sessions from which data was analyzed. Treadmill 3 is a Pro-Form® XP 580s Cross Trainer. This treadmill has a 1306 watt (1.75 hp) continuous duty motor, 0-4.47 m/s (0-10 mph) speed capability adjustable in increments of 0.045 m/s (0.1 mph), and a powered incline range of 0-10% grade in increments of 1%. All three treadmills are equipped with a safety key system for automatic termination in case of emergency.

4.1.3 Data Collection

Sensor data is collected using a National Instruments® USB-6008 multifunction data acquisition module [25], illustrated in Figure 4-5. Three of the eight 12-bit analog input channels are used to collect data from the oxygen, carbon dioxide, and heart rate sensors. The raw voltage data is recorded at a rate of 100 Hz using the included NI-DAQmx software for later conversion and analysis. Complete technical specifications of this module can be found in Appendix A.1.

Figure 4-5: National Instruments® USB-6008 data acquisition module [25]

The USB-6008 also provides analog outputs at 5 Volts DC and 10 Volts DC. The oxygen and heart rate sensors are powered from this 5 Volt DC analog output. The carbon dioxide sensor requires a higher voltage and power for it is provided through an independent 15 Volt power supply.

4.1.4 Oxygen Sensor

The oxygen sensor used is the Vernier® Oxygen Gas Sensor [26], pictured in Figure 4-6. This electrochemical, or Galvanic, oxygen sensor requires an input of +5 Volts DC, outputs a 0-4.8 Volts DC signal, and has a range of 0-27% oxygen. The rated accuracy is +/- 1% oxygen. The sensor is not very sensitive to temperature or pressure within the operational range. However, corrections must be made for relative humidity. More technical details about this sensor can be found in Appendix A.2.

Figure 4-6: Vernier® oxygen gas sensor

The oxygen gas sensor contains an electrochemical cell with a lead anode and gold cathode immersed in electrolyte. Oxygen molecules in the cell are reduced at the cathode and this generates a current proportional to the oxygen concentration. The current is then measured across a resistance and generates a small voltage, which is conditioned and amplified. This sensor is essentially a battery which produces electricity when exposed to oxygen. Therefore, the reactants are continually depleted, even when not in use actively but still exposed to air. For this reason, electrochemical oxygen sensors have a limited lifetime and require calibration with every use. The sensor used in this experiment was about 6 months old and, according to Vernier, these sensors should last for several years.

The Vernier® Oxygen Gas Sensor is designed for use with the Vernier® LabPro interface. Since the National Instrument® USB-6008 was used instead, preprogrammed calibrations and functions had to be replicated in the software described in Section 4.4.1.

An electrochemical oxygen gas sensor was selected over other sensing technologies because of its affordability. Within the selection of possible electrochemical sensors in the same price range and rated accuracies, the Vernier® sensor included built-in signal amplification, which made integration with the data acquisition module simple.

4.1.5 Carbon Dioxide Sensor

The carbon dioxide sensor selected is the Vaisala CARBOCAP® Carbon Dioxide GMM221 Module [27], pictured in Figure 4-7. It has a range of 0-3% carbon dioxide. The input it requires is less than 2.5 W at 11-30 Volts DC and the output is 0-5 Volts DC. The rated accuracy is less than 0.02% CO_2 plus 2% of reading. This sensor has a slight dependence on pressure and temperature; however, this experiment took place at standard conditions and no corrections were necessary. The dependence on relative humidity is insignificant. The calibration is preset by the manufacturer. It is recommended to send the sensor for recalibration annually. This experiment took place six months after the date on the calibration certificate for this sensor. Full technical specifications are available in Appendix A.3.

Figure 4-7: Vaisala CARBOCAP® Carbon Dioxide GMM221 Module [27]

This is a silicon based non-dispersive infrared absorbance (NDIR) sensor [28]. Its working principle is Single-Beam Dual-Wavelength NDIR. An infrared light is emitted at one end of the chamber, where part of it is absorbed by the carbon dioxide molecules present. The light is then filtered to pass only the wavelength of light absorbed by the carbon dioxide and measured by the infrared detector at the end of the chamber. Then a reference wavelength of light is emitted. This reference wavelength is not absorbed by the carbon dioxide and all of it is measured by the infrared detector. The ratio of the amounts of light absorbed gives an accurate reading of the concentration of carbon dioxide. The reference signal compensates for sensor aging affects and maintains the stability of the sensor.

The Vaisala sensor was selected for a high rated accuracy relative to price. Additionally, this line of sensors provided flexibility in the ranges available. Selecting a sensor with a range that fits the application reduces the amount of error as a function of the full range and increases the resolution.

4.1.6 Heart Rate Sensor

Heart rate is measured with a Polar® Chest Belt Transmitter and a Vernier® Heart Rate Receiver, pictured in Figure 4-8. The chest belt transmitter is a rubber chest strap with two electrodes which records the electrocardiogram (ECG) signal and transmits the data. It has built-in batteries, which can only be replaced by the manufacturer. There are two interchangeable elastic straps to accommodate various chest circumferences. Like the oxygen sensor, the receiver requires +5 Volts DC and outputs a 0-4.8 Volts DC signal. Unlike a complete ECG tracing, this sensor outputs a flat line signal with a spike when a heart beat occurs. The other components of the cardiac cycle

are filtered out and are not visible. The complete technical specifications of this sensor can be found in Appendix A.4. The receiver must be kept at most 80 cm (31.5 in) from the transmitter to avoid a loss of signal. To minimize interference from surrounding electronics, the receiver was attached to the subject's shirt.

Figure 4-8: Polar® chest strap transmitter and Vernier® heart rate receiver

The D027i heart rate sensor from Learning Things, Inc. was also considered for this application. Unlike an ECG sensor which monitors the electrical signal of the heart, this sensor monitors the changes in blood perfusion. It has a clip with an infrared light emitting diode on one side and an infrared sensor on the other side. The clip attaches to either the ear lobe or a finger. The amount of blood in blood vessels changes regularly with the heart beat and the amount of infrared light detected by the sensor changes with it. The sensor translates the amount of light detected to an output voltage. It was found that this sensor is very sensitive to movement and accurate readings were only obtained when the subject was motionless. This was not possible throughout treadmill exercise and the ECG chest strap was selected instead.

4.1.7 Flow Rate Sensor

The flow rate sensor utilized for this experiment is the Hastings® L-10S laminar flow element and HS-10S mass flow transducer, illustrated in Figure 4-9. This sensor compensates for pressure changes within 7-1700 kPa (1-250 psi) and gas temperature changes within the range of 0°C to 100°C [30]. It has an accuracy of +/- 1% of the full range, which is 0-283 L/min (0-10 scfm) [31]. It is calibrated by the manufacturer and does not require calibration prior to use. Complete technical specifications for this flow meter can be found in Appendix A.5.

Figure 4-9: Hastings® flow rate sensor

The data from the mass flow meter is not collected with the same data acquisition module as the remaining sensors. It is digitally displayed and monitored periodically throughout the exercise session. This sensor is integrated into the MX-2 air system and was not selected specifically for this study.

4.2 Control Session Hardware

The control sessions were performed with a commercially available, top-of-the-line cardiopulmonary exercise testing system. The following sections describe this system, as well as the weighted helmet the subjects were asked to wear to simulate the weight of the experimental helmet assembly and the heart rate measuring method for this portion of the validation study.

4.2.1 Cardiopulmonary Exercise Testing System

The Viasys Healthcare Oxycon Pro® is the commercially available cardiopulmonary exercise testing system utilized during the control sessions. This complete integrated system includes the respiration collection devices, gas and flow analyzers, computer, and treadmill. Figure 4-10 illustrates this system.

Figure 4-10: Viasys Healthcare Oxycon Pro®

This indirect calorimetry system requires the subject to wear an oronasal mask to collect all exhaled air. It seals to the face around the mouth and nose and is held in place with a double head strap. This mask has several one-way valves. They allow the subject to comfortably inhale ambient air but force all exhaled air out through a hose for analysis. The oronasal mask is pictured in Figure 4-11.

Figure 4-11: Oronasal mask with one-way valves

A hose routes air from the mask into the right side of the mixing chamber, pictured in Figure 4-12. This chamber allows the gas concentrations in an exhaled volume of air to become uniform for averaged results with reduced noise. Two small tubes on the left side collect samples of gas for the oxygen and carbon dioxide analyzers. The oxygen analyzer is a high-speed differential paramagnetic sensor and the carbon dioxide sensor's operating principle is infrared absorption [32]. Both of these sensors have an accuracy of 0.05%, a resolution of 0.01%, a stability of 0.02%/hour, and a minimum 90% rise time of 40 milliseconds. The volume sensor is also located on the left

side at the outlet of the mixing chamber. It is a TripleV bidirectional turbine volume sensor. It has an accuracy of 70 mL/s or 3% over a range of 0-15 L/s. At maximum flow, its resistance is less than 0.1 kPa/L/s. Complete technical specifications of this system can be found in Appendix A.6.

Figure 4-12: Oxycon Pro® mixing chamber

Prior to each control session, all components of the Oxycon Pro® system are calibrated. The gas sensors are calibrated with a calibration gas and the volume sensor undergoes an automatic calibration. Atmospheric pressure, temperature, and relative humidity are also measured for internal sensor corrections.

The Oxycon Pro® system calculates 15-second averages of $\dot{V}O_2$ and $\dot{V}CO_2$. The RER is computed at the same rate. The system records a data point every 30 seconds. Metabolic workload is calculated from this data by multiplying the $\dot{V}O_2$ by the caloric equivalent of oxygen in kilocalories per liter, which can be determined with Equation 4-1 [2].

$$CE_{O_2} = 3.9 + 1.1RER \qquad \textbf{Equation 4-1}$$

4.2.2 Weighted Helmet

To simulate the weight of the experimental helmet assembly, subjects wore a weighted helmet throughout the control sessions. This helmet, shown in Figure 4-13, is a bicycle helmet with four small bags of lead shot attached to the outside. The mass of this helmet is 2 kg (4.4 lb). This is 23% lighter than the experimental helmet assembly. However, the entirety of this mass is supported by the head while the mass of the experimental helmet assembly partially sits on the shoulders. This distribution of mass reduces the perceived load and the reduced mass of the weighted helmet compensates for that.

Figure 4-13: Weighted helmet worn during control sessions

This weighted helmet is different from the one proposed in the IRB protocol modification request in Appendix B.7. The previous helmet was a construction hard hat with weight affixed to the top. This high center of gravity made that helmet unstable and the bicycle helmet was chosen for testing instead. The masses of the two helmets were very similar.

4.2.3 Heart Rate Sensor

Throughout the control sessions, the subjects wore the same Polar® Chest Belt Transmitter as during the experimental sessions. However, instead of the Vernier® Heart Rate Receiver, a Polar® receiver watch was used to display the heart rate, which was recorded manually at 1-minute intervals. The Oxycon Pro® system includes an integrated 12-lead ECG measurement option, but this was considered unnecessary for this study.

4.3 Experiment Protocol

The previously described hardware and sensors were used to collect physiological data on subjects throughout both treadmill exercise sessions. The following sections describe the protocol prior to and throughout the experimental and control exercise sessions.

4.3.1 Subject Selection

Since this research includes human subjects, the study had to be approved by the Institutional Review Board (IRB) to assure the protection of rights and welfare of the subjects. An approval was granted on November 9, 2006. A protocol modification request was later submitted and approved. All IRB submissions and associated documents, including the coversheet, proposal, subject recruitment email, consent form,

subject questionnaire, IRB approval, and the protocol modification request and approval can be found in Appendix B.

A total of 12 subjects, including 8 males and 4 females, participated in this study. They were volunteers who responded to a recruitment email and were selected for certain physical attributes for subject safety. To reduce the risk of a cardiovascular event, all subjects were adults under the age of 40 who are reasonably fit and in good health. Though no medical clearance was required, subjects were asked and excluded if they have any medical conditions with which their risk during treadmill exercise is heightened. The risk factors specifically addressed are listed in Table 4-1. However, this is not an exhaustive list and subjects were asked to bring any additional medical concerns to the investigator's attention prior to commencement of testing for possible disqualification.

Table 4-1: Validation study disqualifying conditions

High blood pressure	Seizure
Heart murmur	Head injury
Emphysema	Diseases of the arteries
Diabetes	Diseases of the lungs
Asthma	Frequent headaches
Elevated cholesterol	Heart palpitations
Claustrophobia	Chest pain
Epilepsy	Dizzy spells
Pregnancy	Shortness of breath
Heart attack	Painful joints
Stroke	Blood clots
Aneurysm	Smoking
Open or bleeding lesions near or including the mouth	Taking medications with adverse side effects to exercise

Subject confidentiality is among the issues addressed by the IRB. Data is not associated with subject identity. Throughout this thesis, subjects will be identified by

alphanumeric codes. Females will be labeled F1 through F4 and males will be labeled M1 through M8.

4.3.2 Exercise Sessions

Each subject was scheduled to attend one experimental treadmill session and one control treadmill session. Prior to the sessions, the physical requirements and excluding conditions were discussed with each subject. He or she was asked to fill out a questionnaire, which can be found in Appendix B.5. The questionnaire asked for basic information, such as sex and age, a medical history to check for any disqualifying conditions, and an exercise profile which establishes the frequency, duration, and type of exercise each subject typically participates in. The weight and height were measured. The purpose of the research, procedures, and equipment were described to the subject, any questions were answered, and informed consent was obtained. The consent form is included in Appendix B.4.

The original validation study plan intended for the order of sessions to vary between subjects. Roughly half of the subjects were to participate in an experimental session first and half were to start with the control session. Each subject's two sessions were to be spaced apart by no more than one week. However, issues with availability of facilities for the control sessions forced all of the control sessions to be completed up to ten weeks after the respective experimental session.

Each session took about an hour of the subject's time, though the actual exercise portion lasted 30 minutes. Prior to the experimental sessions, the chest belt transmitter was first donned by the subjects in the bathroom for privacy. Each subject was instructed on how to adjust the strap and wet the electrodes with saline for maximum signal

conduction. The communications earphones and belt packs were then put on and tested. Finally, the helmet assembly, with the air flow already is progress, was carefully placed over the head, adjusted for fit and comfort, and closed off.

Prior to the control sessions, the chest belt transmitter was first donned following the same procedure as during the experimental sessions. The weighted helmet was then adjusted for a tight fit and removed. Next the oronasal mask was placed on the face and the straps were tightened and closed. Leak paths were checked by placing a hand over the hose attachment on the front of the mask and blowing. If any air was escaping through the seal, the straps were readjusted and tightened. Finally, the weighted helmet was donned taking care not to displace the oronasal mask straps.

After the session-appropriate gear has been donned and adjusted for fit, a rest period began. Each subject was asked to sit quietly for 8 minutes. The 30 minutes of treadmill exercise began immediately following the rest period. It was divided into three 10-minute portions at progressively higher speeds of 1.34 m/s (3 mph), 1.65 m/s (3.7 mph), and 1.97 m/s (4.4 mph). These three segments made up one continuous block of exercise. Data was collected throughout the entire exercise session. The treadmill incline was set to 1° grade because this is the minimal value possible on treadmill 1. A subject during an experimental session and a control session is shown in Figure 4-14.

Figure 4-14: A subject during an experimental (left) and a control (right) session

The three speeds used were selected to include a slow, medium, and fast walk. The slowest speed requires a workload noticeably above resting values. The highest was selected to be slightly slower than the human walk-run gait transition speed for the shortest subject (subject F3 is 1.55 m or 61 in). The transition speed was calculated using Equation 4-2, which is derived from an inverted pendulum mechanical model [33]. The transition speed (m/s), v, is a function of the Froude number, f, acceleration due to gravity (m/s^2), g, and leg length (m), l, measured from the hip to the floor. The Froude number is a dimensionless number defined as the ratio of centripetal and gravitational forces at the preferred walk-run transition. It was experimentally determined to be 0.5 for humans [33].

$$v = \sqrt{fgl}$$ **Equation 4-2**

Historically, a typical average workload during EVA has been 215 kcal/hr and the minimum and peak workloads have been 86 kcal/hr and 516 kcal/hr, respectively [14]. Typical metabolic workloads during walking are 114-228 kcal/hr at 0.89 m/s (2 mph), 150-318 kcal/hr at 1.34 m/s (3 mph), and 192-420 kcal/hr at a speed of 1.79 m/s (4 mph) [4]. There is sufficient overlap between these typical values to assume that the workloads during walking are representative of those experienced during EVA.

At the conclusion of each exercise session, the subjects filled out the response to experiment portion of the subject questionnaire which related to the session just completed. Questions probed the perceived exertion and comfort during the sessions.

Calibration data was collected immediately before and after each experimental session. It is necessary for oxygen sensor calibration and for determination of baseline carbon dioxide concentration in the cascade air without human respiration. The helmet assembly was bypassed by connecting the inlet hose to the outlet hose, as illustrated in Figure 4-15, and air was delivered directly into the outlet hose at the same flow rate.

Figure 4-15: Helmet assembly bypass for calibration

Each time, the system was first allowed to flush out for about 5 minutes followed by 5 minutes of data collection. When two experimental sessions were scheduled

consecutively, only one calibration was taken in between and was used as the after calibration for the first session and the before calibration for the second session.

4.4 Experimental Session Data Processing

The data collected from the oxygen, carbon dioxide, and heart rate sensors is recorded by the NI-DAQmx software as raw voltage values between 0 and 5 Volts at a rate of 100 Hz. This rate was chosen for sufficient resolution in the ECG signal from the heart rate sensor. A lower sampling rate would result in an imprecise determination of the time at which a heart beat occurs and would lead to an irregular calculation of heart rate. Though this high sampling rate is not necessary for either of the gas sensors, the data acquisition module is not capable of different sampling rates at various pins. A short sample of the Ni-DAQmx output is shown in Appendix C.5. The data analysis software later calculated 1-second averages to smooth and reduce the quantity of gas sensor data.

The post-session data processing takes place in three stages, all programmed in Matlab. The gas sensor calibration data obtained before and after each session at a rate of 10 Hz is first averaged and plotted for visual inspection with the code shown in Appendix C.3. The Ni-DAQmx output *data* is then processed with the code included in Appendix C.4 by filtering the heart rate data, adding a column with time in seconds, and saving into a new text file labeled *MHcleandata*. A sample of this output file can be found in Appendix C.6. This process is described in more detail in Section 4.4.3.

Finally, the code found in Appendix C.1 is used to calculate the metabolic rates. It takes two inputs. The first is an Excel file labeled *parameters.* It contains information specific to the subject and the exercise session including age, sex, weight, times of speed transitions, before and after calibration data for the gas sensors, relative humidity, and the

flow rates and times of transitions between them. A sample *parameters* file is included in Appendix C.2. The second is a text *MHcleandata* file with four columns: O_2, CO_2, and heart rate sensor voltages and time in seconds.

The outputs of this data processing are values of heart rate and metabolic workload calculated from each of three sets of sensor data at each speed, the theoretically predicted metabolic workload values as calculated by the Pandolf [35] model, and multiple plots displaying all relevant data. The Pandolf model will be discussed in greater detail in Section 5.1.

The following sections describe the conversion of the raw voltage data from each sensor to metabolic workloads.

4.4.1 Oxygen Sensor Data

Since the oxygen sensor is an electrochemical sensor and its lifetime depends on the amount of reactants present for the reaction, a calibration update is required before every use. Equation 4-3 is the linear calibration equation used.

$$\%O_2 = \frac{\%O_{2\max}(RH)}{V_{\max}}V \qquad \textbf{Equation 4-3}$$

The slope of the calibration equation between the raw voltage (V) and the percentage of oxygen ($\%O_2$) is a ratio of the maximum values of each. The maximum percentage of oxygen ($\%O_{2max}$), or the percentage of oxygen in cascade air without human respiration, is a function of the percentage of relative humidity (RH) shown in Equation 4-4. This equation is derived from tabulated data published in the Vernier® oxygen sensor manual [26].

$$\%O_{2\max}(RH) = 20.9 - 0.008RH \qquad \textbf{Equation 4-4}$$

As the workload increases throughout each experimental session, the respiration, and therefore the relative humidity in the outlet air, increases. Perspiration also contributes to an increase in relative humidity. An Onset HOBO® H08 data logger was used to measure the relative humidity of the outlet air through several experimental sessions. However, this sensor has a 10 minute settling time and a measurement range of 25-95%, making it inadequate for measurements at rest and low workloads. Relative humidity data was only obtained for the medium and fast walking speeds for 4 subjects. Figure 4-16 illustrates the relative humidity profile assumed for all of the experimental sessions. It was developed from averages of collected data and extrapolation to lower workloads. Transitions between each workload were assumed to be linear and last 3 minutes from the time a speed change occurred.

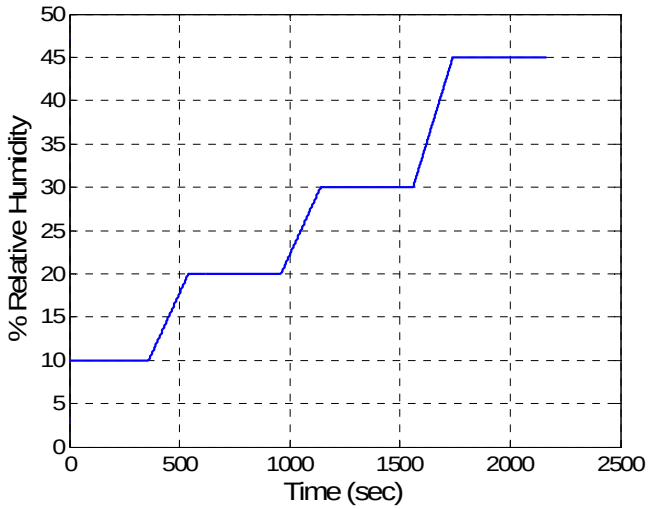

Figure 4-16: Relative humidity profile

The maximum voltage (V_{max}) in Equation 4-3 is the voltage the sensor measured without human respiration when the helmet assembly was bypassed. It was taken to be a linearized function between the mean voltages of the before and after calibrations.

$\dot{V}O_2$ was calculated by multiplying the difference of the maximum ($\%O_{2max}$) and measured ($\%O_2$) percentage of oxygen by the measured flow rate. The $\dot{V}O_2$ was then used to calculate metabolic rate with a caloric equivalent of oxygen of 5.0 kilocalories per liter of oxygen. This value is recommended by the American College of Sports Medicine (ACSM) to be used when a RQ is unknown [34]. According to Equation 2-1, this corresponds to an assumed RQ of 1.0.

4.4.2 Carbon Dioxide Sensor Data

The carbon dioxide sensor's measurements are not affected significantly by relative humidity and corrections for pressure and temperature were not necessary because the testing conditions did not vary substantially from standard conditions. It was calibrated by the manufacturer against accurate gas concentrations and did not require recalibration prior to each session. The sensor has an input range of 0-5 Volts and an output range of 0-3% carbon dioxide. Therefore, the carbon dioxide percentage is calculated simply by multiplying the raw voltage by a factor of 0.6.

Metabolic workload was derived from carbon dioxide data by way of $\dot{V}O_2$. The calculation of $\dot{V}CO_2$ from carbon dioxide sensor data followed the same procedure as the calculation of $\dot{V}O_2$ from oxygen sensor data in Section 4.4.1. An assumed respiratory exchange ratio of 1.0 was used to convert $\dot{V}CO_2$ to $\dot{V}O_2$ and the caloric equivalent of

oxygen of 5.0 kilocalories per liter of was used to calculate the metabolic workload from carbon dioxide sensor data.

4.4.3 Heart Rate Sensor Data

The heart rate sensor data collected is a flat line at about 1.2 Volts, with spikes up to about 2.6 Volts when a heart beat occurs. The duration of the heart beat spikes is about 0.04-0.06 seconds. Electromagnetic interference creates some additional spikes in the data which could be read as heart beats. Fortunately, the duration of the majority of these spikes is shorter than that of a heart beat. Software was written to remove spikes that are shorter than a set threshold. This threshold was typically set to 0.04 seconds, but was adjusted on a case by case basis for optimum results. This code can be found in Appendix C.4. After the heart rate data was cleaned with software, a few spikes had to be removed manually as well. These were instances when interference caused an increase in the voltage that lasted longer than the threshold. These cases were obvious by the fact that heart beats appeared closer than naturally possible and the heart rates jumped to at least twice the previous value.

Heart rate was derived from the cleaned heart rate data. First the times at which a heart beat occurred, or the times the voltage exceeded a threshold of 1.5 Volts, were recorded in a new matrix. The time periods between these beats were then calculated and inverted for beat-to-beat heart rates. Finally, 15-second averages were taken every 5 seconds to smooth the data.

The metabolic rate was calculated from heart rate data using equations for $\dot{V}O_2$ and its dependents published by Johnson [4]. $\dot{V}O_2$ (L/min) was calculated using Equation 4-5.

$$\dot{V}O_2 = \dot{V}O_{2\max} \frac{HR - HR_{rest}}{HR_{\max} - HR_{rest}}$$ **Equation 4-5**

In this equation, HR is the measured heart rate in beats per minute. HR_{rest} is the resting heart rate. It was measured on three occasions for each subject: prior to the experimental and control sessions and a 10 minute independent measurement in a sitting position. During the latter, each subject was asked to sit quietly for 10 minutes with the chest belt heart rate monitor. The average of the final 5 minutes of this rest period was taken to be the resting heart rate. The lowest of these three was used as HR_{rest} in this calculation. Like the RMR, the resting heart rate is not at basal conditions. Subjects are likely digesting food and not in a thermoneutral environment. HR_{max} in beats per minute was calculated using Equation 4-6 as a function of age.

$$HR_{\max} = 220 - age$$ **Equation 4-6**

The $\dot{V}O_2$ max equations vary for males and females. Equation 4-7 is the equation for $\dot{V}O_2$ max (L/min) for males.

$$\dot{V}O_{2\max} = 4.2 - 0.03 \cdot age$$ **Equation 4-7**

Equation 4-8 is the female equation for $\dot{V}O_2$ max (L/min).

$$\dot{V}O_{2\max} = 2.6 - 0.01 \cdot age$$ **Equation 4-8**

Metabolic rate was calculated from $\dot{V}O_2$ using the same caloric equivalent of oxygen (5.0 kilocalories per liter) as discussed in Section 4.4.1.

Chapter 5 : RESULTS AND ANALYSIS

The experimental and control sessions were both completed by each of 10 subjects. The following sections present quantitative and qualitative data from these sessions as well as theoretically predicted results. All of the data is discussed and statistically analyzed. Also included are results from three system characterization tests and a detailed investigation of error sources.

5.1 Theoretical Predictions

Numerous models exist for the prediction of metabolic workload during walking and running with variables such as surface types, incline, loads carried, and physical characteristics of subjects. These models were developed under different conditions with varying numbers of subjects. The model for walking with loads developed by Pandolf, et al. [35] was selected to serve as the source of predicted data for this experiment. The following sections explain why it was selected over others and describe the model and its parameters.

5.1.1 Model Selection

A study was performed by Hall, et al. [36] to compare many of the existing energy expenditure models for walking and running. Male and female subjects were asked to walk and run 1600 m (1 mile) at 1.41 m/s (3.15 mph) and 2.82 m/s (6.31 mph), respectively, while their metabolic workload was measured using indirect calorimetry. Tests were performed on a track and a treadmill. It was found that there was no

significant difference between energy expenditure of walking or running between the track and the treadmill. However, a significant difference was found between the males and females performing the same exercise. This is mostly due to the fact that males tend to have a higher fat-free mass, which is metabolically active.

The data collected was then compared against existing prediction formulas. The walking models considered include those derived by the American College of Sports Medicine (ACSM) [34], Van der Walt, et al., Pandolf, et al. [35], and tables by McArdle, et al. It was found that the experimental values did not differ significantly from those calculated using the ACSM or Pandolf's equations. McArdle's tables and Van der Walt's equation were both found to significantly overestimate the metabolic rate.

The equation listed by ACSM [34] is a function of only walking speed and percent grade. Pandolf's equation is a function of walking speed, percent grade, subject mass, and the mass of the load carried. This model was selected to serve as the source of reference data for this study because it takes into account the physical size of the subject as well as load carried. The experimental helmet assembly has a mass of 3.7 kg (6 lb) was taken into consideration using Pandolf's equation. Additionally, this model was developed for walking and standing so it can be used for resting values as well.

5.1.2 The Pandolf Model

Equation 5-1 shows the Pandolf model for predicting energy expenditure for walking while carrying a load.

$$M = 1.5W + 2.0(W + L)(\tfrac{L}{W})^2 + \eta(W + L)(1.5V^2 + 0.35VG) \quad \textbf{Equation 5-1}$$

In this model, M is the metabolic rate (watts), W is the subject mass (kg), L is the load carried (kg), V is the speed of walking (m/s), G is the percent grade, and η is the terrain factor (η = 1 for a treadmill). All energy expenditures in this thesis are given in kilocalories per hour. The conversion between the two units used is listed in Equation 5-2.

$$1\ kcal/hr = \tfrac{3600}{4184}\ watts = 0.8604\ watts \qquad \textbf{Equation 5-2}$$

The predicted results calculated with this model are shown in Appendix D.2. The variables in this calculation are 3.7 kg (6 lb) for load carried, terrain factor of 1, and a fractional percent grade of 0.01. The subject masses are given in Section 5.2.1.

5.2 Quantitative Results

The discussion of the quantitative results obtained is organized as follows. First is the overview of subject physical characteristics. This is followed by the detailed results from one sample subject to illustrate typical data obtained. The metabolic workloads from all subjects are then presented and trends are discussed. Finally, the heart rates measured during each session are compared.

5.2.1 Physical Characteristics of Subjects

A total of 12 subjects participated in this study. Their physical characteristics, including age, mass, height, and resting heart rate, are listed in Table 5-1.

Table 5-1: Subject physical characteristics

Subject	*Age years*	*Mass kg (lb)*	*Height m (in)*	*Resting Heart Rate bpm*
F1	24	61.8 (136)	1.65 (65)	62.2
F2	24	51.8 (114)	1.63 (64)	94.6
F3	24	59.1 (130)	1.55 (61)	70.4
F4	20	60.9 (134)	1.63 (64)	66.5
M1	20	80.0 (176)	1.88 (74)	66.3
M2	25	77.3 (170)	1.73 (68)	67.0
M3	23	77.7 (171)	1.70 (67)	79.2
M4	23	60.5 (133)	1.68 (66)	77.3
M5	23	68.2 (150)	1.83 (72)	68.4
M6	26	74.5 (164)	1.78 (70)	69.7
M7	20	62.3 (137)	1.73 (68)	74.6
M8	25	70.5 (155)	1.83 (72)	82.2

Of the 12 subjects, 10 completed both sessions. Subject F2 chose to terminate the experimental session prematurely. The experimental session for subject M5 was cut short because of a treadmill malfunction and was never repeated. Neither of these subjects participated in a control session. The average mass of the final 10 subjects was 68.5 kg (150.6 lb) with a standard deviation of 8.4 kg (18.4 lb) and their average height was 1.72 m (67.7 in) with a standard deviation 0.11 m (4.2 in). The average and standard deviation of the age was 23 years and 2.3 years, respectively.

The treadmill malfunctions did present an operational problem in the experimental sessions. Of the 10 subjects who completed the entire experimental session, 5 did so on treadmill 1 (F1, F3, M1, M2, M3) and 5 on treadmill 3 (F4, M4, M6, M7, M8). Those subjects who attempted to complete the protocol on treadmill 1 after it began to malfunction or on treadmill 2 repeated the entire session on treadmill 3. Notes on the specific occurrences during each session can be found in Appendix D.1.

5.2.2 Sample Subject Results

Subject F3 was selected as a sample of all results because she completed both sessions without any anomalies in the protocol and the results are a typical representation of the majority of the subjects. Figure 5-1 displays a plot of the data obtained from all three sensors during the experimental session.

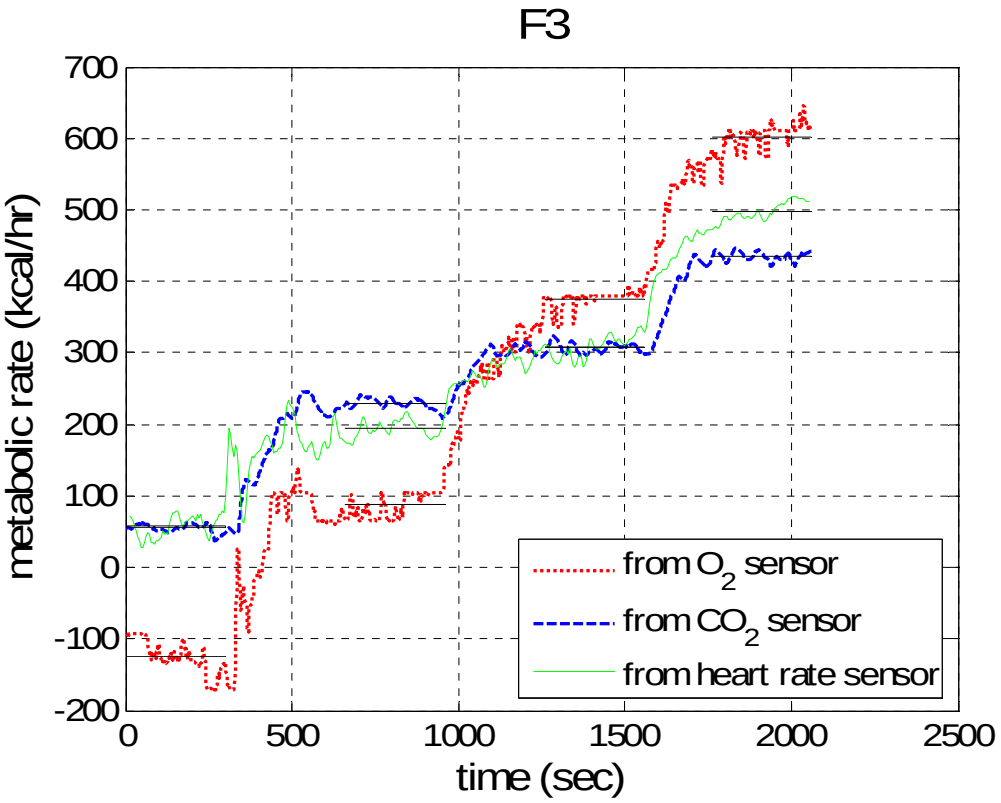

Figure 5-1: Metabolic rate obtained during the control session for subject F3

All three methods display distinct transition regions and plateaus. The horizontal black line through each plateau indicates the averaged metabolic workload at that speed from that sensor and the 5-minute time range over which it was averaged. The carbon dioxide data has a plateau at each of the four workloads, while the remaining two methods do not reach a steady state at the highest workload.

There is some chatter in the data at each plateau. The standard deviations from the mean were calculated for each sensor at each workload for subject F3 and are displayed in Table 5-2. As can be seen from the data for each workload and the averages, the carbon dioxide sensor is the most stable of the three.

Table 5-2: Standard deviations of metabolic workloads at plateaus (kcal/hr)

	Rest	*Slow*	*Medium*	*Fast*	***Average***
O_2 Sensor	22.7	17.7	11.7	17.8	**17.5**
CO_2 Sensor	6.4	7.5	6.9	6.4	**6.8**
HR Sensor	15.2	12.1	13.8	12.0	**13.3**

The metabolic workload and the respiratory exchange ratio obtained from the control sessions for subject F3 is displayed in Figure 5-2.

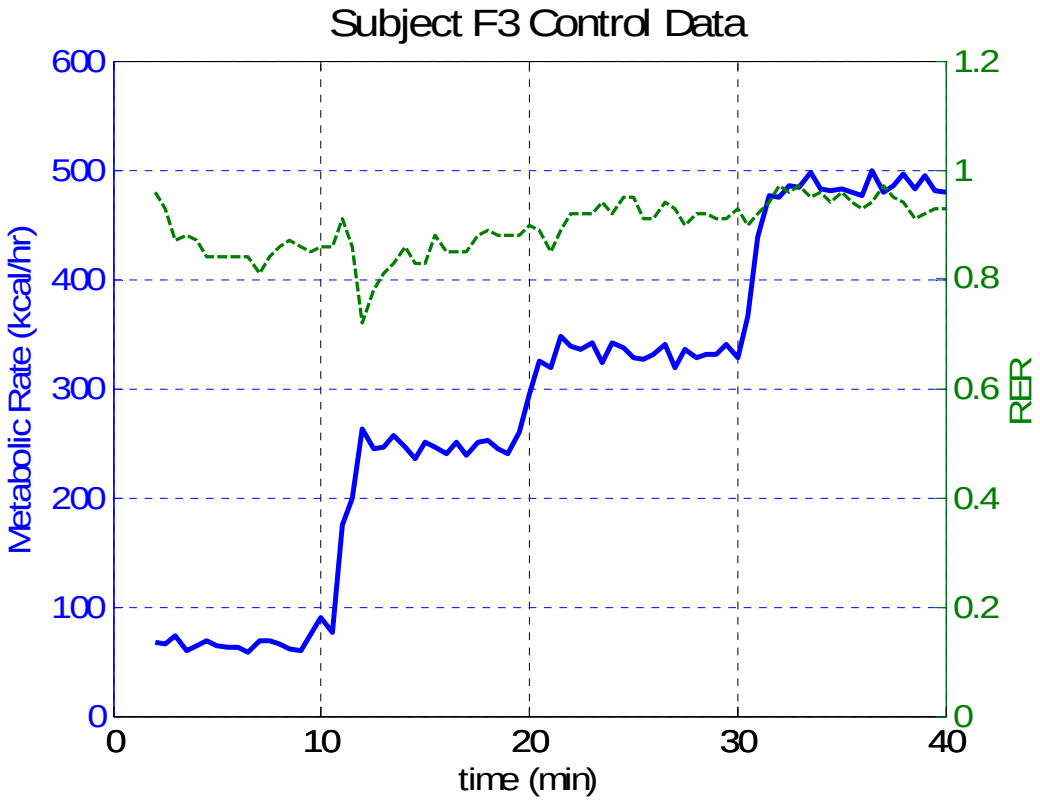

Figure 5-2: Metabolic rate and RER obtained during the control session for subject F3

The control data also results in steady plateaus at each workload. The standard deviations of the metabolic workloads of subject F3 at rest and the slow, medium, and fast walking speeds are 4.5 kcal/hr, 5.8 kcal/hr, 6.5 kcal/hr, and 8.0 kcal/hr, respectively. The average of these four values is 6.2 kcal/hr. This is just slightly lower than the amount of chatter in the carbon dioxide sensor.

Similar plots of experimental and control data for each subject can be found in Appendix D.3 and Appendix D.5, respectively.

5.2.3 Results from All Subjects

The metabolic rates were calculated from the mean of the final 5 minutes of data at each workload to avoid the inclusion of any settling effects before steady state was reached. The metabolic workload data calculated for each subject and speed from data collected by the oxygen sensor, carbon dioxide sensor, and heart rate sensor, along with the theoretically expected values according to Pandolf's model and those obtained during the control sessions, is tabulated in Appendix D.2. These results are displayed in Figure 5-3 through Figure 5-6.

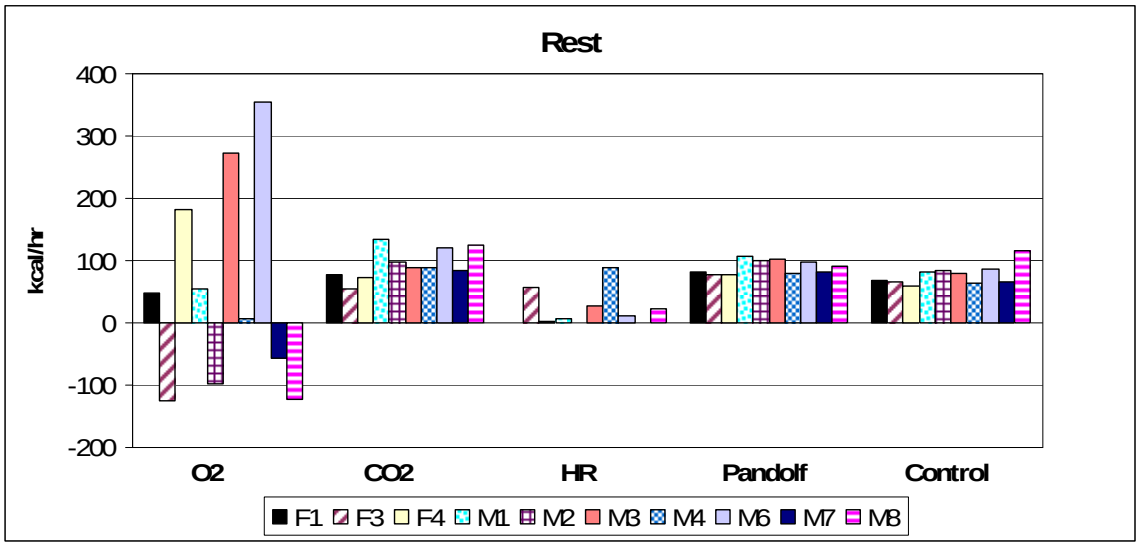

Figure 5-3: Metabolic rates during the rest period for all subjects calculated from the oxygen, carbon dioxide, and heart rate sensors, Pandolf's model, and control data

The rest period data presented in Figure 5-3 is the most variable of the four workloads. Oxygen sensor data shows a negative metabolic workload for four subjects. This is physically impossible and implies problems with sensor calibration and determining the absolute amount of oxygen in the air. The negative values indicate that the amount of oxygen measured in the cascade air during the calibration before or possibly after the exercise session was lower than with human respiration consuming oxygen in the loop. Conversely, the metabolic workloads for three subjects appear very high compared to the predicted and control values. It is likely that the resolution and accuracy of the oxygen sensor within this small portion of its range is not sufficient.

The heart rate sensor shows no workload for three subjects and very low workloads for five subjects. This supports the claim in Section 2.2.4 that the correlation between metabolic workloads and heart rate is not strong at low workloads. The linear approximation used to calculate metabolic workload from heart rate assumes no

workload at rest and depends very heavily on the accuracy of the resting heart rate measurement. As mentioned in Section 4.4.3, the resting heart rate is the lowest of three heart rate measurements for each subject. For the subjects whose lowest heart rate occurred prior to the experimental session, the metabolic workload calculated by Equation 4-5 is 0 kcal/hr.

Carbon dioxide sensor data appears to be closest to predicted and control values. It does not exhibit any highly irregular behavior like the oxygen and heart rate sensors.

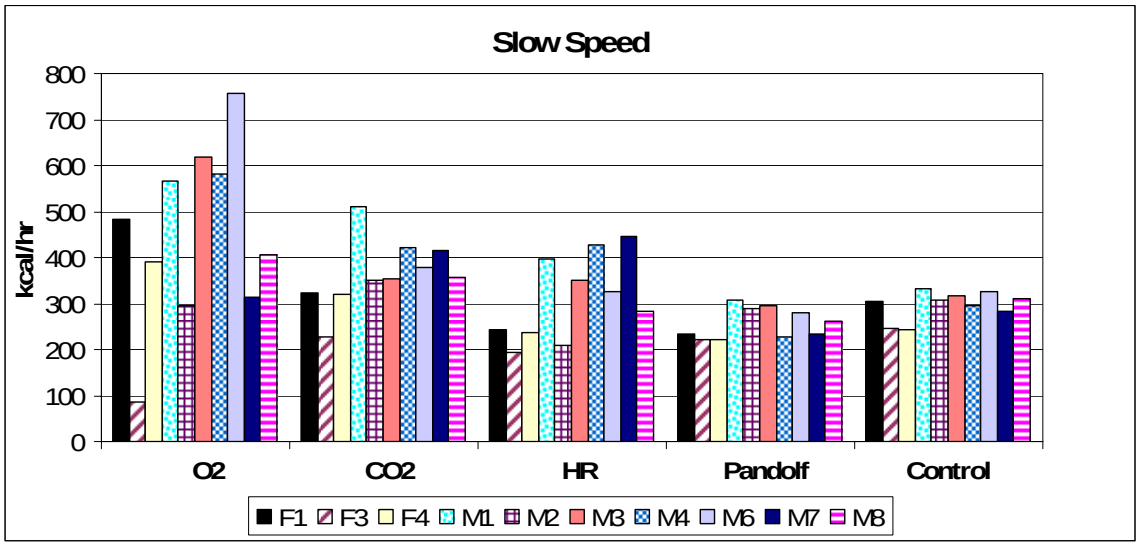

Figure 5-4: Metabolic rates during the slow speed for all subjects calculated from the oxygen, carbon dioxide, and heart rate sensors, Pandolf's model, and control data

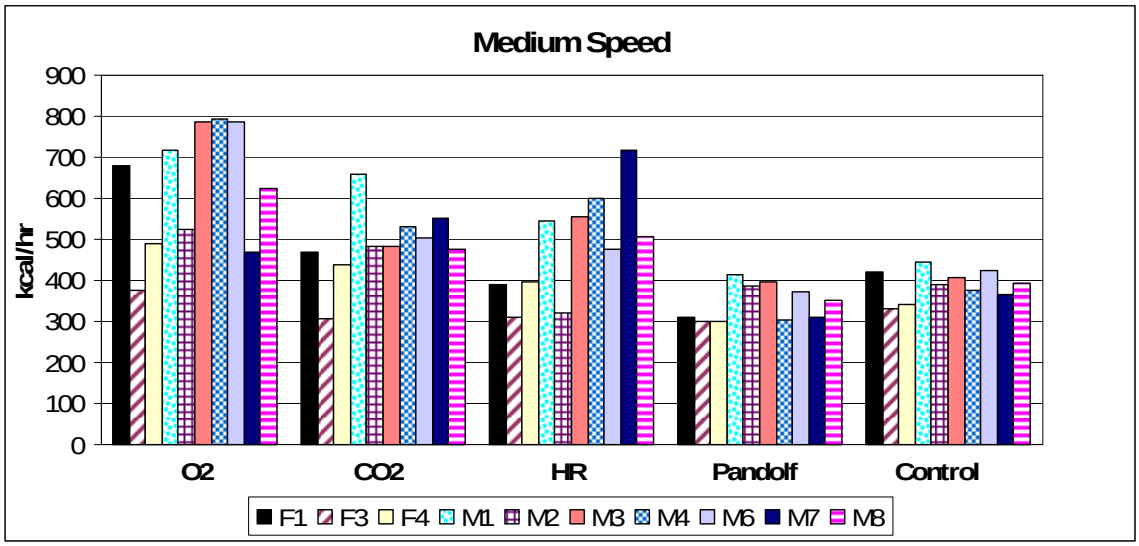

Figure 5-5: Metabolic rates during the medium speed for all subjects calculated from the oxygen, carbon dioxide, and heart rate sensors, Pandolf's model, and control data

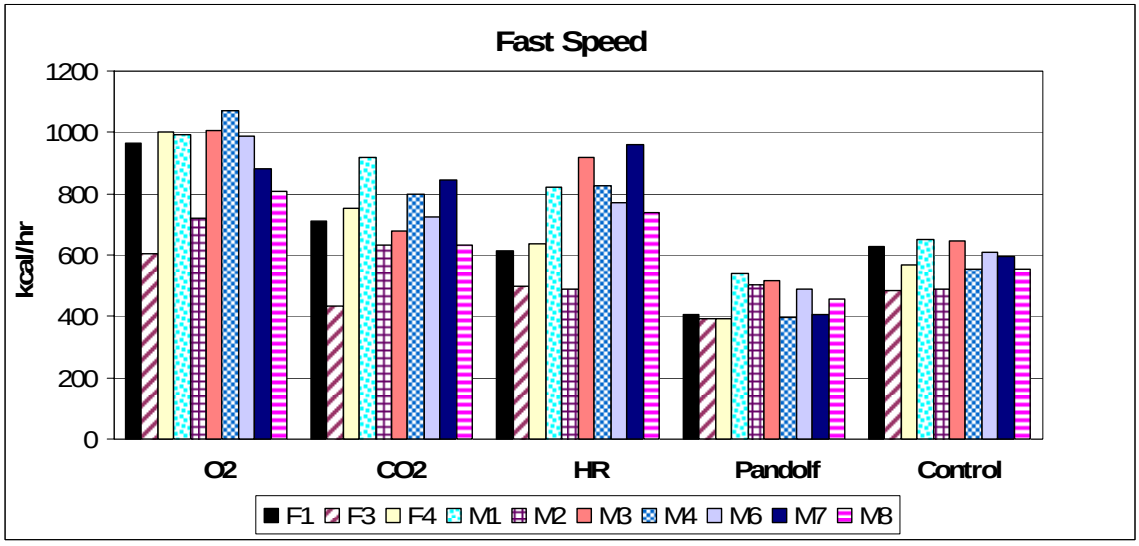

Figure 5-6: Metabolic rates during the fast speed for all subjects calculated from the oxygen, carbon dioxide, and heart rate sensors, Pandolf's model, and control data

A lot of variability was found in the experimental data during the slow, medium, and fast walking periods as well. In general, experimental data showed higher workloads

than control data. This phenomenon will be explored in greater detail in the following sections.

The Pandolf model resulted in values close to the control results. This gives a general indication that the experimental data is likely overestimating the metabolic workload rather than the control data underestimating it. However, the Pandolf model was experimentally derived with data from a limited number of subjects in conditions that were not identical to those in this study, and it will not be quantitatively compared to the experimental data.

5.2.4 Heart Rates

Heart rates were measured throughout each experimental and control session. The means of the final 5 minutes of each workload for each subject are tabulated in Appendix D.2. The heart rates from both sessions at each speed averaged across all 10 subjects, along with their average difference (not difference of the averages) and the standard deviation of this difference can be found in Table 5-3.

Table 5-3: Average heart rates (bpm) from each session and their difference

	Experiment	*Control*	*Difference*	*St. Dev. of Diff.*
Rest	74	82	-8	10
Slow	112	110	3	9
Medium	135	128	7	11
Fast	168	160	8	8

It was found that average heart rates were higher during the experimental sessions than the control sessions at all workloads other than rest. However, paired T tests at a significance level of 0.05 support the hypothesis that the experimental and control heart rates at the slow and medium speeds come from distributions with equal means. At rest and at the fast walking speed this hypothesis can be rejected; therefore, the heart rates are

not statistically the same. This implies that the experimental session workload was only higher than its control counterpart at the fastest walking speed and this cannot be said for the slow or medium walking speeds.

5.3 Statistical Analysis

Statistical analysis was performed on several aspects of the quantitative data collected from the experimental and control sessions. The following sections explain the relationship between the metabolic workloads from the experimental and control sessions, the analysis of the energy expenditures relative to subject body mass, and the search for correlations between metabolic rates and various body parameters.

5.3.1 Correlations with Control Measurements

To determine the accuracy of the experimental system, the metabolic rates from each of the three sensors were correlated against the data obtained during the control sessions. The results of this investigation are displayed in Figure 5-7 through Figure 5-9. Each of these plots displays the equation of the best fit linear regression and the coefficient of determination (R^2) for this regression.

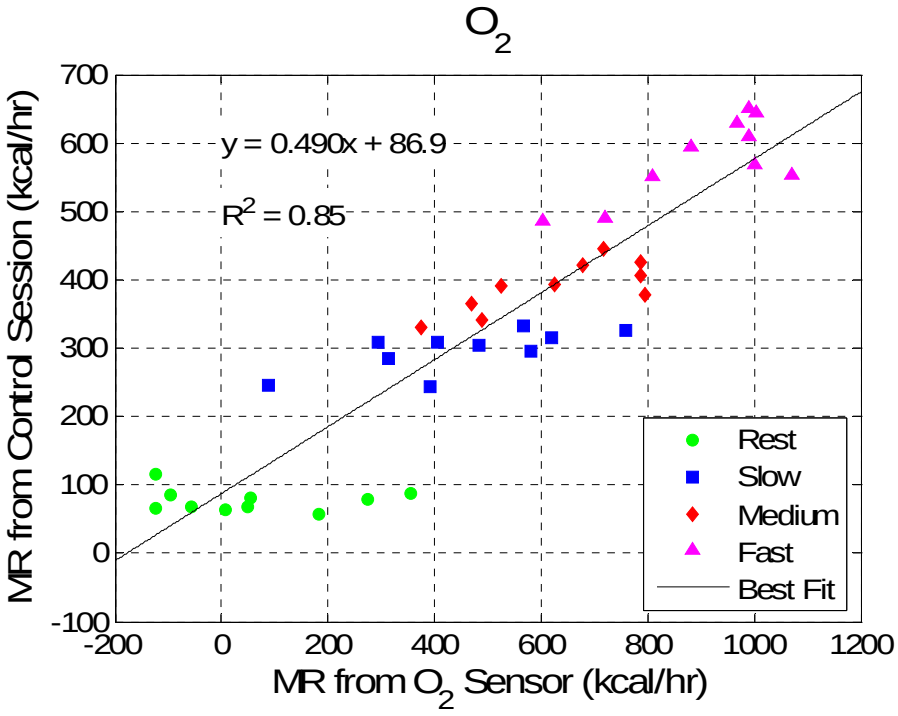

Figure 5-7: Metabolic rates calculated from O_2 sensor data correlated against control session measurements

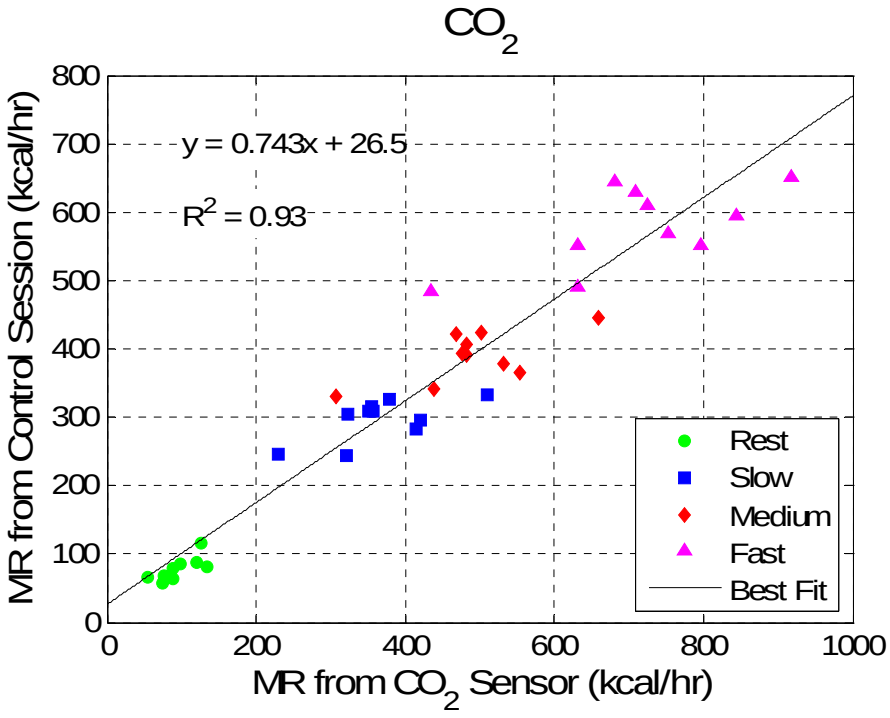

Figure 5-8: Metabolic rates calculated from CO_2 sensor data correlated against control session measurements

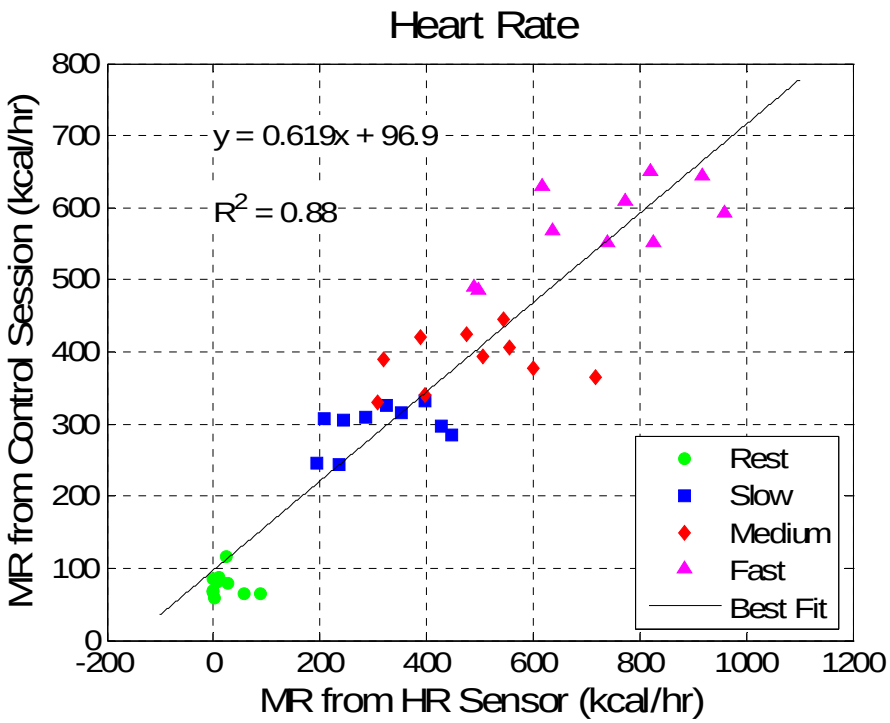

Figure 5-9: Metabolic rates calculated from heart rate sensor data correlated against control session measurements

The Pearson correlation coefficients (R) between the control metabolic workloads and those from the oxygen, carbon dioxide, and heart rate sensors are 0.92, 0.96, and 0.94, respectively. All three of these are statistically significant. This is a very encouraging result because it indicates that all three of these sensors could serve as predictors of metabolic workload.

The correlation of the carbon dioxide sensor data with the control data is the strongest of the three. Visual inspection of the correlation plots indicates that the carbon dioxide sensor data is a lot closer to the regression line than the oxygen sensor data at rest. As was shown in Figure 5-3, there is a lot of variability and even negative values in oxygen sensor data at rest. This is likely the reason that the correlation with control data

is not as strong with the oxygen sensor. The same is true with the heart rate sensor data, though to a lesser extent.

5.3.2 Relative Metabolic Workloads

Section 2.1.1 described the dependence of BMR and metabolic workload on body mass. A measurement of metabolic workload per unit body mass can eliminate this variable and allow the direct comparison of workloads among subjects. The metabolic rates computed from data during the experimental and control sessions were divided by the mass of the subject. The averages and standard deviations of these relative workloads across all 10 subjects can be found in Table 5-4.

The standard deviations indicate that the variability in the results from all three sensors is greater than in the control data. At rest, the variability in the carbon dioxide data is on par with that of the control data. It is the only one of the three sensors which has a standard deviation that is smaller than the mean. Since the metabolic workload should never be negative, this implies that the oxygen and heart rate sensor methods are not satisfactory at resting workloads.

Table 5-4: Averages and standard deviations of metabolic workload per unit body mass (kcal/hr/kg)

	O_2	*CO_2*	*Heart Rate*	*Control*
Rest	0.7 (2.4)	1.4 (0.3)	0.3 (0.5)	1.1 (0.2)
Slow	6.5 (2.6)	5.4 (1.0)	4.6 (1.5)	4.4 (0.3)
Medium	9.1 (2.1)	7.2 (1.2)	7.1 (2.2)	5.7 (0.5)
Fast	13.4 (2.7)	10.5 (2.2)	10.7 (2.5)	8.5 (1.1)

The averages for the three experimental sensors are higher than the control session averages in all cases except for the rest values from the oxygen and heart rate sensors at rest. This is in agreement with the observations in Section 5.2.3. However, it is possible that this assessment is not statistically significant.

T tests at a significance level of 0.05 were performed at each speed between the relative control workloads and relative workloads from each of the sensors to determine if they come from distributions with identical means. It was found that only the rest oxygen sensor data and the slow and medium heart rate sensor data share a mean with their control data counterparts. This implies that at all workloads the carbon dioxide sensor, which has thus far been shown to be the most reliable of the three methods, requires a calibration. This linear calibration is the regression line displayed in Figure 5-8, and is given in Equation 5-3 in units of kilocalories per hour.

$$MR = 0.743MR_{CO_2} + 26.5 \qquad \textbf{Equation 5-3}$$

5.3.3 Correlations with Body Parameters

In an attempt to find some meaningful trends, the metabolic workloads from the experimental and control sessions were correlated against body parameters including body mass, height, and body mass index (BMI). Pearson correlation coefficients (R) were found for each of these combinations. With a significance level of 0.05 and a sample size of 10, R needs to be greater than 0.632 to be considered significant.

Significant correlations with body mass were only found for the slow and medium speeds during the control sessions and at the resting workload for the carbon dioxide sensor data. Theoretically, some correlation is expected between body mass and metabolic workload and these results are slightly surprising. However, the sample size is not very large and the test conditions do include extraneous factors such as the experimental helmet assembly. Additionally, the increased variability of data during the experimental sessions, discussed in Section 5.3.2, can blur correlation calculations.

The correlation results with height are more encouraging. Significant correlations were found for the rest, and slow and medium speeds for both the carbon dioxide sensor data and the control session data. No significant correlations were found for either the oxygen sensor or the heart rate sensor at any workload. It is possible that correlations are stronger with height than weight because the headgear used during both sessions could affect the walking gait by forcing the subjects to maintain a stiff neck and back to maintain the stability of the headgear. This could affect the taller subjects more because the distance from their heads to their centers of gravity is greater and more static torque may be required to stabilize the helmets. The similar correlations between the carbon dioxide sensor data and the control session data with subject height do not shed light on the accuracy of the carbon dioxide sensor. However, similar behavior between these two methods of measuring the metabolic workload is another indication that, with the proper calibration, the carbon dioxide sensor may provide sensible estimates of energy expenditure.

BMI is a parameter used to assess weight relative to height and determine if an adult is overweight or underweight. BMI is the body mass (kg) divided by the square of the height (m) [34]. A BMI of less than 18.5 is considered underweight, 18.5-24.9 is normal weight, 25-29.9 is overweight, and 30 or greater is considered obese. BMI is related to percent of body fat. As mentioned in Section 2.1.1, the BMR and metabolic workload depend on fat-free body mass. However, no significant correlations were found between BMI and metabolic rate at any workload during any exercise session. The BMI values for the 10 subjects ranged from 20.8 to 26.8, with only two subjects falling into the overweight category.

5.4 Qualitative Results

Subjects were asked to complete a questionnaire about their medical history, exercise profile, and rated and qualitative response to the exercise sessions. The following sections explore the responses given and attempt to draw some meaningful information from them. The complete questionnaire can be found in Appendix B.5.

5.4.1 Experiment Response Ratings

The following questions were asked of the subjects after completing the exercise sessions.

1. *Was the experimental session strenuous?*
2. *Was the apparatus worn during the experimental session comfortable?*
3. *Did the apparatus worn during the experimental session make the work more strenuous?*
4. *Was the control session strenuous?*
5. *Was the apparatus worn during the control session comfortable?*
6. *Did the apparatus worn during the control session make the work more strenuous?*
7. *Was the workload during the experimental and control sessions similar?*
8. *Was the heart rate monitor comfortable?*
9. *Did the heart rate monitor make the work more strenuous?*

The responses to these questions are tabulated in Table 5-5. Subjects were asked to check one of five boxes in response to each question. A rating of 1 meant *not at all* and a rating of 5 meant *very*.

Table 5-5: Subject responses to questionnaire

Subject	*Q1*	*Q2*	*Q3*	*Q4*	*Q5*	*Q6*	*Q7*	*Q8*	*Q9*
F1	3	2	4	3	3	4	4	4	2
F3	2	2	4	2	3	1	4	5	1
F4	5	3	2	5	4	2	5	5	1
M1	2	3	1	3	2	3	4	4	1
M2	2	3	3	2	3	3	4	5	1
M3	4	2	3	3	4	2	3.5	5	1
M4	4	4	3	4	4	2	2	5	1
M6	3	2	1	1	1	1	5	5	1
M7	5	1	4	3	4	2	3	4	1
M8	3	3	4	4	4	4	4	4	2

There was no consensus on which session was more strenuous. According to the responses to questions 1 and 4, 5 subjects indicated that the sessions were the same, 3 said that the experimental session was more strenuous and 2 said that the control session was more strenuous. However, when asked if each apparatus made the work more strenuous in questions 3 and 6, 5 said both elevated the workload equally, 4 stated that the experimental helmet assembly hindered their workload more and only 1 said the opposite. When asked if the workload during the sessions was similar in question 7, the average response was a 3.9 with a standard deviation of 0.9. This indicates that subjects were leaning towards yes, but it is not unanimous.

In general, the experiment response portion of the subject questionnaire did not yield any unanimous opinion or conclusive response to the question of whether the workload during the experimental sessions was higher than during the control sessions. However, it should be noted that the control sessions were performed up to ten weeks after the experimental sessions. After the experimental sessions, subjects were asked to respond to the questions that apply and the complete the rest after the control sessions. This large lag time may have affected the subjects' relative memory of the experimental sessions.

5.4.2 Subject Comments

After the completion of each session, subjects were asked to write down or state any general comments they may have about the experiment and the workloads of each session. A complete list of subject comments can be found in Appendix D.1. Four subjects indicated that the experimental helmet assembly affected their workload because it rests on the shoulders and institutes a motion constraint. One subject complained that this headgear forced him to look down throughout the walking portion of the session and caused his glasses to slide off his nose. However, not all subjects chose to comment and it is possible that those who did not respond were the ones without complaints.

Breathing comfort was also mentioned. One subject mentioned being bothered by the very low humidity of the cascade air compared to ambient air. It is not clear whether this actually inhibited his performance. Another subject noted that the control session was more difficult because it takes more effort to breathe out directly into the hose rather than the open space of the experimental helmet assembly. Only one subject indicated anything to this effect.

In general, there is a slight tendency within the subjects to make comments that indicate the experimental session was more strenuous. However, it is nearly impossible to draw conclusive results from a few subject comments.

5.4.3 Subject Exercise Profiles

The subject questionnaire, found in Appendix B.5, included questions about the subjects' typical exercise routine. Table 5-6 lists the frequency and duration of weekly exercise as well as a list of the activities each subject participates in.

Table 5-6: Subject exercise profiles

Subject	*Exercise Frequency (per week)*	*Exercise Duration (min)*	*Fitness Score*	*Exercise Type*
F1	2 to 4	30-60	4	Running, swimming, biking, martial arts, climbing
F3	5 to 7	60-120	9	Swimming, running
F4	0 to 1	N/A	0	
M1	0 to 1	30-60	2	Swimming, running, lifting
M2	5 to 7	30-60	6	Running, swimming, soccer
M3	2 to 4	30-60	4	Racquetball, climbing
M4	2 to 4	<30	2	Jogging, sit-ups, push-ups
M6	5 to 7	<30	3	Biking
M7	2 to 4	<30	2	Biking, Frisbee
M8	2 to 4	30-60	4	Swimming, volleyball

In an attempt to quantify the fitness level of the subjects, a scoring system was developed. Point values were awarded for both frequency and duration of exercise according to the values set forth in Table 5-7. The fitness scores, listed in Table 5-6, are the products of the frequency and duration point values for each subject.

Table 5-7: Fitness score point system

Exercise Frequency (per week)	*Frequency Points*	*Exercise Duration (min)*	*Duration Points*
0 to 1	1	<30	1
2 to 4	2	30-60	2
5 to 7	3	60-120	3

The metabolic workloads per unit mass from the experimental and control sessions were correlated against the fitness scores. The relative workloads were used instead of the absolute to eliminate the variation due to body size and only look at the effects of physical fitness. With a significance level of 0.05 and a sample size of 10, the absolute value of the Pearson correlation coefficient (R) needs to be greater than 0.632 to be considered significant. Significant correlations were only found for the oxygen sensor at the slow and fast walking speeds and for the carbon dioxide sensor for all three walking speeds. No significant correlations were found for workloads from the heart rate sensor and the control sessions at any speed.

A correlation was expected because regular physical activity improves cardiovascular and respiratory function [34]. Trained athletes tend to have lower heart rates, ventilation rates, and oxygen uptakes at a given submaximal workload because their bodies can utilize the aerobic metabolism more efficiently. It was expected that more physically fit subjects will have lower relative workloads, as exhibited in the correlations of fitness with workloads from the carbon dioxide sensor. However, it was surprising that the same correlations were not present for the control sessions. It is possible that experimental helmet assembly required a higher level of adaptation of the walking gait that fit subjects were more capable of doing efficiently, but this is difficult to confirm.

There are several possible sources of error within this study. First of all, the exercise profile is self-reported by each subject. There may be a tendency to overestimate the amount of exercise performed regularly. It is also possible that some regular activities which require physical exertion were not reported. Examples of this could be long walks or lifting heavy objects outside the gym. Additionally, the scoring system placed on the exercise profiles attempts to quantify fitness for analysis. However, it does not capture the amount of exertion during the reported exercise periods and may not be a very accurate method.

5.5 System Characterization

Several tests were performed to characterize the behavior of the system as much as possible. The following section addresses the decision to assume a respiratory exchange ratio rather than calculating one. The measurement repeatability, sensor stability, and time step response are then explored.

5.5.1 Respiratory Exchange Ratio Measurements

The respiratory exchange ratio was calculated during each experimental session from the $\dot{V}CO_2$ and $\dot{V}O_2$, which were derived from data from the respective sensors. Typical results are plotted in Figure 5-10 and plots from all 10 subjects are included in Appendix D.4.

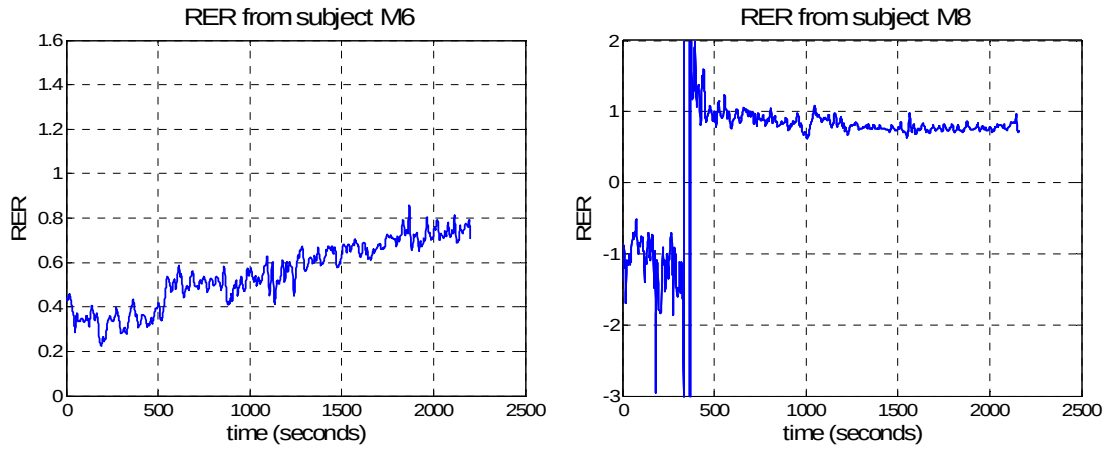

Figure 5-10: Sample RER plots from experimental session

As discussed in Section 2.1.4, RER should typically remain within the range of 0.7 to 1.0. Under conditions of prolonged strenuous activity, it can rise to slightly above 1.0 due to the buffering of lactic acid and hyperventilation. The results from the experimental sessions include respiratory exchange ratios significantly outside of this range. Subject M6 is an example where the RER was below the reasonably expected range throughout the first three quarters of the session. This implies that the $\dot{V}CO_2$ was lower than the $\dot{V}O_2$. Subject M8 had even more unreasonable RER values. Since the oxygen sensor measured a negative workload during the rest portion of this session, the RER is also negative. Not a single one of the 10 subjects had RER results that were reasonable throughout the entire exercise session. The likely culprit is the oxygen sensor,

particularly for the subjects with a negative metabolic workload during the rest period. In these instances the RER blew up near the $\dot{V}O_2$ crossover from negative to positive values.

For these reasons, the measured RER from the experimental sessions was not used for the calculation of $\dot{V}O_2$ from $\dot{V}CO_2$ or the caloric equivalent of oxygen. Instead, a value of 1.0 was assumed. This value is also assumed in the COSMED® K2 portable $\dot{V}O_2$ measurement system, a predecessor to the COSMED® K2b[4]. This instrument does not have a carbon dioxide sensor and assumes an RER of 1.0. A study was performed to test the accuracy of this system against a metabolic measurement cart in a laboratory and showed that it is accurate and precise at submaximal workloads [37]. However, the RER assumption in the K2 is only used to calculate the caloric equivalent of oxygen and not to calculate $\dot{V}O_2$ from $\dot{V}CO_2$. As explained in Section 5.6.4, the caloric equivalent of oxygen is less sensitive to RER.

This assumed value may appear high compared the RER data from the control sessions. However, the assumed RER is directly proportional to the metabolic workload calculated from the carbon dioxide sensor data. A different assumption would simply change the calibration equation but yield similar results in the end.

5.5.2 Repeatability

To test the repeatability, or the variation of measurements provided by this system, subject F3 was asked to perform the experimental protocol on five separate occasions. The results from these tests are listed in Table 5-8. Session 1 is the primary data collection experimental session for subject F3. It was performed in the morning.

Session 2 was performed 48 days later in the afternoon. The preliminary data from these two sessions showed a large discrepancy. Paired T-tests with a significance level of 0.05 showed that the values from all three sensors were statistically different. A more controlled repeatability study was then initiated. Sessions 3, 4, and 5 occurred on three consecutive mornings (beginning at 10:40, 9:20, and 9:50am). The ambient temperature was similar on all three days. To eliminate the effect on the energy expenditure due to the thermic effect of feeding, the subject was asked to fast for 12 hours prior to these experimental sessions.

Table 5-8: Results of repeatability study

Oxygen Sensor	*Session 1*	*Session 2*	*Session 3*	*Session 4*	*Session 5*
Rest	-118*	117	321	291	-42
Slow Walk	84	337	515	473	214
Medium Walk	369	480	478	491	464
Fast Walk	593	700	683	655	705
Carbon Dioxide Sensor	*Session 1*	*Session 2*	*Session 3*	*Session 4*	*Session 5*
Rest	52	85	72	73	73
Slow Walk	222	263	253	243	250
Medium Walk	302	381	346	362	341
Fast Walk	429	546	543	538	511
Heart Rate Sensor	*Session 1*	*Session 2*	*Session 3*	*Session 4*	*Session 5*
Rest	49	146	-7	-9	-18
Slow Walk	188	261	166	154	153
Medium Walk	304	337	267	269	271
Fast Walk	495	518	493	489	521
**all metabolic workload values are given in kcal/hr*					

Paired T-tests were performed on the results of every possible pair of the five sessions for each of the three sensors. The purpose of this is to test the hypothesis that the two matched (paired) samples come from distributions with equal means by analyzing the difference between each pair and the variance. Figure 5-11 shows the T-test results at a significance level of 0.05.

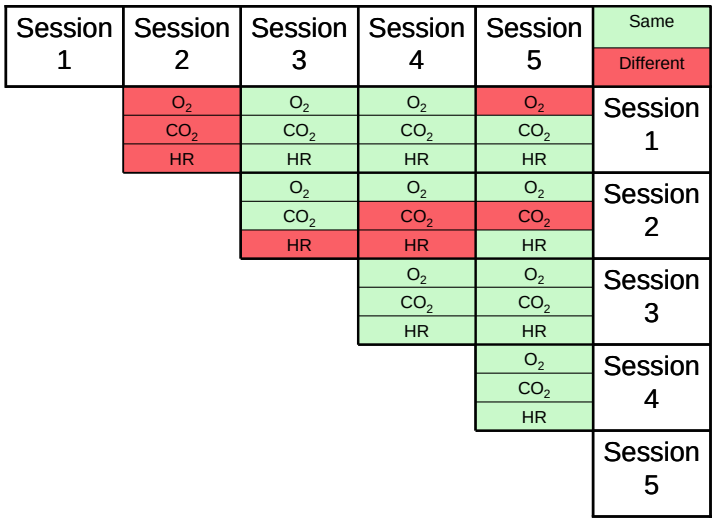

Figure 5-11: Between-session T-test results for all sensors

As mentioned previously, there was a statistically significant difference between the sessions 1 and 2. These two were performed at various times of day in various stages of food metabolism. Conversely, the paired T-tests performed on the highly controlled sessions, sessions 3, 4, and 5, for each of the three sensors showed that the results were statistically the same. The T-tests performed to compare sessions 1 and 2 to sessions 3, 4, and 5 show mixed results. The discrepancies found are not specific to one sensor.

Additional insight can be gained from a visual inspection of the repeatability data. Plots of data for each of the three sensors throughout the five sessions are displayed in Figure 5-12, Figure 5-13, and Figure 5-14.

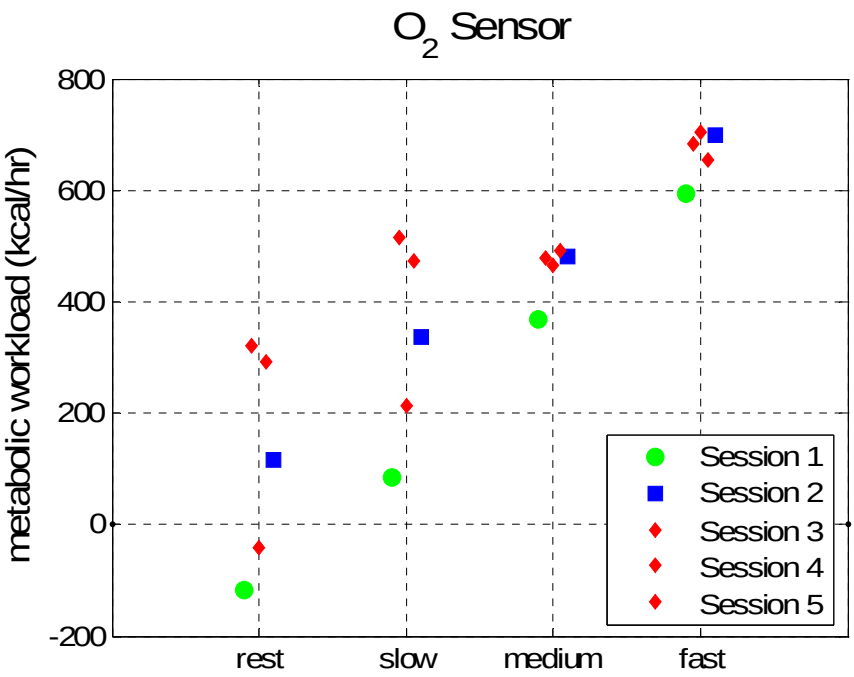

Figure 5-12: Plot of O_2 sensor data from repeatability study

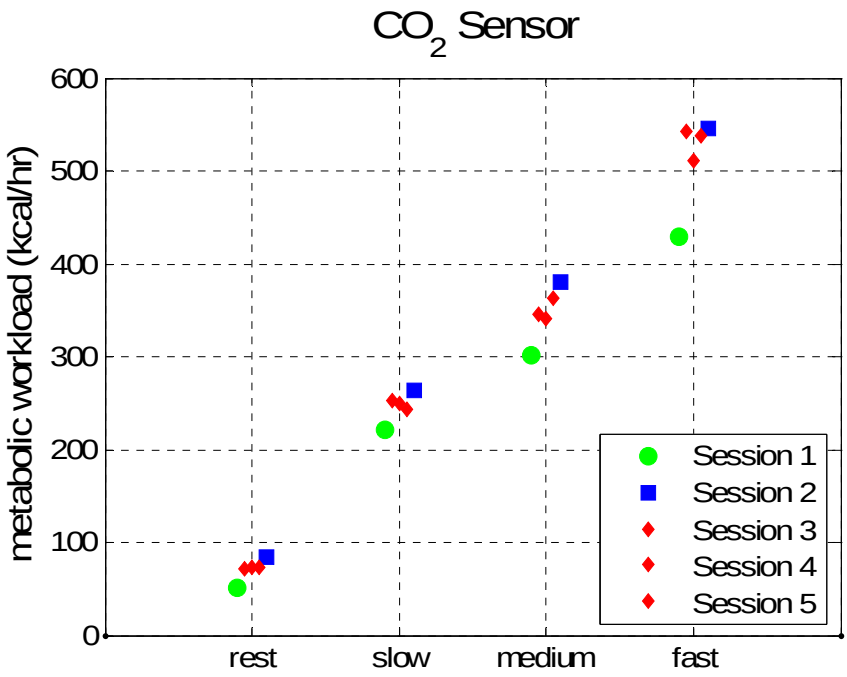

Figure 5-13: Plot of CO_2 sensor data from repeatability study

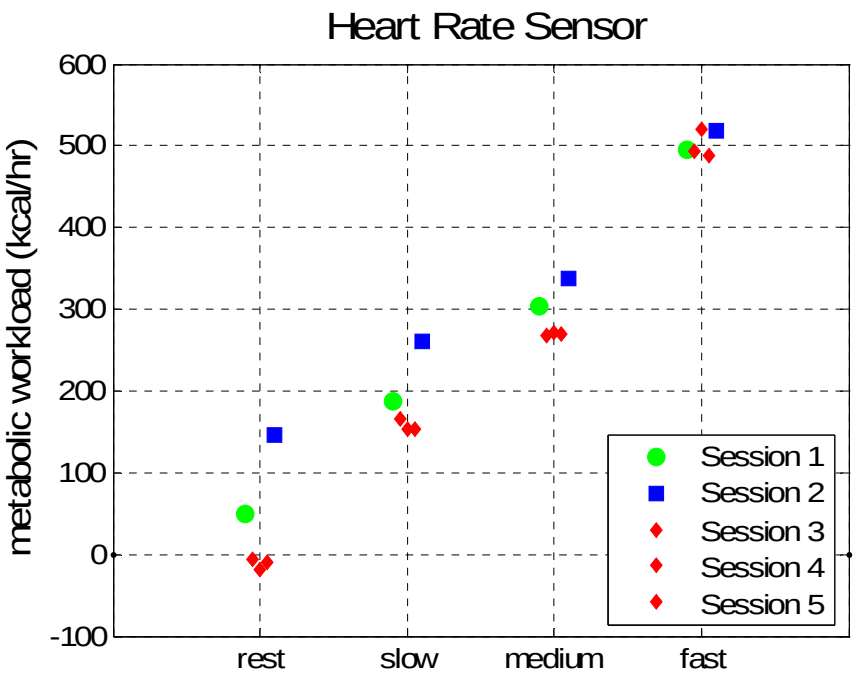

Figure 5-14: Plot of heart rate sensor data from repeatability study

Once again it is evident from the plots from the carbon dioxide and heart rate sensors in Figure 5-13 and Figure 5-14 that the results of sessions 3, 4, and 5 are much more constant than those from sessions 1 and 2. These findings lead to two results. It was found that the metabolic workload measurement system has good repeatability of its measurements when input conditions are replicated closely. However, some doubt has been cast over the conditions under which data was obtained during the experimental and control sessions, which did not control the time of the subject's most recent meal. The energy expenditure due to the thermic effect of feeding is a potential source of error between the experimental and control sessions.

Of the three sensors, the most variation is found in data from the oxygen sensor. This is determined from visual inspection of the oxygen sensor plot in Figure 5-12 compared to the remaining two sensors in Figure 5-13 and Figure 5-14. It is particularly

true during the rest and slow walk periods. Since $\dot{V}O_2$ and $\dot{V}CO_2$ are related by RER, a relatively constant value, the amount of variation should not differ much between the oxygen and carbon dioxide sensors. Furthermore, the similarity in the amount of variation in the data from the carbon dioxide and heart rate sensors indicates a problem with the reliability of the oxygen sensor.

5.5.3 Sensor Stability

To examine the stability of the two gas sensors, the experimental helmet assembly was bypassed as done for calibration and described in Section 4.3.2. Data was recorded at a rate of 10 Hz for a time period of 69.6 minutes. The results from this study are plotted in Figure 5-15 and Figure 5-16. The oxygen sensor displays behavior that appears to be sinusoidal, while the carbon dioxide sensor seems to be slowly drifting upwards. It is possible that these changes are a result of variation in the air rather than the sensor. However, this is unlikely because the sensors display different behaviors during the same data collection period.

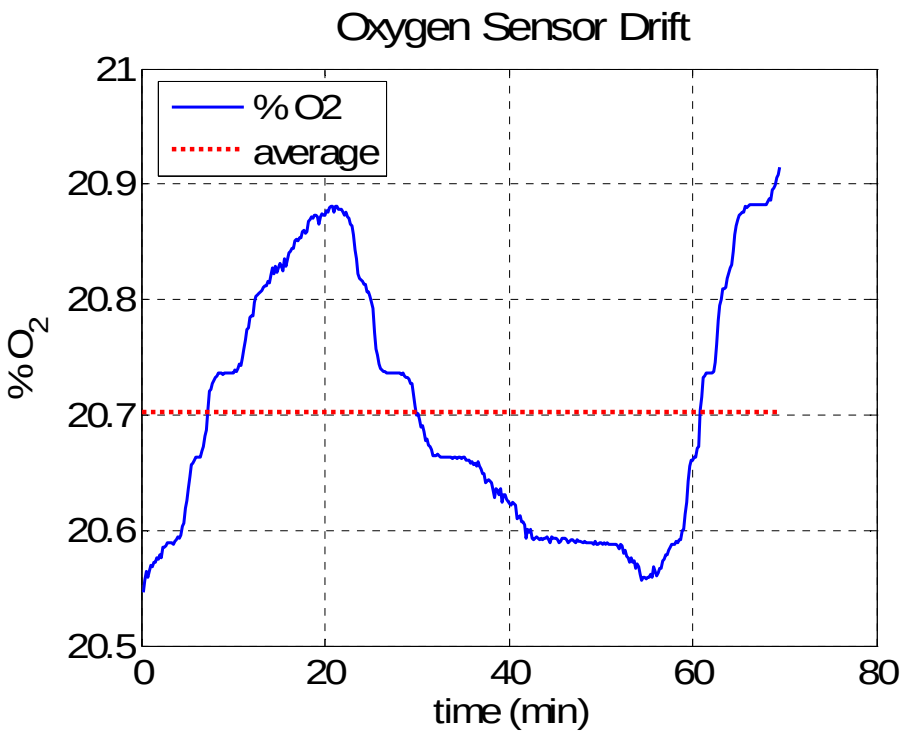

Figure 5-15: Oxygen sensor drift

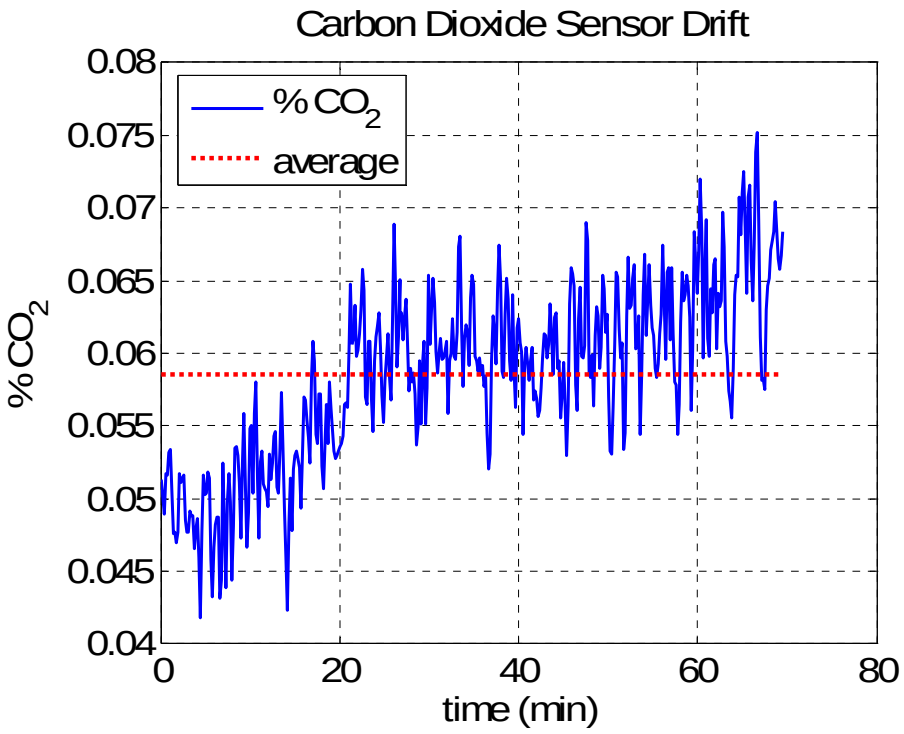

Figure 5-16: Carbon dioxide sensor drift

The magnitude of these changes is important to note. Throughout this time, the oxygen measurement varies by about 0.35% O_2. The carbon dioxide sensor measurement varies by only 0.02% CO_2. These changes translate to about 180 kcal/hr and 10 kcal/hr, respectively. The carbon dioxide sensor exhibits significantly more stability.

5.5.4 System Response Time

The lag time and step response time of the gas sensors are important to quantify for system characterization. A test was performed by bypassing the experimental helmet assembly as described in Section 4.3.2. A T-connection was installed in the system such that air could enter from two different sources. One was the cascade of air used during all testing and the other was a cylinder of nitrogen gas. Air was flown through the system at a flow rate of 170 L/min (6 scfm) for several minutes. Then, the cascade was closed and the nitrogen cylinder was opened at the same instant. The flow rate of nitrogen was unknown but the regulator was set to a pressure of 103 kPa (15 psi). The data collection rate was 10 Hz. The results from this test are plotted in Figure 5-17 and Figure 5-18. After the transition, the percentages of oxygen and carbon dioxide should theoretically be 0. However, small leaks in the system and the possible reverse flow of air from the outlet back to the gas sensors lead to small amounts of oxygen and carbon dioxide in this measurement.

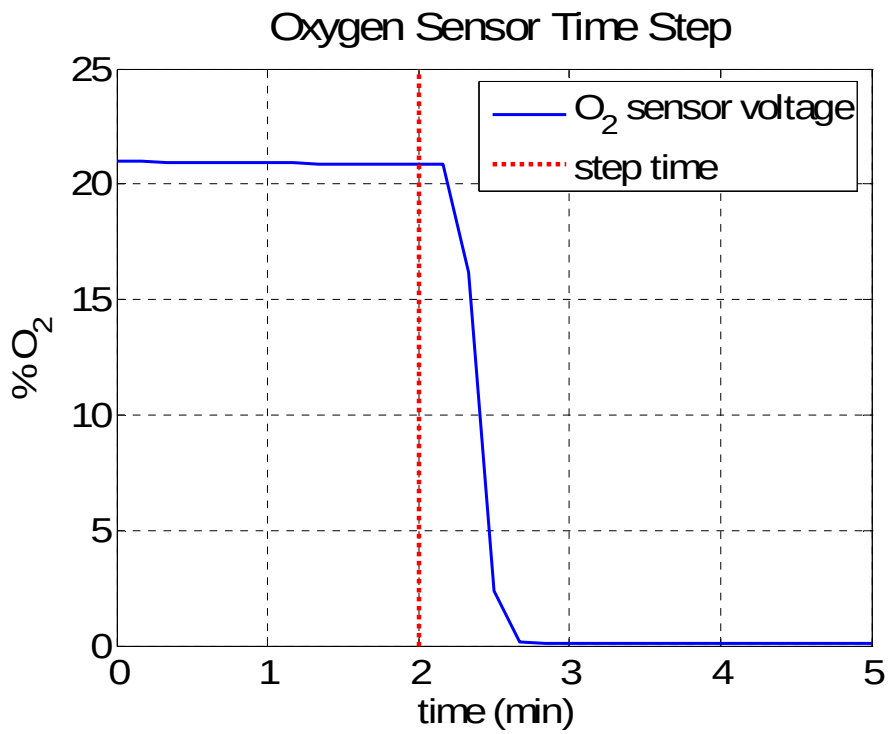

Figure 5-17: Oxygen sensor response time

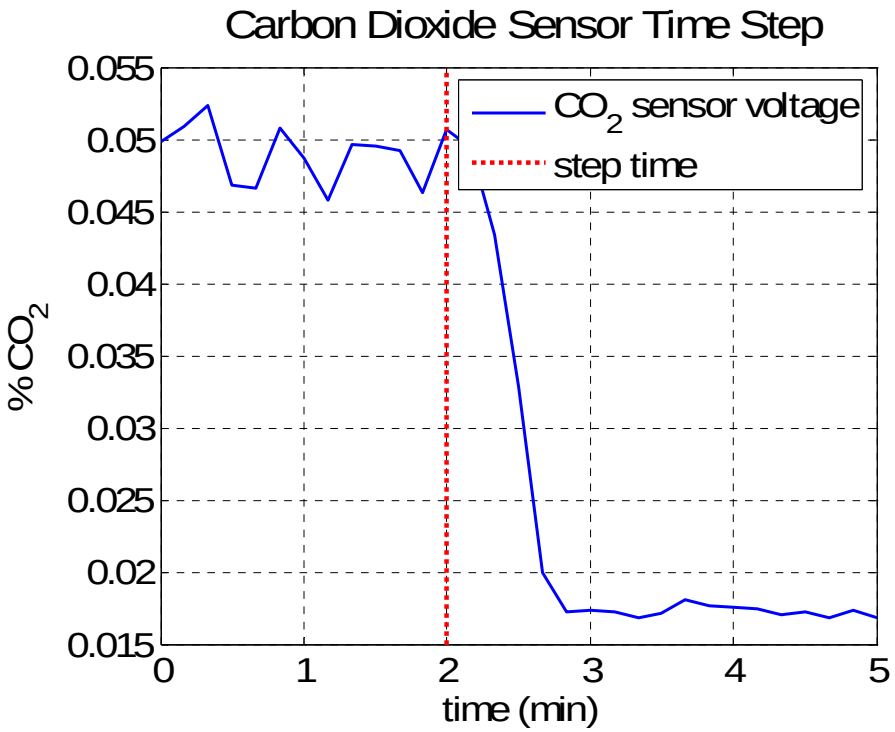

Figure 5-18: Carbon dioxide sensor response time

Both gas sensors exhibit a similar time response of about 10 seconds of lag before the sensor began to respond and a transition period of about 30 seconds. The lag time is the duration of the new gas traveling through the system to the sensors at the outlet. This depends on the lengths of air inlet and outlet hoses and is likely to change with the implementation into MX-2. The MX-2 umbilical is 15 m (50 ft) long and the experimental helmet assembly air outlet hose length is only 3 m (10 ft). This lag time may also be affected by some inaccuracy in turning the cascade air off and opening the nitrogen bottle because two people were required to complete these tasks at the same instant. However, the time difference during this operation was significantly lower than the 10 second time lag, perhaps about 1 second.

The transition time of about 30 seconds is acceptable for this application. The time constant, or the time to reach 63.2% of the final value, for $\dot{V}O_2$ at the onset of exercise is about 49 seconds [4]. The steady state $\dot{V}O_2$ after the onset or change in exercise intensity is typically reached within 1-4 minutes [1]. This implies that the sensor settling time is not dominating in the measurements obtained.

5.6 Error Analysis

The oxygen, carbon dioxide, and heart rate sensors have been shown to output some amount of error in their readings. This section takes a closer look at the possible sources of error and how they affect each of the sensor readings individually. The potential sources of error analyzed include: the pre- and post-session calibrations, relative humidity estimation, variability in flow rate, assumed respiratory exchange ratio,

published sensor accuracy, ambient temperature, treadmill calibration, and electromagnetic interference. Table 5-9 displays a summary of the error sources and a rating of how significantly each error affects each of the three sensors.

Table 5-9: Comparison of error sources at a glance

Error Source	*O_2 Sensor*	*CO_2 Sensor*	*Heart Rate Sensor*
Pre- and post-session calibration	**High**	Very low	None
Estimation of relative humidity	**Medium**	None	None
Variability of flow rate	Low	Low	None
Estimation of respiratory quotient	Low	**High**	Low
Published sensor accuracy	**High**	Low	None
Ambient temperature	None	Very low	None
Treadmill calibration	Low	Low	Low
Electromagnetic interference	None	None	Low

The sensitivity was rated as *high* if an expected or observed error can cause a change in the output equivalent to 100 kcal/hr or greater, *medium* if the effect can be 51-100 kcal/hr, *low* for an error of 11-50 kcal/hr, *very low* for 1-10 kcal/hr, and *none* if the sensor reading is not affected by the source of error.

The error sources fall into two possible categories: absolute or relative. Absolute errors are those from measurements of the oxygen or carbon dioxide in the air and are flat quantities regardless of the workload. Therefore, these errors account for a greater percentage error at lower workloads. For example, if a source of error translates to 10 kcal/hr, this is a 10% error at a workload of 100 kcal/hr, but only a 2% error at a workload of 500 kcal/hr. Conversely, relative errors are a certain percentage error and translate to a larger amount at higher workloads. For example, a relative error of 5% translates to 5 kcal/hr at a workload of 100 kcal/hr, but at a workload of 500 kcal/hr it translates to 25 kcal/hr. This distinction is the reason the possible errors are calculated in kilocalories per hour instead of percentages and given for the worst possible situation in Table 5-9.

In general, the oxygen sensor is most prone to errors. It has a high sensitivity to the pre- and post-session calibrations, the estimation of relative humidity, and the published accuracy is not very high for this application. The only very large source of error attributed to the carbon dioxide sensor is the estimation of respiratory quotient or respiratory exchange ratio. The heart rate sensor itself was not found to have a lot of considerable errors. However, as discussed in Section 2.2.4, heart rate has been shown to be an unreliable predictor of metabolic rate for various emotional and environmental reasons, even when measured very accurately.

The following sections delve into the details of the sensitivity analysis for each of the error sources and their effect on each of the three sensors.

5.6.1 Sensitivity to Calibration Errors

Calibration data with the experimental helmet assembly bypassed was collected prior to and following each experimental exercise session. There is a discrepancy between the averaged voltages from the before and after calibration for each subject for both the oxygen and carbon dioxide sensor. The voltage difference between each before and after calibration was translated into a workload quantity by following the equations described in Section 4.4. It was found that the variation in the before and after oxygen sensor calibration data converts to an average of 61 kcal/hr and the maximum value found was 195 kcal/hr for subject M1. For the carbon dioxide sensor, these errors amount to an average of only 3 kcal/hr and the maximum found was 10 kcal/hr for subject M7. The maximum values were the ones represented in Table 5-9 as *high* for the oxygen sensor and *very low* for the carbon dioxide sensor.

The errors from the calibrations are considered to be absolute errors. They are based on the measurement of the amount of oxygen or carbon dioxide in the air naturally without human respiration and do not depend on the workload. For this reason, they are more significant at low workloads.

This analysis shows that the carbon dioxide sensor provides a consistent reading of the carbon dioxide content in the cascade air and the sensor calibration and conversion of voltage data to metabolic workload do not yield high errors. Conversely, the oxygen sensor is very sensitive to the calibration process. There is a lot of variability in the sensor readings of ambient oxygen content, which implies that there may also be variability in the values during human respiration. A contributing factor is likely the fact that only a small portion of the sensor range is utilized for this application. The range of the sensor is 0–27% but the utilized range is only about 18-21% and the resolution within this diminished range is reduced.

The heart rate sensor does not require or even have the possibility of calibration and is not affected by this error source (*none* in Table 5-9).

5.6.2 Sensitivity to Relative Humidity

The relative humidity estimate only affects the oxygen gas sensor readings. The carbon dioxide sensor output does not significantly depend on the relative humidity and the heart rate sensor is completely independent of it (*none* in Table 5-9).

The percentage of oxygen in ambient air depends on the relative humidity. With a higher amount of water vapor, the same physical amount of oxygen constitutes a lower percentage. Since the relative humidity profile utilized was created from a few measurements and extrapolation, this assumption could lead to an unknown amount of

error. It was found that every 1% RH error translates to about 4.5 kcal/hr. Since the relative humidity measurements obtained vary by as much as 11% RH between subjects (6% RH from the mean) for a given workload and the profile was extrapolated for lower workloads, it is assumed that the error could be as much as 15% RH. This translates to about 70 kcal/hr and is rated as *medium* Table 5-9.

Like the calibration errors discussed in Section 5.6.1, relative humidity errors are absolute and do not vary with the workload. Therefore, the errors accumulated from this source are more significant at lower workloads.

5.6.3 Sensitivity to Flow Rate

The flow rate is directly proportional to the $\dot{V}O_2$ and $\dot{V}CO_2$, and therefore directly proportional to the calculated metabolic workload from these two sensors. The heart rate measurements are not affected by the flow rate (*none* in Table 5-9).

Throughout most of the sessions, the flow rate sensor showed a very gradual increase in flow rate throughout the exercise period, usually no more than 5.7 L/min (0.2 scfm) overall. The valves on the air system were not touched throughout the experiments so the physical amount of air flow should not have changed. This sensor has a 67% settling time of less then 10 seconds [31]. However, the residual settling may occur over a much greater period of time. The final flow rate value recorded was assumed to be the actual rate and was used in the calculations. Additionally, this sensor has an accuracy of +/- 2.8 L/min (+/- 0.1 scfm). At a flow rate of 169.9 L/min (6.0 scfm), a variation of 2.8 L/min (0.1 scfm) translates to 1.7 % error in the final metabolic workload value.

Errors in the flow rate reading are relative. They account for a certain percentage of error. A 1.7% error accounts for less than 2 kcal/hr at rest and for up to 20 kcal/hr at high workloads. In Table 5-9, this error source was rated as *low* for the gas sensors.

Flow rate errors can also be caused by a leak between the flow meter and the experimental helmet assembly. This would not be the fault of the sensor. However, the flow rate utilized in the calculations would be higher than actual and would lead to an elevated metabolic workload in both gas sensor calculations. Since the experimental helmet assembly is not designed to be airtight, the difference between the inlet and outlet flow rates would not yield useful information for quantifying this source of error. On occasion, a small leak was manually detected in a connection on the air inlet hose, but it was not quantified. Opening and reconnecting the joint mitigated this apparent problem each time.

5.6.4 Sensitivity to Respiratory Exchange Ratio Estimate

As mentioned in Section 5.5.1, the RER measurements did not yield good results and a value of 1.0 was assumed in lieu of measured data. The respiratory quotient has an effect on the metabolic rate measurements in two distinct ways. All three of the methods of measurement are a form of indirect calorimetry, in which the metabolic workload is estimated from $\dot{V}O_2$. As described in Section 2.2.2, the caloric equivalent of oxygen used to convert $\dot{V}O_2$ to metabolic workload depends on the RQ. It was found that a difference of 0.2 in RQ leads to 4% error in the caloric equivalent of oxygen and therefore 4% error in the calculated metabolic workload.

The RQ also has a greater impact on carbon dioxide measurements. It is used to directly convert $\dot{V}CO_2$ to $\dot{V}O_2$. Therefore, a difference of 0.2 between the assumed and actual RQ translates into 20% error.

Both of these errors are relative errors. They account for a greater amount of error at higher workloads. A 4% error in the caloric equivalent of oxygen translates to about 3 kcal/hour at rest and up to 40 kcal/hr at a high workload for a heavy person. The 20% error in the conversion from $\dot{V}CO_2$ to $\dot{V}O_2$ can lead to about 15 kcal/hour error at low workloads and up to 200 kcal/hr for a large subject at the highest walking speed. For these reasons, the significance of errors in RQ estimation has been rated *low* for the oxygen and heart rate sensors and *high* for the carbon dioxide sensor, as listed in Table 5-9.

5.6.5 Sensitivity to Published Sensor Accuracy and Resolution

The oxygen gas sensor is listed to have an accuracy of +/- 1% volume of oxygen [26]. This is not a high accuracy considering that the range used in this application is only about 18%-21% oxygen. This is possibly the reason for the unpredictably varying $\dot{V}O_2$ values compared to $\dot{V}CO_2$. An error of 1% volume of oxygen translates to an absolute error of about 500 kcal/hr at any workload. The published accuracy of the oxygen sensor is rated as a *high* error source in Table 5-9.

The carbon dioxide sensor has a published accuracy of 1.5% of the full range plus 2% of the reading [27]. The range is 0%-3%. This error is both absolute and relative because it has a portion that does not depend on the workload and a portion that does. The absolute portion of the error is significantly larger. This error source translates to

about 25 kcal/hr at rest and about 35 kcal/hr at the fast walking speed. It was classified as *low* in Table 5-9.

The heart rate monitor does not have a published accuracy. Though it has an analog output voltage, it is essentially a digital signal because it only has two distinct narrow ranges. The sensor has a constant low voltage output and switches to a significantly higher voltage for a few hundredths of a second when a heart beat occurs. As long as the receiver is within range of the transmitter, no errors are generated and the rating for this sensor is *none* in Table 5-9.

5.6.6 Sensitivity to Ambient Temperature

Only the carbon dioxide sensor is affected by temperature. The oxygen and heart rate sensors do not depend on ambient temperature and are rated as *none* for this category in Table 5-9. The air temperature was not measured throughout all of the experimental sessions. The Onset HOBO® H08 data logger used to measure the relative humidity also recorded temperature for four of the subjects. It was found that the temperature stays within 2°C of 25°C, which is the temperature the carbon dioxide sensor is calibrated for. The sensor temperature dependence is -0.1% of full scale per 1°C [27]. A temperature difference of 2°C translates into only 3 kcal/hr, therefore, this error source was rated *very low* in Table 5-9 for the carbon dioxide sensor. Since the error depends on the full scale instead of the actual reading, it is an absolute error, which is more significant at lower workloads.

5.6.7 Sensitivity to Treadmill Calibration

A calibration check was performed on treadmills 1 and 3 used in the experimental sessions. The belt length of each treadmill was measured by placing three marks in various positions and summing the distances between them. The treadmills were then set to each of the three speeds and the passing of a mark on the belt was counted during a 1-minute interval while a person was walking. The results are listed in Table 5-10. No calibration was performed on treadmill 1 at the fast speed or the treadmill used during the control sessions.

Table 5-10: Treadmill calibration results

Treadmill 1			*Treadmill 3*		
Intended Speed	*Measured Speed*	*Difference*	*Intended Speed*	*Measured Speed*	*Difference*
3.0 mph	3.002 mph	0.07%	3.0 mph	3.093 mph	3.1%
3.7 mph	3.752 mph	1.4%	3.7 mph	3.839 mph	3.8%
4.4 mph	-	-	4.4 mph	4.479 mph	1.8%

All measured speeds were slightly above those intended by up to 3.8%. This may be an artifact of an imperfect measuring method. However, since two different treadmills were used during the experimental sessions and a third was used during the control sessions, it is worthwhile to explore the sensitivity to speed variation between treadmills. The Pandolf model [35] applied to subject F3 was used to determine the effect of speed variation on metabolic workload. When the slow, medium, and fast speeds are each increased by 0.1 mph, the workload increases by 10 kcal/hr (4.4 %), 12 kcal/hr (4.1 %), and 14 kcal/hr (3.7 %), respectively. This source of error does not fall into either the relative or absolute categories of error because both the absolute workload differences and the percentages of error vary with workload.

Treadmill calibration affects the metabolic workload itself and therefore the measurements from all three sensors are affected equally. This error is rated *low* in Table 5-9.

5.6.8 Electromagnetic Interference

The heart rate sensor is unaffected by most error sources which degrade the data obtained from the two gas sensors. Electromagnetic interference does create some spikes in the raw voltage data which could be read as heart beats and elevate the heart rate. The inclusion of an additional heart beat in a 15 second time segment results in a relative error of about 3%. This can translate to over 30 kcal/hr at high workloads and was rated as a *low* source of error in Table 5-9. Fortunately, the duration of these voltage spikes is shorter than that of heart beats and they can be easily filtered out with software and some manual data cleaning. The addition or omission of a single heart beat is easily recognizable in a plot of the data and is always corrected.

However, as mentioned in Section 2.2.4, heart rate has been shown to be an unreliable predictor of metabolic rate for various emotional and environmental reasons, even when measured very accurately. Additional error is caused by the use of standardized equations for $\dot{V}O_2$ as a function of heart rate, rather than personal laboratory calibrations for each subject.

Electromagnetic interference does not affect the measurements from the two gas sensors and this is reflected in Table 5-9 with ratings of *none.*

Chapter 6 : CONCLUSIONS AND FUTURE RESEARCH

The final chapter of this thesis contains a summary of the research that has been performed, the conclusions that have been drawn, and a recommendation for the metabolic workload measurement system to be implemented into the MX-2 neutral buoyancy space suit analogue. Finally, a few suggestions for future testing and system improvements are outlined.

6.1 Conclusions

In an attempt to develop a metabolic workload measurement system for the MX-2, a neutral buoyancy space suit analogue developed by the University of Maryland Space Systems Laboratory, three independent indirect calorimetry methods were tested. The energy expenditure was calculated from oxygen consumption via the caloric equivalent of oxygen. Oxygen consumption was computed from measurements of flow rate and those from an oxygen sensor and a carbon dioxide sensor located at the air outlet of the space suit and also from heart rate measurements with standardized equations. All three methods were implemented into a space suit simulation system, which included an isolated experimental helmet assembly that allowed subjects to breathe in an enclosed environment similar to the MX-2 but retain full mobility below the neck. This system was validated against the Viasys Healthcare Oxycon Pro®, a commercially available metabolic measurement system used by exercise physiologists. 10 subjects completed two exercise sessions each: an experimental session and a control session. The protocol for each session was an 8-minute sitting rest period followed by 30 minutes of continuous

walking on a treadmill, which included three 10-minute periods at progressively faster speeds. The experimental sessions were performed with the experimental helmet assembly and control sessions were performed with the Oxycon Pro®. For each subject, three metabolic workloads were calculated from the experimental session data and one was calculated from data obtained during the control session. These results, along with subject heart rates and verbal and written feedback, were analyzed statistically, graphically, and qualitatively.

6.1.1 System Performance

Results indicate that the carbon dioxide sensor method is the best of the three. This sensor was found to have the least chatter of the three, a level comparable to the control system. It was the most reliable at rest and low workloads. The oxygen sensor indicated some negative metabolic workloads, which is physically impossible, and the heart rate sensor method indicated some workloads too close to zero to be plausible. At rest, the carbon dioxide sensor supplied data which was closest to the control data. Pearson correlation coefficients were found between the control results and the results from each of the three sensors. It was found that the carbon dioxide sensor data had strongest correlation with the control data ($R = 0.96$). Metabolic rate results were also correlated against subject body parameters. Significant correlations were only found for the carbon dioxide sensor and the control sessions with height. A possible reason for this correlation is the fact that the additional load on the head was further from the center of gravity of taller subjects and more difficult to stabilize. However, it is another example of the carbon dioxide sensor displaying behavior similar to the control system and unlike either the oxygen or the heart rate sensors.

A few tests were performed to better characterize the system. A repeatability study was carried out, which included a single subject executing the experimental session protocol on five separate occasions. While all three sensor methods demonstrated repeatability, the metabolic rate values from the carbon dioxide sensor were the most consistent. When the gas sensors were left to collect data for over an hour to quantify the amount of drift, the carbon dioxide sensor performed significantly better than the oxygen sensor. Both of these sensors have a similar response time to a step input, which has been determined to be acceptable for this application.

Finally, an error analysis was performed on all three experimental methods to determine the sensitivity of each sensor to various parameters and how it may impact the final results. The oxygen sensor method was found to have three very significant sources of error: calibration, accurate knowledge of relative humidity, and the published sensor accuracy. The heart rate sensor is not very prone to error due to various outside factors. However, heart rate has been shown to be an unreliable predictor of metabolic workload due to various environmental and psychological issues. The carbon dioxide was shown to have only one significant source of error: the estimation of respiratory exchange ratio. While it would be ideal to measure this parameter, assumptions have been previously used in commercially available products and studies have shown these to be sufficient.

6.1.2 Recommendations for MX-2

It is recommended that the carbon dioxide sensor method be implemented into the MX-2 neutral buoyancy space suit analogue. Additionally, the heart rate sensor can be implemented to monitor heart rate. However, it should not be used to calculate the metabolic workload.

Though the intention of this experiment design was for the experimental and control sessions to be identical and require the same amount of workload, there were some differences between the headgear worn during both sessions and the environments they were performed in. Several types of results were analyzed to determine whether sessions were identical. The heart rates obtained during the experimental sessions appeared to be higher than those from the control sessions; however, T tests showed that they were only statistically different at the fastest walking speed. The metabolic workloads relative to body weight (for direct comparison among subjects) from each of the three sensors were compared to those from the control sessions. T test analysis found that the carbon dioxide sensor values were higher than their control session counterparts at each of the four workloads. This indicates the need for a calibration for this system. Such a linear calibration was found to have slope of 0.743 and an intercept of 26.5 kcal/hr.

Metabolic rate and heart rate information should be displayed in real time during MX-2 operations as well as stored for future analysis. This implies that calibration information taken after each session cannot be utilized in the metabolic workload calculation. For this reason, it should be assumed that the amount of carbon dioxide found in the cascade air without human respiration is 0.05%. This is the mean from calibrations taken before and after each exercise session. The effect of the calibration of the carbon dioxide sensor on the metabolic workload results has been found to be very low compared to other errors.

The recommended method for calculating the metabolic workload from the raw voltage from the carbon dioxide sensor is displayed in Equation 6-1. This equation

incorporates the calculations performed during the study with the calibration equation that was developed as a result of this research. In this equation, *V* is the raw carbon dioxide sensor voltage, *flow* is the air flow rate (L/min), and *RER* is the respiratory exchange ratio. The calibration was developed for the assumption that RER is 1.0 and this value should be used in this formula. It is best to include real time values for flow rate in this equation. However, if this is not possible, a value of 170 L/min (6 scfm) can be used if the flow is carefully monitored and adjusted manually to be kept at this value.

$$MR = 0.743\left[\frac{60\,flow(0.6V - 0.05)}{100RER}\right](3.9 + 1.1RER) + 26.5 \qquad \textbf{Equation 6-1}$$

To display the heart rate in real time, a change in algorithm will be necessary. A simple approach is to count the number of heart beats in the past 15 seconds and multiply this number by a factor of 4. However, for more accurate results, the time intervals between heart beats should be considered. For example, the heart rate can be calculated from the duration of the last 10 heart beat intervals. This method looks at irregular sample times depending on the workload. Another option is to calculate the heart rate from the time interval between the last two heart beats; however, this has been shown to be a noisy approach. Any of these options are viable depending on what is most desired: simplicity, low noise, or accuracy.

6.2 Future Research

Many approaches can be taken in the continuation of this research. A few are discussed in the following sections. The first issue touched on is the replacement of the electrochemical oxygen sensor with one that is more accurate and precise. The topic of implementing a direct calorimetry metabolic workload measurement system into the LCG

is then overviewed. Finally, a suggestion for final validation testing after implementation into the MX-2 neutral buoyancy space suit analogue is made.

6.2.1 Oxygen Sensor Replacement

The electrochemical oxygen sensor utilized in this experiment was not accurate or precise enough for this application. Though the carbon dioxide sensor method was recommended for implementation into the MX-2, a capable oxygen sensor would be beneficial in the long run. The knowledge of the concentration of oxygen would be instrumental in reducing error by removing the need for assumptions when calculating $\dot{V}O_2$ from $\dot{V}CO_2$ and the caloric equivalent of oxygen.

A paramagnetic oxygen sensor is recommended for this application. This is the type of oxygen sensor used in the Oxycon Pro®. This sensor type takes advantage of the paramagnetic behavior of oxygen [38]. A small glass dumbbell is suspended inside a nitrogen-filled cylindrical container. Oxygen molecules are attracted to the magnetic field and this causes a displacement of the dumbbell. The applied current necessary to restore the position of the dumbbell is directly proportional to the partial pressure of oxygen in the gas sample.

These sensors are generally very accurate, except for trace concentrations of oxygen. The percentages of oxygen in this application are about 16-21% and are not near trace concentrations. Paramagnetic oxygen sensors are also very delicate and sensitive to vibration and should only be used in a fixed testing environment, which is the case in the MX-2 metabolic workload measurement system. However, the largest disadvantage of this sensor is the price as it tends to be significantly above the price of the electrochemical sensors. [38]

6.2.2 Direct Calorimetry Measurements with the LCG

It may be beneficial to implement another redundant and completely independent method of metabolic workload measurement into the MX-2 system. This can be achieved by direct calorimetry. The measurement of LCG inlet and outlet water temperatures and flow rate through it could provide sufficient data to estimate metabolic rate by measuring the amount of heat carried away by the LCG. This method would be completely unobtrusive since a LCG is already worn by the suit subjects. However, the heat exchange with the environment through the wall of the MX-2 would have to be estimated or ignored. Additionally, any LCG leaks inside the suit would reduce the actual flow rate and cause an overestimation of metabolic workload. Nevertheless, this is a worthwhile endeavor for redundancy and calibration.

6.2.3 Simultaneous Experimental and Control Testing

A method of final verification of this system is a simultaneous workload measurement with the carbon dioxide sensor method implemented into the MX-2 and a portable system. A portable cardiopulmonary exercise system, such as the COSMED® $K4b^2$, can easily fit inside the large interior volume of the MX-2. It includes an oronasal mask with one-way valves, similar to that of the Oxycon Pro®. Air from inside the suit would be inhaled and exhaled, measured with the portable system, released into the volume of the suit, and finally exit through the air outlet hose past the gas sensor located at the exit. It can also be used in conjunction with the LCG direct calorimetry metabolic measurement method. The benefit of this test is the direct comparison of metabolic workloads without the need for standardizing conditions and repeating simulations. The difference between the two measurements is the error of the experimental system only

and does not include physiological, environmental and hardware differences between two different sessions. Unfortunately, the drawback to this method and the reason it wasn't utilized during this study is the staggering cost of the COSMED® $K4b^2$ or similar systems.

Appendix A : COMPONENT SPECIFICATIONS

A.1 Data Acquisition Module

Low-Cost Multifunction DAQ for USB

NI USB-6008, NI USB-6009

- Small and portable
- 12 or 14-bit input resolution, at up to 48 kS/s
- Built-in, removable connectors for easier and more cost-effective connectivity
- 2 true DAC analog outputs for accurate output signals
- 12 digital I/O lines (TTL/LVTTL/CMOS)
- 32-bit event counter
- Student kits available
- OEM versions available

Operating Systems
- Windows 2000/XP
- Mac OS X[1]
- Linux®[1]
- Pocket PC
- Win CE

Recommended Software
- LabVIEW
- LabWindows/CVI

Measurement Services Software (included)
- NI-DAQmx
- Ready-to-run data logger

[1]Mac OS X and Linux users need to download NI-DAQmx Base.

Product	Bus	Analog Inputs[1]	Input Resolution (bits)	Max Sampling Rate (kS/s)	Input Range (V)	Analog Outputs	Output Resolution (bits)	Output Rate (Hz)	Output Range (V)	Digital I/O Lines	32-Bit Counter	Trigger
USB-6009	USB	8 SE/4 DI	14	48	±1 to ±20	2	12	150	0 to 5	12	1	Digital
USB-6008	USB	8 SE/4 DI	12	10	±1 to ±20	2	12	150	0 to 5	12	1	Digital

[1]SE = single-ended, DI = differential

Hardware Description

The National Instruments USB-6008 and USB-6009 multifunction data acquisition (DAQ) modules provide reliable data acquisition at a low price. With plug-and-play USB connectivity, these modules are simple enough for quick measurements but versatile enough for more complex measurement applications.

Software Description

The NI USB-6008 and USB-6009 use NI-DAQmx high-performance, multithreaded driver software for interactive configuration and data acquisition on Windows OSs. All NI data acquisition devices shipped with NI-DAQmx also include VI Logger Lite, a configuration-based data-logging software package.

Mac OS X and Linux users can download NI-DAQmx Base, a multiplatform driver with a limited NI-DAQmx programming interface. You can use NI-DAQmx Base to develop customized data acquisition applications with National Instruments LabVIEW or C-based development environments. NI-DAQmx Base includes a ready-to-run data logger application that acquires and logs up to eight channels of analog data.

PDA users can download NI-DAQmx Base for Pocket PC and Win CE to develop customized handheld data acquisition applications.

Recommended Accessories

The USB-6008 and USB-6009 have removable screw terminals for easy signal connectivity. For extra flexibility when handling multiple wiring configurations, NI offers the USB-6008/09 Accessory Kit, which includes two extra sets of screw terminals, extra labels, and a screwdriver.

In addition, the USB-6008/09 Prototyping Accessory provides space for adding more circuitry to the inputs of the USB-6008 or USB-6009.

Common Applications

The USB-6008 and USB-6009 are ideal for a number of applications where economy, small size, and simplicity are essential, such as:
- Data logging – Log environmental or voltage data quickly and easily.
- Academic lab use – The low price facilitates student ownership of DAQ hardware for completely interactive lab-based courses. (Academic pricing available. Visit ni.com/academic for details.)
- Embedded OEM applications.

NATIONAL INSTRUMENTS

Information for Student Ownership

To supplement simulation, measurement, and automation theory courses with practical experiments, NI has developed the USB-6008 and USB-6009 student kits, which include the LabVIEW Student Edition and a ready-to-run data logger application. These kits are exclusively for students, giving them a powerful, low-cost hands-on learning tool. Visit ni.com/academic for more details.

Information for OEM Customers

For information on special configurations and pricing, call (800) 813 3693 (U.S. only) or visit ni.com/oem. Go to the Ordering Information section for part numbers.

Ordering Information

NI USB-6008[1]	779051-01
NI USB-6009[1]	779026-01
NI USB-6008 OEM	193132-02
NI USB-6009 OEM	193132-01
NI USB-6008 Student Kit[1,2]	779320-22
NI USB-6009 Student Kit[1,2]	779321-22

[1] Includes NI-DAQmx software, NI ready-to-run data logger software, and a USB cable.

[2] Includes LabVIEW Student Edition.

BUY NOW!

For complete product specifications, pricing, and accessory information, call 800 265 9891 (U.S. only) or go to ni.com/usb.

Specifications

Typical at 25 °C unless otherwise noted.

Analog Input

Absolute accuracy, single-ended

Range	Typical at 25 °C (mV)	Maximum (0 to 55 °C) (mV)
±10	14.7	138

Absolute accuracy at full scale, differential[1]

Range	Typical at 25 °C (mV)	Maximum (0 to 55 °C) (mV)
±20	14.7	138
±10	7.73	84.8
±5	4.28	58.4
±4	3.59	53.1
±2.5	2.56	45.1
±2	2.21	42.5
±1.25	1.70	38.9
±1	1.53	37.5

Number of channels ..... 8 single-ended/4 differential
Type of ADC ..... Successive approximation

ADC resolution (bits)

Module	Differential	Single-Ended
USB-6008	12	11
USB-6009	14	13

Maximum sampling rate (system dependent)

Module	Maximum Sampling Rate (kS/s)
USB-6008	10
USB-6009	48

Input range, single-ended ..... ±10 V
Input range, differential ..... ±20, ±10, ±5, ±4, ±2.5, ±2, ±1.25, ±1 V
Maximum working voltage ..... ±10 V
Overvoltage protection ..... ±35 V
FIFO buffer size ..... 512 B
Timing resolution ..... 41.67 ns (24 MHz timebase)
Timing accuracy ..... 100 ppm of actual sample rate
Input impedance ..... 144 k
Trigger source ..... Software or external digital trigger
System noise ..... 0.3 LSB_{rms} (±10 V range)

Analog Output

Absolute accuracy (no load) ..... 7 mV typical, 36.4 mV maximum at full scale
Number of channels 2
Type of DAC ..... Successive approximation
DAC resolution ..... 12 bits
Maximum update rate ..... 150 Hz, software-timed
Output range ..... 0 to +5 V
Output impedance ..... 50 Ω
Output current drive ..... 5 mA
Power-on state ..... 0 V
Slew rate ..... 1 V/µs
Short-circuit current ..... 50 mA

Digital I/O

Number of channels ..... 12 total
8 (P0.<0..7>)
4 (P1.<0..3>)
Direction control ..... Each channel individually programmable as input or output
Output driver type
USB-6008 ..... Open-drain
USB-6009 ..... Each channel individually programmable as push-pull or open-drain
Compatibility ..... CMOS, TTL, LVTTL
Internal pull-up resistor ..... 4.7 kΩ to +5 V
Power-on state ..... Input (high impedance)
Absolute maximum voltage range ..... -0.5 to +5.8 V

Digital logic levels

Level	Min	Max	Units
Input low voltage	-0.3	0.8	V
Input high voltage	2.0	5.8	V
Input leakage current	–	50	µA
Output low voltage (I = 8.5 mA)	–	0.8	V
Output high voltage (push-pull, I = -8.5 mA)	2.0	3.5	V
Output high voltage (open-drain, I = -0.6 mA, nominal)	2.0	5.0	V
Output high voltage (open-drain, I = -8.5 mA, with external pull-up resistor)	2.0	–	V

Counter

Number of counters 1
Resolution ..... 32 bits
Counter measurements ..... Edge counting (falling edge)
Pull-up resistor ..... 4.7 kΩ to 5 V
Maximum input frequency ..... 5 MHz
Minimum high pulse width ..... 100 ns
Minimum low pulse width ..... 100 ns
Input high voltage ..... 2.0 V
Input low voltage ..... 0.8 V

Power available at I/O connector

+5 V output (200 mA maximum) ..... +5 V typical
+4.85 V minimum
+2.5 V output (1 mA maximum) ..... +2.5 V typical
+2.5 V output accuracy ..... 0.25% max
Voltage reference temperature drift ..... 50 ppm/°C max

[1]Input voltages may not exceed the working voltage range.

Physical Characteristics

If you need to clean the module, wipe it with a dry towel.

Dimensions (without connectors)	6.35 by 8.51 by 2.31 cm (2.50 by 3.35 by 0.91 in.)
Dimensions (with connectors)	8.18 by 8.51 by 2.31 cm (3.22 by 3.35 by 0.91 in.)
Weight (without connectors)	59 g (2.1 oz)
Weight (with connectors)	84 g (3 oz)
I/O connectors	USB series B receptacle (2) 16-position (screw-terminal) plug headers
Screw-terminal wiring	16 to 28 AWG
Screw-terminal torque	0.22 to 0.25 N•m (2.0 to 2.2 lb•in.)

Power Requirement

USB (4.10 to 5.25 VDC)	80 mA typical 500 mA maximum
USB suspend	300 µA typical 500 µA maximum

Environmental

The USB-6008 and USB-6009 are intended for indoor use only.

Operating environment	
Ambient temperature range	0 to 55 °C (tested in accordance with IEC-60068-2-1 and IEC-60068-2-2)
Relative humidity range	10 to 90%, noncondensing (tested in accordance with IEC-60068-2-56)
Storage environment	
Ambient temperature range	-40 to 85 °C (tested in accordance with IEC-60068-2-1 and IEC-60068-2-2)
Relative humidity range	5 to 90%, noncondensing (tested in accordance with IEC-60068-2-56)
Maximum altitude	2,000 m (at 25 °C ambient temperature)
Pollution degree	2

Safety and Compliance

Safety

This product is designed to meet the requirements of the following standards of safety for electrical equipment for measurement, control, and laboratory use:

- IEC 61010-1, EN 61010-1
- UL 61010-1, CAN/CSA-C22.2 No. 61010-1

Note: For UL and other safety certifications, refer to the product label or visit ni.com/certification, search by model number or product line, and click the appropriate link in the Certification column.

Electromagnetic Compatibility

This product is designed to meet the requirements of the following standards of EMC for electrical equipment for measurement, control, and laboratory use:

- EN 61326 EMC requirements; Minimum Immunity
- EN 55011 Emissions; Group 1, Class A
- CE, C-Tick, ICES, and FCC Part 15 Emissions; Class A

Note: For EMC compliance, operate this device according to product documentation.

CE Compliance

This product meets the essential requirements of applicable European Directives, as amended for CE marking, as follows:

- 73/23/EEC; Low-Voltage Directive (safety)
- 89/336/EEC; Electromagnetic Compatibility Directive (EMC)

Note: Refer to the Declaration of Conformity (DoC) for this product for any additional regulatory compliance information. To obtain the DoC for this product, visit ni.com/certification, search by model number or product line, and click the appropriate link in the Certification column.

Waste Electrical and Electronic Equipment (WEEE)

EU Customers: At the end of their life cycle, all products must be sent to a WEEE recycling center. For more information about WEEE recycling centers and National Instruments WEEE initiatives, visit ni.com/environment/weee.htm.

NI Services and Support

NI has the services and support to meet your needs around the globe and through the application life cycle – from planning and development through deployment and ongoing maintenance. We offer services and service levels to meet customer requirements in research, design, validation, and manufacturing. Visit ni.com/services.

Training and Certification

NI training is the fastest, most certain route to productivity with our products. NI training can shorten your learning curve, save development time, and reduce maintenance costs over the application life cycle. We schedule instructor-led courses in cities worldwide, or we can hold a course at your facility. We also offer a professional certification program that identifies individuals who have high levels of skill and knowledge on using NI products. Visit ni.com/training.

Professional Services

Our Professional Services Team is comprised of NI applications engineers, NI Consulting Services, and a worldwide National Instruments Alliance Partner program of more than 600 independent consultants and integrators. Services range from start-up assistance to turnkey system integration. Visit ni.com/alliance.

NATIONAL INSTRUMENTS Certified Alliance Partner

OEM Support

We offer design-in consulting and product integration assistance if you want to use our products for OEM applications. For information about special pricing and services for OEM customers, visit ni.com/oem.

Local Sales and Technical Support

In offices worldwide, our staff is local to the country, giving you access to engineers who speak your language. NI delivers industry-leading technical support through online knowledge bases, our applications engineers, and access to 14,000 measurement and automation professionals within NI Developer Exchange forums. Find immediate answers to your questions at ni.com/support.

We also offer service programs that provide automatic upgrades to your application development environment and higher levels of technical support. Visit ni.com/ssp.

Hardware Services

NI Factory Installation Services

NI Factory Installation Services (FIS) is the fastest and easiest way to use your PXI or PXI/SCXI combination systems right out of the box. Trained NI technicians install the software and hardware and configure the system to your specifications. NI extends the standard warranty by one year on hardware components (controllers, chassis, modules) purchased with FIS. To use FIS, simply configure your system online with ni.com/pxiadvisor.

Calibration Services

NI recognizes the need to maintain properly calibrated devices for high-accuracy measurements. We provide manual calibration procedures, services to recalibrate your products, and automated calibration software specifically designed for use by metrology laboratories. Visit ni.com/calibration.

Repair and Extended Warranty

NI provides complete repair services for our products. Express repair and advance replacement services are also available. We offer extended warranties to help you meet project life-cycle requirements. Visit ni.com/services.

NATIONAL INSTRUMENTS

ni.com • (800) 813 3693
National Instruments • info@ni.com

351378A-01 2006-7323-301-101-D

A.2 Oxygen Gas Sensor

O_2 Gas Sensor

(Order Code O2-BTA or O2-DIN)

The Vernier O_2 Gas Sensor is used to monitor gaseous oxygen levels in a variety of biology and chemistry experiments. The O_2 Gas Sensor can be used for the following experiments:

- Monitor human respiration during exercise.
- Measure concentration of oxygen gas generated during decomposition of hydrogen peroxide by catalase.
- Monitor changes in oxygen concentration during photosynthesis and respiration of plants.
- Monitor respiration of animals, insects, or germinating seeds.
- Monitor oxidation of metals such as iron.
- Monitor consumption of oxygen by yeast during respiration of sugars.

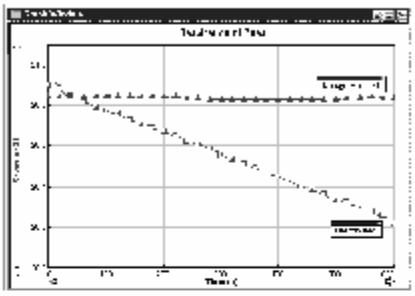

Cell Respiration of Germinated Peas

Inventory of Items Included with the O_2 Gas Sensor

Check to be sure that each of these items is included with your O_2 Gas Sensor:

- O_2 Gas Sensor
- 250 mL gas sampling bottle (Nalgene bottle with lid)
- O_2 Gas Sensor booklet

Note: This product is to be used for educational purposes only. It is not appropriate for industrial, medical, research, or commercial applications.

Using the O_2 Gas Sensor with a Computer

This sensor can be used with a computer and any of the following lab interfaces: Vernier LabPro®, Go!®Link, Universal Lab Interface, or Serial Box Interface.

1. Connect the O_2 Gas Sensor, interface, and computer.
2. Start the Logger *Pro*® or Logger Lite® software.
3. The program will automatically identify the O_2 Gas Sensor, and you are ready to collect data.[1]

Using the O_2 Gas Sensor with TI Graphing Calculators

This sensor can be used with a TI graphing calculator and any of the following lab interfaces: LabPro, CBL 2™, and Vernier EasyLink®. Here is the general procedure to follow when using the O_2 Gas Sensor with a graphing calculator:

1. Connect the data-collection interface to the graphing calculator.

[1] If your system does not support auto-ID, open an experiment file in Logger *Pro*, and you are ready to collect data.

2. Connect the O_2 Gas Sensor to any of the analog ports on the interface or to EasyLink.
3. Start the EasyData® or DataMate App—the application you choose to use depends on your calculator and interface. See the chart for more information.

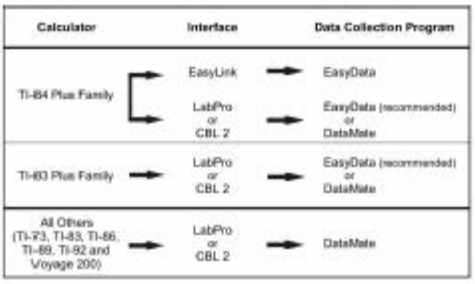

4. The O_2 Gas Sensor will be identified automatically, and you are ready to collect data.

If the data-collection application is not on your calculator, use the following instructions to load it onto the calculator.

- **EasyData App**–This program may already be installed on your calculator. Check to see that it is EasyData version 2.0 or newer. If it is not installed or is an older version, it can be downloaded to your computer from the Vernier web site, www.vernier.com/easy/easydata.html. It can then be transferred from the computer to the calculator using TI-Connect and a TI unit-to-computer cable or TI-GRAPH LINK cable. See the Vernier web site, www.vernier.com/calc/software/index.html for more information on the App and Program Transfer Guidebook.
- **DataMate program**–This program can be transferred directly from LabPro or CBL 2 to the TI graphing calculator. Use the calculator-to-calculator link cable to connect the two devices. Put the calculator into Receive mode, and then press the Transfer button on the interface.

Using the O_2 Gas Sensor with a Palm Powered™ Device

1. Connect the Palm Powered handheld, LabPro, and the O2 Gas Sensor.
2. Start Data Pro.
3. Tap New, or choose New from the Data Pro menu. Tap New again. The O2 Gas Sensor will be identified automatically.
4. You are now ready to collect data.

How the O_2 Gas Sensor Works

The Vernier O_2 Gas Sensor measures the oxygen concentration in the range of 0 to 27% using an electrochemical cell. The cell contains a lead anode and a gold cathode immersed in an electrolyte. When oxygen molecules enter the cell, they get electrochemically reduced at the gold cathode. This electrochemical reaction generates a current that is proportional to the oxygen concentration between the electrodes. The current is measured across a resistance to generate a small voltage output. The voltage output is conditioned and read by a Vernier interface or the CBL 2.

IMPORTANT: The O_2 Gas Sensor must be stored upright when not being used. This is necessary to maintain the sensor. Failure to store upright will reduce the life of the sensor.

Do I Need to Calibrate the O_2 Gas Sensor?

For many measurements, it will not be necessary to calibrate the O_2 Gas Sensor. We have set the sensor to match our stored calibration before shipping it. You can simply use the appropriate calibration file, which is stored in your data-collection program from Vernier.

For more accurate measurements, the sensor can be calibrated at 0 and 20.9% oxygen. Follow the normal 2-point calibration procedure. For the first point, push and hold the zero button located on the top of the sensor. Enter a value of 0 for this reading. Release the button and take a second reading. Enter a value of 20.9% oxygen or a corrected value from the table below. Once finished, the sensor should now read 20.9 (or the value entered from the table below) while resting in the gas sampling bottle. To calibrate in parts per thousand, multiply the second value by 10 (for example, you would enter 209 instead of 20.9).

If your O_2 Gas sensor is several years old, you may see readings in air that are considerably lower than 20.9%. This does not mean the sensor is no longer functional; rather, it simply requires that you perform the easy two-point calibration described in the previous paragraph.

Atmospheric Considerations

Because the % of oxygen varies with the amount of water vapor in the atmosphere, you may want to adjust your atmospheric oxygen calibration value to improve accuracy when using the O_2 Gas Sensor. The accepted value of 20.9% for atmospheric oxygen levels is calculated in dry air (0% humidity). If you know the relative humidity of the location at which you are calibrating, you can substitute one of the values below in place of 20.9%.

Relative Humidity	0%	25%	50%	75%	100%
Oxygen in % by volume	20.9	20.7	20.5	20.3	20.1

Tips

- Even though the sensor responds rather quickly to changes in O2 concentration, remember that gas has to diffuse into the electrochemical cell located at the top of the sensor shaft before any changes in concentration can be detected. Since diffusion of gases is a fairly slow process, there can be some delay in readings. This is especially important to keep in mind when using this sensor with the CO2-O2 Tee.
- To collect data in a controlled environment, we recommend that you use the 250 mL Nalgene collection bottle that is included with your sensor. Place the tip of the sensor into the opening of the bottle and push the sensor into the bottle. When the sensor will go no further, you have a seal. Very important: Do not place the sensor into any liquid. The sensor is intended only for measuring gaseous, not aqueous, O2 concentration.
- The O2 Gas Sensor must be stored upright when not being used. This is necessary to maintain the sensor. Failure to store upright will reduce the life of the sensor.

Specifications

Measurement Range of O_2 Gas Sensor	0%–27%
Accuracy (@ Standard Pressure 760 mmHg)	+/- 1% volume O_2
Resolution	12 bit (ULI, Serial Box, LabPro) = 0.01% 10 bit (CBL2) = 0.04%
Response Time	~12 seconds to 90% of final value
Warm-Up Time	Less than 5 seconds to 90% of final value
Pressure Effect	Directly proportional $V_{out} = V_{out}$ (standard) x (P/1013) Pressure range: 0.5 atm to 1.5 atm
Output Signal Range	0 to 4.8 VDC, 2.7 to 3.8 VDC @ 21% O_2
Output Impedance	1 K
Input Voltage	5 VDC +/–0.25 VDC
Gas Sampling Mode	Diffusion
Operating Temperature Range	5 to 40°C
Operating Humidity Range	0 to 95% RH
Storage Temperature Range	–20 to +60°C
Dimensions	Sensor Tube: 76 mm length (32 mm largest OD)
Calibration information:	slope (gain): 6.769 pct/ppt/ppm/V intercept (offset): pct/ppt/ppm

This sensor is equipped with circuitry that supports auto-ID. When used with LabPro, Go! Link, EasyLink, or CBL 2, the data-collection software identifies the sensor and uses pre-defined parameters to configure an experiment appropriate to the recognized sensor.

Warranty

Vernier warrants this product to be free from defects in materials and workmanship for a period of five years from the date of shipment to the customer. This warranty does not cover damage to the product caused by abuse or improper use.

Measure. Analyze. Learn.®
Vernier Software & Technology
13979 S.W. Millikan Way • Beaverton, OR 97005-2886
Toll Free (888) 837-6437 • (503) 277-2299 • FAX (503) 277-2440
info@vernier.com • www.vernier.com

A.3 Carbon Dioxide Sensor

VAISALA

10-D Gill Street, Woburn, MA 01801
Tel: 1-888-VAISALA (824-7252)
Fax: (781) 933-8029
Email: instruments@vaisala.com
www.vaisala.com

GMM220 Carbon Dioxide Modules for Harsh and Demanding OEM Applications

The Vaisala CARBOCAP® Carbon Dioxide Module Series GMM220 withstand harsh conditions. They provide high carbon dioxide measurement accuracy over wide temperature and relative humidity ranges.

Features/Benefits

- Incorporates Vaisala CARBOCAP® Sensor - the silicon based NDIR sensor
- Choice of several measurement ranges
- IP65 (NEMA 4) protected probe against dust and spray water
- Interchangeable probes provide easy maintenance

For harsh environments

The Vaisala CARBOCAP® Carbon Dioxide Module Series GMM220 are designed for Original Equipment Manufacturers (OEM's) requiring carbon dioxide measurements in harsh and demanding applications.

The modules are optimized for integration into equipment for greenhouse control, incubators, fermentors, safety alarming and integrated systems.

Vaisala CARBOCAP® – the silicon based CO_2 sensor

The GMM220 series modules incorporate the industrial Vaisala CARBOCAP® Sensor. The patented sensor has unique reference measurement capabilities. Its critical parts are made of silicon; this gives the sensor outstanding stability over both time and temperature.

Since water vapor, dust, and most chemicals do not effect the measurement, the GMM220 series modules can be used in harsh and humid environments.

Interchangeable probes

The GMP220 probes are interchangeable. They can be removed, reattached or replaced at any time – without the need for calibration and adjustment. The interchangeable probes make calibration and field service easy. In addition, the measurement range can be changed simply by replacing one probe with another.

Different configurations to meet demanding applications

The user has a choice of measurement ranges up to 20 % CO_2: the Vaisala CARBOCAP® Carbon Dioxide Module GMM221 for higher and the Vaisala CARBOCAP® Carbon Dioxide Module GMM222 for lower concentrations of CO_2.

Different power supply voltages, output options, as well as cable lengths, connectors, and mounting gear are also available.

Technical Data

PRICE:

GMM220 The GMM220 is an OEM product. Please call 1-888-VAISALA (824-7252) for pricing.

Carbon Dioxide

Measurement Ranges	
GMM221	0..2% CO_2
for high concentrations	0..3% CO_2
	0..5% CO_2
	0..10% CO_2
	0..20% CO_2
GMM222	0...2000 ppm
for low concentrations	0...3000 ppm
	0...5000 ppm
	0...7000 ppm
	0...10 000 ppm
Accuracy at +25 °C (+77 °F) against certified factory references	
GMM221	<±(0.02% CO_2 + 2% of reading)
GMM222	<±(20 ppm CO_2 +2% of reading)
(incl. repeatability and calibration uncertainty)	
Nonlinearity	<±1.0 %FS
Temperature dependence of output (typ.)	0.1 %FS/°C (0.1 %FS/°F)
Pressure dependence (typ.)	0.15% of reading/hPa
Long-term stability	<±5 %FS/2 years
Response time (63%)	
GMM221	20 seconds
GMM222	30 seconds

General

Analog output signals	0..20 or 4..20 mA
	0..1 V or 0..2 V, 0..2.5 V, 0..5 V
Resolution of analog outputs	0.03 %FS
Recommended external load:	
current output	max. 200 Ohm
voltage output	min. 1 kOhm
Power supply	11-20 VDC or
	18..30 VDC
Power consumption	<2.5 W
Warm-up time	<15 minutes
Operating temperature range	-20..+60 °C (-4...+140 °F)
Storage temperature range	-30...+70 °C (-22..+158 °F)
Operating humidity range	
probe	0..100 %RH
	non-condensing
mother board	0..85 %RH
	non-condensing
Probe housing material	PC plastic
Housing classification	
(probe only)	IP65 (NEMA 4)
Weight:	
GMM221 (w/2m cable)	max. 180 g
GMM222 (w/2m cable)	max. 200 g
Probe cable length	0.6 m, 2 m, 6 m or 10 m

Accessories

GMP221, GMP222	spare probe
(use the order form to define measurement range etc.)	
25245GM	clips (2 pcs) for attaching the probe
GM45156	mounting flange for the probe
GMM220Z600	6.0 m probe cable
GMM220Z1000	10.0 m probe cable
19040GM	serial COM adapter

Electromagnetic compatibility

Complies with EMC standard EN61326-1:1997 + Am1:1998 + Am2:2001; Generic Environment.

Dimensions

Dimensions in mm (inches)

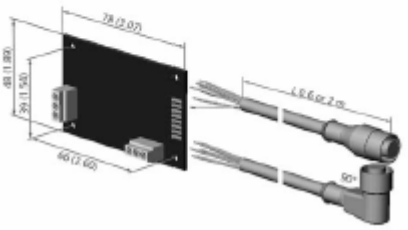

CARBOCAP® is a registered trademark of Vaisala.

Specifications subject to change without prior notice.

VAISALA

P.O. Box 26, FIN-00421 Helsinki, FINLAND
Tel: +358 9 894 91
Fax: +358 9 8949 2485
Email: industrialsales@vaisala.com
www.vaisala.com

Vaisala CARBOCAP® Sensor Technology for Stable Carbon Dioxide Measurement

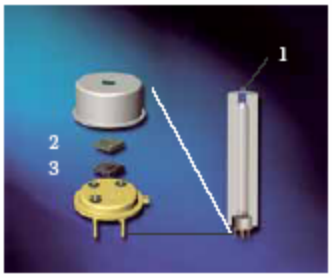

The Vaisala CARBOCAP® Sensor components:
1. Infrared source
2. Tunable FPI filter
3. Infrared detector

Features/Benefits

- Vaisala CARBOCAP® Sensor, a silicon-based non-dispersive infrared (NDIR) sensor
- Built-in reference measurement – superior stability
- No moving parts - excellent durability

The Vaisala CARBOCAP® Sensor is a silicon based, non-dispersive infrared (NDIR) sensor for the measurement of gaseous carbon dioxide. Its working principle is Single-Beam Dual-Wavelength NDIR, the same method that is commonly used in expensive high performance NDIR analyzers. However, in the Vaisala CARBOCAP® Sensor, the traditional rotating filter wheel is replaced with a tiny, electrically controlled Fabry-Perot Interferometer (FPI) made of silicon. A true Dual-Wavelength measurement can be provided in a very simple and practically solid-state structure.

The operating principle

An infrared source at the end of the measurement chamber emits light into the gas chamber, where any carbon dioxide gas present absorbs a part of the light at its characteristic wavelength. The FPI interference filter is electrically tuned so that its pass band coincides with the absorption wavelength of carbon dioxide. The IR detector measures the strength of the signal that passes through.

After this the pass band of the FPI is shifted to a wavelength where no absorption occurs. This provides the reference signal. The ratio of these two signals, one at the absorption wavelength and the other at the reference wavelength, indicates the degree of light absorption in the gas and thus the gas concentration. The reference signal compensates for the possible effects of sensor aging and contamination, making the sensor very stable over time.

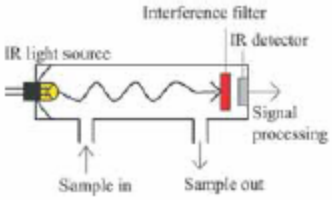

The Vaisala CARBOCAP® Sensor is simple in structure, yet it offers high performance.

The Vaisala CARBOCAP® sensors have excellent stability, both in terms of time and temperature. The sensor is accurate and durable, and its small size enables the measurement system to be truly miniaturized. Due to the simplicity of the structure, Vaisala is able to offer customers a high quality sensor at an affordable price. In particular, Vaisala CARBOCAP® solutions will prove themselves economical over time: their stability will decrease maintenance costs significantly over the years.

Applications

Vaisala's line of CO_2 instruments meets the needs of ecological measurements as well as industrial measurements and HVAC. Fixed transmitters and portable meters, as well as OEM modules, are available.

For ecological measurements Vaisala offers instruments, such as Vaisala CARBOCAP® Carbon Dioxide Probe GMP343, for diffusion based CO_2 measurement. The instruments can be used both in below-ground CO_2 measurements and soil respiration boxes.

The Vaisala CARBOCAP® Carbon Dioxide Transmitter Series GMT220 are designed to measure CO_2 in harsh and humid environments, such as greenhouses and industrial process sites.

For HVAC applications, Vaisala product range consist of both duct and wall mount transmitters. They are a cost-effective solution for demand controlled ventilation and related applications. The Vaisala CARBOCAP® technology is so stable that these instruments only require a calibration check every five years.

The Vaisala CARBOCAP® Hand-Held Carbon Dioxide Meter GM70 is ideal for various spot-checking applications, like laboratories, greenhouses, mushroom farms, breweries and bottling plants and as a tool for checking fixed CO_2 instruments.

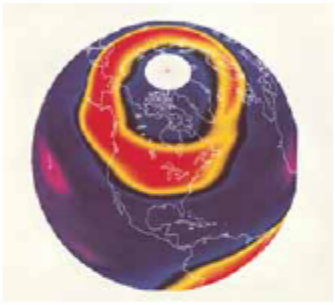

A small change in the soil respiration can have a major impact on the whole atmospheric CO_2 budget and on the global ecosystem.

Forests have an important role in world's ecosystem.

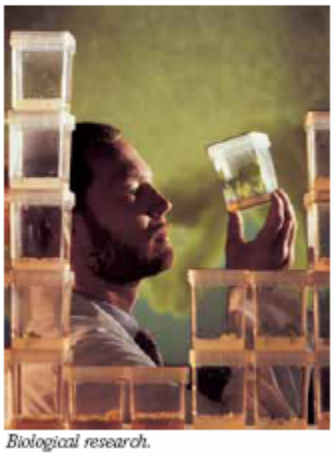

Biological research.

The productivity in a greenhouse can be increased up to 30% with proper CO_2 fertilization. The optimum CO2 concentration depend on the plant and the light conditions in the greenhouse.

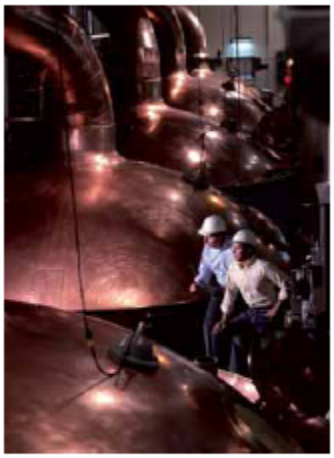

Carbon dioxide is used for carbonation of beverages - CO_2 is the gas that gives the fizz to soft drinks. In breweries and wineries, CO_2 is recovered as a by-product of fermentation. CO_2 is also injected into bottles when the bottles are capped to remove oxygen.

By monitoring CO_2 and humidity levels, certain broiler houses have observed improved growth rate, feed conversion, and carcass quality

The top reasons for maintaining good indoor air quality are human comfort and health aspects, energy savings, which can grow up to 50%, and well-being of the building and it's structures.

Too low ventilation means bad air quality and an unpleasant environment.

A.4 Heart Rate Monitor

Hand-Grip Heart Rate Monitor

(Order Code HGH-BTA)

The Hand-Grip Heart Rate Monitor measures a person's heart rate by registering the small electrical signals carried across the surface of a person's skin each time his or her heart contracts. This signal is measured at the surface of the skin by electrodes embedded in the hand grips of the Hand-Grip Heart Rate Monitor. By graphing this signal, the heart rate can be determined. A sample graph is shown below:

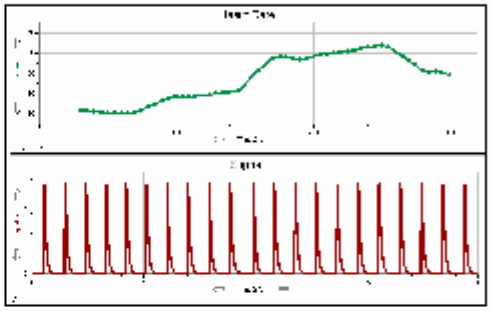

Suggested Experiments

- Compare the heart rate of different individuals.
- Compare the heart rate of athletes and sedentary people.
- Monitor a person's heart rate before, during, and after a short period of vigorous activity (such as doing jumping jacks).
- Monitor how fast a person's heart rate returns to normal after exercise (recovery rate).
- Check for baroreceptor reflex; that is, changes in heart rate for a person when reclined, sitting, and standing caused by the need for the heart to pump blood to different levels.
- Check a person's heart rate before and after caffeine consumption.
- Check a person's heart rate before and after eating.
- Check your own heart rate at different times of the day.
- Monitor a person's heart rate as his or her breath is held.

NOTE: This product is to be used for educational purposes only. It is not appropriate for industrial, medical, research, or commercial applications.

Using the Hand-Grip Heart Rate Monitor with a Computer

This sensor can be used with a Vernier LabPro® or Go!®Link. Here is the general procedure to follow when using the Hand-Grip Heart Rate Monitor with a computer:

1. Connect the Hand-Grip Heart Rate Monitor, interface, and computer.
2. Start the Logger *Pro*® or Logger Lite® software.
3. The program will automatically identify the Hand-Grip Heart Rate Monitor, and you are ready to collect data.[1]

[1] If your system does not support auto-ID, open an experiment file in Logger *Pro*, and you are ready to collect data.

Using the Hand-Grip Heart Rate Monitor with TI Graphing Calculator

This sensor can be used with a TI graphing calculator and any of the following lab interfaces: LabPro, CBL 2™, and Vernier EasyLink®. Here is the general procedure to follow when using the Hand-Grip Heart Rate Monitor with a graphing calculator:

1. Connect the data-collection interface to the graphing calculator.
2. Connect the Hand-Grip Heart Rate Monitor to any of the analog ports on the interface or to EasyLink.
3. Start the Vernier EasyData® or DataMate App—the application you choose to use depends on your calculator and interface. See the chart for more information.

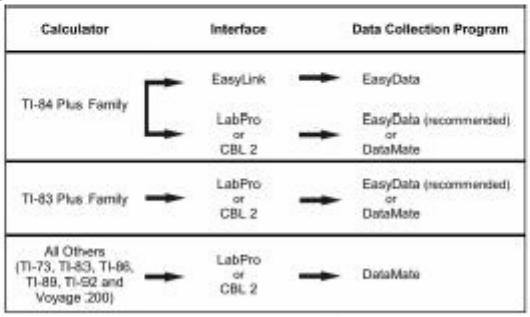

4. The Hand-Grip Heart Rate Monitor will be identified automatically[2], and you are ready to collect data.

If the data-collection application is not on your calculator, use the following instructions to load it onto the calculator.

- **EasyData App**–This program may already be installed on your calculator. Check to see that it is EasyData version 2.0 or newer. If it is not installed or is an older version, it can be downloaded to your computer from the Vernier web site, www.vernier.com/easy/easydata.html. It can then be transferred from the computer to the calculator using TI-Connect and a TI unit-to-computer cable or TI-GRAPH LINK cable. See the Vernier web site, www.vernier.com/calc/software/index.html for more information on the App and Program Transfer Guidebook.
- **DataMate program**–This program can be transferred directly from LabPro or CBL 2 to the TI graphing calculator. Use the calculator-to-calculator link cable to connect the two devices. Put the calculator into Receive mode, and then press the Transfer button on the interface.

Using the Hand-Grip Heart Rate Monitor with Palm Powered™ Handhelds

1. Connect the Palm Powered handheld, LabPro, and the Hand-Grip Heart Rate Monitor.

---

[2] If your system does not support auto-ID, choose SETUP and then Other Sensors. See the EasyData Guidebook for information on setting up a sensor manually, www2.vernier.com/manuals/easydata_guidebook.pdf

2. Start Data Pro.
3. Tap New, or choose New from the Data Pro menu. Tap New again. The Hand-Grip Heart Rate Monitor will be identified automatically.[3]
4. You are now ready to collect data.

Specifications

Receiver range: 80–100 cm

Receiver current consumption: 30–55 μA

Transmitter transmission frequency: 5 kHz ±10%

Transmitter operating temperature: 0–60°C

This sensor is equipped with circuitry that supports auto-ID. When used with LabPro, Go! Link, EasyLink, or CBL 2, the data-collection software identifies the sensor and uses pre-defined parameters to configure an experiment appropriate to the recognized sensor.

How the Hand-Grip Heart Rate Monitor Works

The Hand-Grip Heart Rate Monitor consists of a set of hand grips and a plug-in receiver. The hand grips are held, one in each hand, by the individual whose heart rate is being monitored. The hand grips are marked for the right or left hand and each has the necessary markings showing where the individuals' fingers and palms should be placed. The left hand grip and the receiver are both marked with an alignment arrow. When collecting data, it is **important** that the arrow labels on each of these devices be in alignment (see figure below).

The plug-in receiver connects to any of the interfaces listed above. The transmitter detects each heart beat through the electrodes on the two hand grips with ECG accuracy and transmits the heart rate information to the plug-in receiver with the help of a low frequency electromagnetic field. The plug-in receiver wirelessly receives the transmission, and passes a 3-volt pulse for each heart beat detected to the Vernier interface. The reception range of the plug-in receiver is 80–100 cm or about 3 feet.

In general, you can use the Hand-Grip Heart Rate Monitor as you would any other sensor connected to your interface. You can plot a pulse for each heart beat and analyze the time between the peaks to determine the heart rate. Often it is more convenient to use a program that simply displays the heart rate in beats per minute on the screen. Our data-collection programs perform this task for all of our interfaces.

Do I Need to Calibrate the Hand-Grip Heart Rate Monitor? "No."

The Hand-Grip Heart Rate Monitor does not need to be, nor can it be, calibrated. It provides very accurate heart rate values.

[3] If your sensor does not auto-ID, tap Setup and set up an experiment.

Using a Chest Belt Transmitter

The Chest Belt Transmitter, which is ordered separately (Order Code CBT), works in place of the hand grips, allowing a hands-free option of measuring heart rate. The chest belt is worn on or below the chest and held in place by an elastic strap. Make sure that the belt fits snugly around the chest and is resting directly against the subject's skin. Make sure to re-wet the electrodes each time the belt is positioned.

Helpful Tips

Listed below are some tips to insure successful data collection .

1. Make sure that the hand grips and the receiver are in alignment. The arrow symbol on the left hand grip and the receiver should be held in parallel alignment.
2. Be sure to hold the receiver within 80 cm of the hand grips. This is the maximum transmission range of the transmitter in the chest belt.
3. Dirty electrodes on the hand grips can cause poor readings. In between uses, it is a good idea to gently wipe the electrodes clean using alcohol wipes. Do not immerse the hand grips in solution, simply spray or wipe alcohol onto them.
4. The receiver of the Hand-Grip Heart Rate Monitor will receive signals from other hand grips if they are within range; be sure to maintain a distance of at least 2 meters between other individuals that are monitoring heart rate.
5. Interference from electrical devices, such as computer monitors, electronic exercise equipment (treadmills, stationary bicycles, etc.), televisions, TV antennas, and high voltage lines (both above and below ground) can result in poor readings. Keep the receiver of the Hand-Grip Heart Rate Monitor as far away as possible from such equipment.
6. With certain individuals, readings from the Hand-Grip Heart Rate Monitor may take a minute or two to stabilize. In such cases, allow the readings to stabilize before starting data collection.

Warranty

Vernier warrants this product to be free from defects in materials and workmanship for a period of five years from the date of shipment to the customer. This warranty does not cover damage to the product caused by abuse or improper use.

Measure. Analyze. Learn.™
Vernier Software & Technology
13979 S.W. Millikan Way • Beaverton, OR 97005-2886
Toll Free (888) 837-6437 • (503) 277-2299 • FAX (503) 277-2440
info@vernier.com • www.vernier.com

A.5 Flow Rate Meter

TELEDYNE HASTINGS INSTRUMENTS

NALL-SERIES MASS FLOWMETERS

Model NALL

FEATURES

- The Original Hastings Mass Flowmeter
- 15 Standard Flow Ranges
- No Corrections for 20% Variations in Temperature or Pressure

APPLICATIONS

For All of Your Gas Flow Measuring Needs:

- Vapor Deposition
- Leak Testing
- Gas Blending
- Semiconductor Processes
- Measurement of Toxic and Hazardous Gases
- High Temperature, High Pressure, and Hermetically Sealed Uses

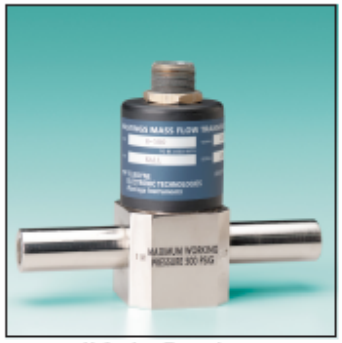

H Series Transducer

Model NALL Power Supply

DESIGN FEATURES

The Hastings NALL-Series Flowmeter is the original model that has generated repeat customers for over 50 years. It operates on a unique thermal principle which permits inherently linear response to flow. The flow passage is constructed entirely of metal and contains no O-rings. The transducer is also separate from any electronic circuitry, making it ideal for high temperature or other adverse environmental applications. The power supply features a bright digital display and is contained in either a cabinet or panel mountable case.

All models feature high accuracy and excellent repeatability.

TELEDYNE INSTRUMENTS
Hastings Instruments
A Teledyne Technologies Company

SELECTION CHART

Each flowmeter requires one Power Supply; one Cable; one Transducer; and (if using a range higher than 0-50 slpm) one Laminar Flow Element.

Power Supplies

Stock #	Model #	Description	Dimensions
54-113	NALL	Digital Cabinet	7.75"W x 5.75"H x 5.75"D
54-096	NALL-P	Digital Panel	5.41"W x 8.71"H x 9.68"D
54-121	NALL-P/CC	Digital Panel, 4.20 mA output	same as above
54-111	TNALL-P	Digital Panel Flowmeter/Totalizer	same as above
54-115	NALL-C	Digital Chassis	10.0"W x 3.25"H x 6.50"D

Cables

Stock #	Model #	Transducer Cable Length
65-060	NF-8-NM	8-foot
65-074	NF-25-NM	25-foot
65-095	NF-50-NM	50-foot
65-079	NF-100-NM	100-foot
65-228	NF-200-NM	200-foot
65-229	NF-300-NM	300-foot
65-313	NF-8T-NM*	8-foot (high-temp)
65-314	NFT-25T-NM*	25-foot (high-temp)

*For use with models with OPT-T (high temperature) ONLY.

Stainless Steel Transducers

Stock #	Model #	Flow Range	Connection
54-131	HS-10S	0-10 sccm	1/8" NPT female
54-173	HS-50S	0-50 sccm	1/4" NPT female
54-174	HS-100S	0-100 sccm	1/4" NPT female
54-175	HS-500S	0-500 sccm	1/4" NPT female
54-176	HS-1KS	0-1 slm	1/2" NPT male
54-177	HS-5KS	0-5 slm	1/2" NPT male
54-129	HS-10KS	0-10 slm	3/4" NPT male
54-130	HS-50KS	0-50 slm	3/4" NPT male

Monel Transducers

Stock #	Model #	Flow Range	Connection
54-153	HS-10M	0-10 sccm	1/8" NPT female
54-178	HS-50M	0-50 sccm	1/4" NPT female
54-179	HS-100M	0-100 sccm	1/4" NPT female
54-180	HS-500M	0-500 sccm	1/4" NPT female
54-181	HS-1KM	0-1 slm	1/2" NPT male
54-182	HS-5KM	0-5 slm	1/2" NPT male
54-156	HS-10KM	0-10 slm	3/4" NPT male
54-157	HS-50KM	0-50 slm	3/4" NPT male

Stainless Steel Laminar Flow Elements (to be used with Model HS-10S transducer)

Stock #	Model #	Flow Range	Connection
P-5-SS-T	L-5S	0-5 scfm (0-150 slm)	1" NPT
P-10-SS-T	L-10S	0-10 scfm (0-300 slm)	1.5" NPT
P-25-SS-T	L-25S	0-25 scfm (0-750 slm)	2" NPT
P-50-SS-F	L-50SF*	0-50 scfm (0-1500 slm)	3" flange
P-100-SS-F	L-100SF*	0-100 scfm (0-3000 slm)	4" flange
P-200-SS-F	L-200SF*	0-200 scfm (0-6000 slm)	6" flange
P-500-SS-F	L-500SF*	0-500 scfm (0-15,000 slm)	8" flange

*250 psig working pressure max. at 100°F. See ASA B16.5 100 lb. std.

Monel Laminar Flow Elements (to be used with Model HS-10M transducer)

Stock #	Model #	Flow Range	Connection
P-5-M-T	L-5M	0-5 scfm (0-150 slm)	1" NPT
P-10-M-T	L-10M	0-10 scfm (0-300 slm)	1.5" NPT
P-25/2-M-T	L-25M	0-25 scfm (0-750 slm)	2" NPT
P-3-M-T	L-50M	0-50 scfm (0-1500 slm)	3" NPT

Monel LFEs, 500 lb. max. working pressure.

SPECIFICATIONS

Accuracy	±1% of range for 20% variation in pressure and temperature
Linearity	±1% of range
Repeatability	±0.25% of F.S.
Working Pressure	500 psig max.; transducers available for 1000 psig
Temperature	Gas temperature, -20°C to 100°C Ambient for transducer and indicator, 0°C to 40°C
Power	115 volt AC, 50/60 hz - 15 watt. For 230 volt, add prefix "E" to power supply model number.
Output	0-5 volts DC into a load of 2000 ohms or greater. The signal is available at binding posts on rear of instrument.
Material	316SS, or monel, gold/nickel braze
Calibration	Direct reading is for air. Calibration available at time of order for oxygen, nitrogen, hydrogen, carbon monoxide, other gases.
Response Time	< 10 secs. to 67% of reading
Options	OPT-T: High temperature transducer to 200°C OPT-P: Working pressures up to 1000 psig; contact factory OPT-H: Hermetically sealed transducer OPT-NIST: NIST traceability OPT-E: 230 VAC/50 Hz

Transducer Dimensions

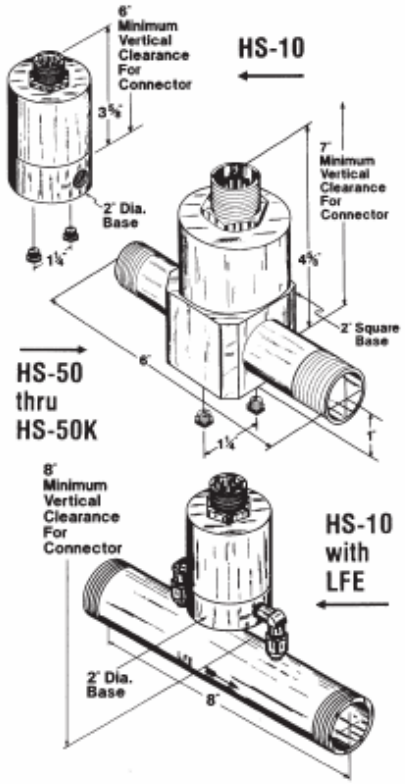

All dimensions shown are in inches

Your Customer Service Representative

TELEDYNE INSTRUMENTS
Hastings Instruments
A Teledyne Technologies Company

Telephone: (757) 723-6531
Toll Free: (800) 950-2468
Fax: (757) 723-3925
World Wide Web: http://www.teledyneinstruments.com
E-mail: hastings_instruments@teledyne.com
P.O. Box 1436
Hampton, VA 23661

A.6 Control Session Metabolic Workload Measurement System

Oxycon Pro® - Comfortable Cardiopulmonary Exercise Testing

Cardiopulmonary Exercise Testing with Ease

A modern diagnostic system must be both technically convincing and tailored to today's clinical needs of laboratory routine. To meet these demands Oxycon Pro was made quicker, more accurate and above all more economical than any piece of equipment ever designed for this field. Oxycon Pro is an expert system for routine CPET and offers you outstanding performance features and unparalleled ease of operation. So you can confidently give your attention to your patient and not to your equipment. The modular concept provides sufficient possibilities for upgrades or subsequent expansion whenever required or allowed by your budget.

Convincing in Every Way

■ Speed and Precision

To meet these high demands, Oxycon Pro uses sensors that exceed the common recommendations.
The patented TripleV volume sensor is a precise volume sensor with low resistance and no flow limitations in the physiological range. TripleV guarantees precise measurements and is smaller and lighter than competitor products, which means, it is more convenient for the patients who have to wear a mask or mouthpiece with the sensor during the test.
Unlike other devices which require manual calibration, the volume sensor and gas analyzers are checked automatically, thus saving time and effort on the part of the operator.

■ Economy

In the time a standard stress ECG or pulmonary exercise test normally takes, Oxycon Pro allows you to run a complete, combined exercise test.
A well-founded diagnosis can be made based on the analysis of all available stress test data measured in one unit. Oxycon Pro combines the necessary tools for cardiopulmonary exercise testing in one small and compact package. Not only are capital costs low in comparison with other less than fully-featured solutions, but operating costs are also remarkably reduced.

Oxycon Pro needs no chemicals, expensive disposable sample tubes or disposable sensors. All that is required to run the system is a calibration gas and disposable ECG electrodes (if you choose not to use our optional lightweight gold suction electrodes).
And, of course, ink and paper to print out your reports!

Recording Modes: Breath-by-Breath, Intrabreath or Mixing Chamber

The „heart" of the Oxycon Pro is its precise and reliable cardiopulmonary exercise testing program. Cardiopulmonary data and resulting parameters can either be recorded in Breath-by-Breath, Intrabreath or Mixing Chamber mode.

User-specific workload protocols for exercise on bicycle or treadmill guide you through the measurement. The screen display is clearly structured. Preset graphs and groups of graphs show the status of the current workload phase with predicted/actual value comparison.

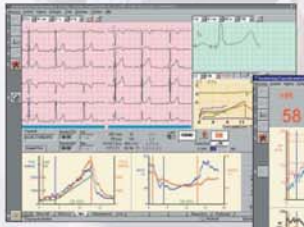

■ *12-lead ECG and CPET data*

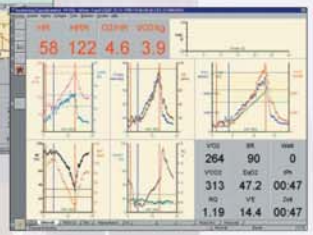

■ *Screen display during test*

An Expert System at your Fingertips

Cardiopulmonary exercise testing produces volumes of data - after all, that's what it is designed to do. However, this data needs to be properly analyzed and evaluated. In designing Oxycon Pro, we considered the time pressures faced by modern clinicians and introduced IntelliSupport, a graphics-based expert system which relieves the busy physician from time-consuming data analysis.

Based on accepted guidelines and predicted ranges described by the world renowned expert in cardiopulmonary exercise testing Professor Karlman Wasserman in his „Principles of Exercise Testing and Interpretation", IntelliSupport guides the clinician step by step through a test to arrive at a suitable interpretation. Some clinicians will use this feature as a fast and reliable route to routine diagnosis; others will prefer to use it as a handy tool for comparing the IntelliSupport diagnosis with their own conclusions. The graphical nature of the IntelliSupport interface makes it an excellent method of communicating data and documentation visually to colleagues and for patient education and counselling.

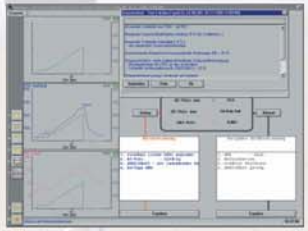

■ *IntelliSupport - your expert interpreter*

Integrated Computer-based ECG: All Parameters at a Glance

A notable feature of the Oxycon Pro is the exceptional stability of the stress ECG baseline traces. 12-channel ST-monitoring is based on a 10-second interval. A clearly structured ST graph displays the ST changes in different color. In addition, automatic arrhythmia detection is provided.

All Available from One Hand

Components which perfectly fit to each other ensure trouble-free test sequence. This is particularly important if you want to expand your system later.

■ *The new ergometer generation: VIAsprint 150P*

■ *CPET unit with ECG screen and suction electrodes*

Perfection in Simplicity

Our developers did their utmost to create a system that you could feel comfortable with right from the start. Because we have used a standard computer with keyboard and mouse and the proven Windows user interface, do not be surprised if Oxycon Pro seems familiar to you right from the start. Consequently, training time can be reduced to a minimum and you can delegate parts of the test to your team.

Appendix B : INSTITUTIONAL REVIEW BOARD

B.1 Application Coversheet

UNIVERSITY OF MARYLAND, COLLEGE PARK
Institutional Review Board
Initial Application for Research Involving Human Subjects
Please complete this cover page AND provide all information requested in the attached instructions.

Name of Principal Investigator (PI) or Project Faculty Advisor David L. Akin **Tel. No** 301-405-1138
(NOT a student or fellow; must be UMD employee)

Name of Co-Investigator (Co-PI) - **Tel. No** -

Department or Unit Administering the Project Aerospace Engineering

E-Mail Address of PI dakin@ssl.umd.edu **E-Mail Address of Co-PI** -

Where should the IRB send the approval letter? University of Maryland Building 382, College Park, MD 20742-2911

Name of Student Investigator Agnieszka Kościelniak **Tel. No.** 301-405-7353

E-Mail Address of Student Investigator notaggy@umd.edu

Check here if this is a student master's thesis ☒ **or a dissertation research project** ☐

Project Duration (mo/yr – mo/yr) 3/06 -- 8/07

Project Title Space Suit Energy Expenditure Measuring System Validation Study

Sponsored Project Data | **Funding Agency** NASA | **ORAA Proposal ID Number** 060620-8364

(PLEASE NOTE: Failure to include data above may result in delay of processing sponsored research award at ORAA.)

Vulnerable Populations: The proposed research will involve the following (Check all that apply): pregnant women ☐, human fetuses ☐, neonates ☐, minors/children ☐, prisoners ☐, students ☒, individuals with mental disabilities ☐, individuals with physical disabilities ☐

Exempt or Nonexempt (Optional): You may recommend your research for exemption or nonexemption by completing the appropriate box below. For exempt recommendation, list the numbers for the exempt category(s) that apply. Refer to pages 5-6 of this document.

☐ **Exempt----List Exemption Category Numbers** *Or* ☒ **Non-Exempt**

If exempt, briefly describe the reason(s) for exemption. Your notation is a suggestion to the IRB Manager and IRB Co-Chairs.

10/30/06 **Date** **Signature of Principal Investigator or Faculty Advisor** *(PLEASE NOTE: Person signing above accepts responsibility for the research even when data collection is performed by other investigators)*

Date **Signature of Co-Principal Investigator**

10/30/06 **Date** **Signature of Student Investigator**

10/1/06 **Date** **REQUIRED** Departmental Signature
Name Dr. Darryll Pines, **Title** ENAE Dept. Chair
(Please also print name of person signing above)

(PLEASE NOTE: The Departmental signature block should not be signed by the investigator or the student investigator's advisor.)

***PLEASE ATTACH THIS COVER PAGE TO EACH SET OF COPIES**

B.2 Proposal

IRB Application

0. Title:
Space Suit Energy Expenditure Measuring System Validation Study

1. Abstract:
The purpose of this study is to validate a new space suit energy expenditure measuring system against the standard open-circuit method. Subjects will participate in two sessions in which they will perform low to medium intensity exercise on a treadmill. The experimental session will be performed at the Space Systems Lab in the Aerospace Engineering Department, where the subject will perform exercise at various speeds while wearing a helmet with constant air circulation at a rate of 6 scfm. This simulates a closed space suit environment. As a backup precaution, the helmet can be removed quickly at any time. The control session will take place at the Human Performance Laboratory in the Biological Engineering Department. The subjects will perform the exact same treadmill exercise while wearing a Hans Rudolph™ Oro-Nasal mask with a one-way valve connected to a mass spectrometer for gas analysis. The intake air is ambient. A questionnaire about basic body parameters, exercise profile, and experiment response will be completed. Subject involvement will be completely voluntary, informed consent will be obtained before commencement of the experiment, and all subject data will be kept confidential.

2. Subject selection:
The subjects will be adult (over 18 years of age) students from the College of Engineering. To reduce the risk of a cardiovascular event, subject selection will be limited to individuals under 40 years of age, who participate in a routine physical activity, are reasonably fit and in good health. Routine physical activity could include organized sports, personal exercise, commuting by cycling, etc. Though no medical clearance is required, subjects will be asked and excluded if they have any medical conditions with which their risk during treadmill exercise is heightened, including:

- High blood pressure
- Heart murmur
- Emphysema
- Diabetes
- Asthma
- Elevated cholesterol
- Claustrophobia
- Epilepsy
- Pregnancy
- Heart attack
- Stroke
- Aneurysm
- Open or bleeding lesions near or including the mouth
- Seizure
- Head injury
- Diseases of the arteries
- Diseases of the lungs
- Frequent headaches
- Heart palpitations
- Chest pain
- Dizzy spells
- Shortness of breath
- Painful joints
- Blood clots
- Smoking

The number of subjects in the study will be between 5 and 10 with an approximately even distribution of men and women. The subjects will not be selected for race, ethnic origin, religion, or any social or economic qualifications. Subjects will be recruited informally through word of mouth or email. A copy of the recruitment email is included with this application. Study participation will be completely voluntary and a subject can withdraw from the study at any time for any reason.

3. Procedures:

Each subject will be scheduled to attend two treadmill sessions, an experimental and a control session. The experimental session will take place at the Neutral Buoyancy Research Facility at the University of Maryland in College Park. The subject will wear a helmet assembly which simulates the closed environment of a space suit with ambient breathing air provided from a compressed air source. The control session will take place in the Human Performance Laboratory in the Biological Engineering Department at the University of Maryland in College Park. Here, the subject will wear a Hans Rudolph™ Oro-Nasal mask with a one-way valve which will route all exhaled air to a mass spectrometer for analysis. The sessions will be scheduled within the same week to eliminate possible errors due to physical conditioning from the subject's regular exercise routine. They will be held at the same time of day to minimize errors from daily metabolic effects. The order of the sessions (experimental or control first) will vary from subject to subject to eliminate any possible learning curve effects. The subjects will be asked to wear loose and comfortable clothing and athletic footwear.

Each session will take up to an hour of the subject's time, though the actual exercise portion will be 30 minutes long. Prior to scheduling the sessions, the physical requirements and excluding conditions will be discussed with each subject. The Basic Information, Medical History, and Exercise Profile portion of the subject questionnaire will be filled out at this time. At the start of the first session, the purpose of the research, procedures, equipment, and risks will be described to the subject, any questions will be answered, and informed consent will be obtained. The resting heart rate of the subject will then be measured in a sitting position. A Polar™ heart rate monitor will be worn by the subject before and during each exercise session to measure resting and exercise heart rate. Since this is worn under a shirt, the subjects will be instructed on how to don this and allowed to don it in a private enclosed space. The monitor is a rubber chest strap with two electrodes which records the ECG signal and transmits the data. The receiver during the experimental sessions is the Vernier™ heart rate receiver which is connected to a data acquisition system. The receiver must be kept within 80 cm of the chest strap transmitter and will be mounted to the treadmill for the exercise session. During the control session, the same chest strap heart rate monitor will be worn, but the receiver will be a Polar™ S810i watch worn by the subject. The chest strap and Vernier™ heart rate receiver are pictured below.

Polar™ chest strap and Vernier™ heart rate receiver

After the resting heart rate is measured and the session-appropriate gear has been donned and adjusted for fit, the treadmill exercise will begin. The 30 minutes of exercise are divided into three 10-minute portions at progressively higher speeds of 3 mph (20 minutes per mile), 4 mph (15 minutes per mile), and 5 mph (12 minutes per mile). These three segments will make up one continuous block of exercise. The treadmill incline will be kept at 0°. At the conclusion of the second exercise session, the subject will fill out the Response to Experiment portion of the subject questionnaire. Water will be available for the subject at the conclusion of each session, but not during. It is impossible to drink with either apparatus.

The subject heart rate will be monitored in real time during the experimental session and the subject oxygen consumption will be monitored in real time during the control session. If either of these value approaches 75% of the age predicted maximum, the session will be terminated early to avoid the associated health risks for the subject.

The apparatus the subjects will be asked to wear during the experimental session is pictured below. It is a 13" spherical helmet made of clear plastic with a 9.5" opening at the bottom. A modified bicycle helmet is glued inside the clear plastic helmet. The purpose of the bicycle helmet is to provide a firm way of supporting the larger helmet on the subject's head and keeping it stable throughout the exercise session. It is also adjustable for various head sizes. The colorful plastic covering was removed from the outside of the bicycle helmet. This allowed easy shaping of the helmet by cutting sections of Styrofoam out. The bicycle helmet was shaped to fit the inside contour of the clear plastic helmet. The front section of the bicycle helmet was removed and a groove over the top of the head was cut out to make room for the air inlet.

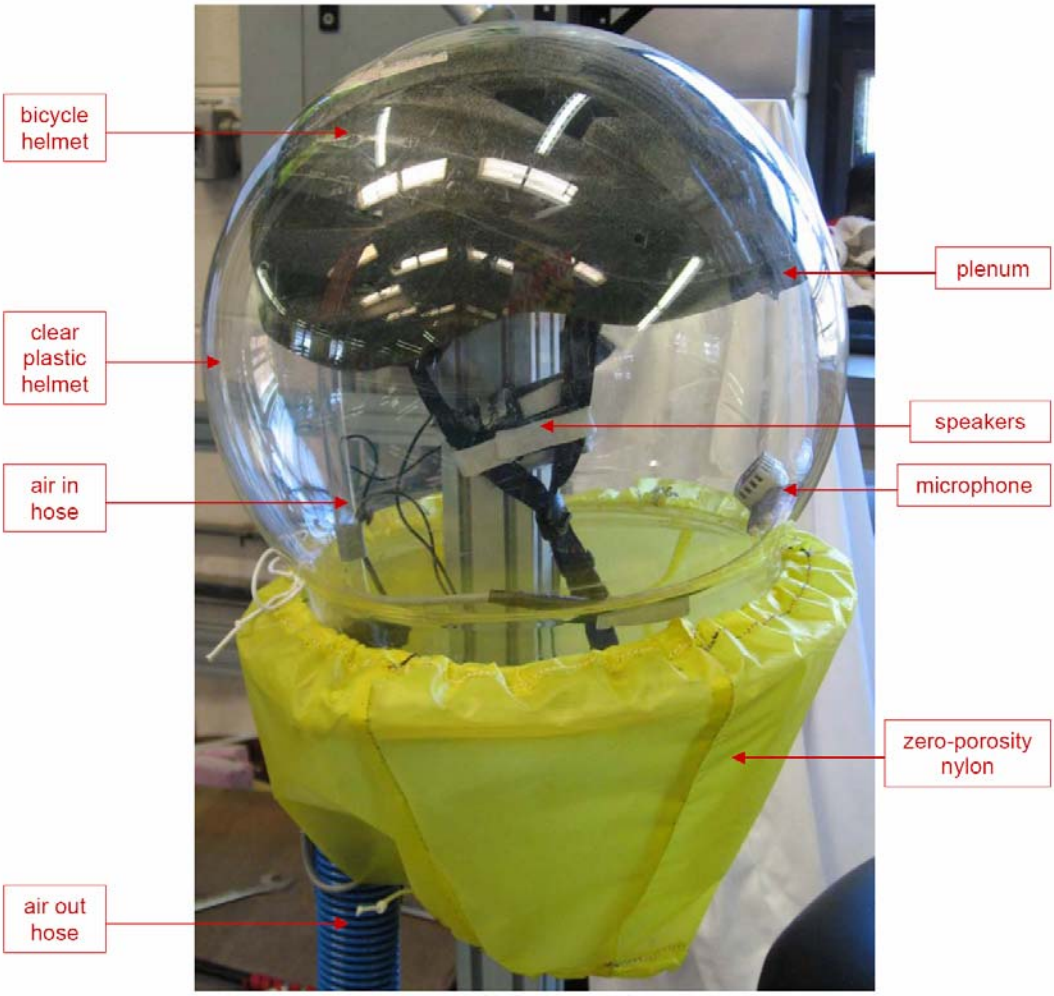

Experimental helmet assembly

A 1.5" diameter hose is attached to the back of the clear plastic helmet at the base of the neck. This is the air outlet hose. It is attached to a bent hose clamp, which is glued to the lip of the clear plastic helmet on the outside. The air inlet line is a ½" clear vinyl hose which enters the helmet assembly through the air outlet hose. It runs straight up and over the top of the bicycle helmet (through the groove mentioned previously) and ends in a plenum at the forehead. The plenum directs the fresh air down over the face and towards the air outlet hose for constant air circulation.

The clear plastic helmet is closed off at the neck with zero-porosity nylon fabric. It is shaped like a cone with the tip cut off. It is attached around the subject's neck and the lip of the clear plastic helmet with loose elastic and has a pass-through for the 1.5" air outlet hose in the back. The purpose of this is to route the majority of the air leaving the helmet through the air outlet hose, however it is not a complete seal and no pressure differential was

measured across it. The air outlet hose is 10' long and has oxygen and carbon dioxide sensors mounted near the end furthest from the helmet. This end is open to ambient air.

The inlet air is provided from compressed air cylinders at a flow rate of 6 scfm. This is the flow rate used in NASA space suits. The Bauer Life Support Compressor for Breathing Air used is certified for grade E air by Trace Analytics, Inc. The compressed air is stored in a cascade of four cylinders after exiting the compressor; therefore, in the unlikely event of a power failure, air will continue flowing for over an hour, which is much more than ample time to terminate the session. The air flow will be started and verified prior to ingress at the beginning of each experimental session.

Though the helmet assembly is not sound proof, it may be difficult for the subject wearing it to carry a conversation with the researcher over the noise of the flowing air and the treadmill. To mitigate this, a two-way communications head set has been integrated into the helmet. Speakers have been incorporated into the straps of the bicycle helmet and a microphone is taped to the inside of the clear plastic helmet right in front of the subject's lips. The communication line also runs through the air outlet hose and is plugged into the communication station on the deck of the Neutral Buoyancy Research Facility. The researcher will be wearing a headset throughout the entire exercise session. In the event of a loss of communications, the researcher and subject can communicate in elevated voice tones directly. If this is not sufficient to the comfort of both the subject and the researcher, the session will be terminated.

Student Investigator wearing experimental helmet assembly

During the control session the subject will wear a Hans Rudolph™ Oro-Nasal mask with a one-way valve, which tightly covers the mouth and nose. Inspired air is ambient and expired air is routed through a mass spectrometer for gas analysis. This is the standard method of obtaining energy expenditure by measuring oxygen consumption. The Human Performance Lab has been using this system in numerous studies for many years. An experienced exercise physiologist will be responsible for monitoring the exercise sessions. The control set-up at the Human Performance Lab is illustrated below.

The control set-up at the Human Performance Lab
Image from http://www.bre.umd.edu/humanper.htm

The equipment will be cleaned following each session. The Polar™ chest strap will be washed with soap and water and dried thoroughly. The product instructions state that alcohol or a solvent-based detergent should not be used on the chest strap. The inside of the experimental helmet assembly will also be cleaned. The inside of the clear plastic helmet will be washed with antibacterial soap and water. This surface cannot be cleaned with any alcohol because it would react with the plastic and make the surface opaque. All other surfaces, including the microphone, will be wiped with 70% isopropyl alcohol. The equipment used in the Human Performance Lab, including the Hans Rudolph™ Oro-Nasal mask, will also be disinfected after each use.

4. Risks and Benefits:

There may be some risks from participating in this research study. As with all exercise, subjects may experience mild fatigue. Both the helmet assembly and the Hans Rudolph™ Oro-Nasal mask may cause some minimal discomfort during wear because of fit or additional mass. There is a slight possibility of over-pressure in the helmet which could lead to a lung overexpansion injury such as edema or pulmonary embolism; however, this is unlikely because the helmet assembly is not sealed in. Pressure testing has been performed and showed no pressure differential between the inside of the experimental helmet assembly and ambient air. The subject will be breathing ambient (not compressed) air. There is also a slight risk of a cardiovascular event due to the elevated physical workload of treadmill exercise. This risk is not unlike to that of any cardiovascular activity and the subjects have been selected for lack of additional risk factors. Through 15 years of diving operations, the Space Systems Lab has developed safety measures and emergency protocols and most students and staff are trained in first aid and CPR.

5. Confidentiality:

To help protect confidentiality, the subjects' name will not be included on the collected data. Instead, a code will be placed on the collected data and the researcher will be able to link data to subject identities through the use of an identification key. Only the principal investigator and the student investigator will have access to the identification key. All data will be stored on password-protected computers. If a report or article about this research project is written, subject identities will be protected to the maximum extent possible.

6. Information and Consent Forms:

Informed consent will be obtained from each subject in writing before the commencement of the experiment. The purpose, background information, detailed procedures, equipment, and risks will be described as above. Any of the subjects' questions will be answered. The subjects will then be presented with the consent form and given the opportunity to read it and ask more questions if needed. All subjects will be fluid English speakers and the consent form will not need to be translated into another language.

7. Conflict of Interest:

This research is not conducted in collaboration with the private sector. No party has financial or employment interest in the outcome of this research. There are no known conflicts of interest.

8. HIPAA Compliance:

No HIPAA protected information will be used. No information will be obtained from health care providers.

9. Research Outside of the United States: N/A

10. Research Involving Prisoners: N/A

B.3 Subject Recruitment Email

Recruitment Email

Subject: Call for subjects for space suit study!

Greetings!

I am looking for subjects for my research. The experiment is called *Space Suit Energy Expenditure Measuring System Validation Study*. The procedures involve two sessions, during which you will be asked to perform 30 minutes of exercise on a treadmill. Each 30 minute session will be broken up into three blocks at increasing speeds of 3 mph (20 minute mile), 4 mph (15 minute mile), and 5 mph (12 minute mile). The experimental session will take place at the Space Systems Lab. There you will be asked to perform treadmill exercise while wearing a helmet assembly connected to an air system with constant air circulation at a rate of 6 scfm. The helmet will provide constant two-way communication with the investigator (me). The control session will take place at the Human Performance Laboratory. There you will perform the exact same treadmill exercise while wearing a Hans Rudolph™ Oro-Nasal mask, which will be connected to a system that analyzes exhaled air. The intake air is ambient. Each of these sessions will take about 1 hour. You will wear a Polar™ heart rate monitor during both of these sessions and your resting heart rate will be measured at the beginning of each session. You will also fill out a short questionnaire about basic personal information, medical history, your exercise profile, and your feedback on the experiment.

I am looking for about 8-10 subjects with an even distribution of males and females. You need to be between the ages of 18 and 40, in reasonably good health and fitness level, and participate in a routine physical activity. This could include organized sports, personal exercise, commuting by cycling, etc. Attached is a questionnaire that all subjects will be asked to fill out. Please look over the medical history section in particular. If you answer *yes* to any of the questions, you will not be able to participate in this study.

If you are eligible and interested, let me know. It would be a great help. Thanks!

Agnieszka

Agnieszka Kościelniak
Graduate Research Assistant
Space Systems Lab
University of Maryland
Email: notaggy@umd.edu
Phone: 301-405-7353

B.4 Consent Form

Initials _____ Date _____

CONSENT FORM

Project Title	***Space Suit Energy Expenditure Measuring System Validation Study***
Why is this research being done?	*This is a research project being conducted by Dr. David Akin and Agnieszka Kościelniak of the Space Systems Laboratory at the University of Maryland, College Park. We are inviting you to participate in this research project because you are between the ages of 18 and 40, are generally healthy, fit, participate in a routine physical activity, and are free of the following medical conditions or any other heightened risk factors.* • *High blood pressure* • *Heart murmur* • *Emphysema* • *Diabetes* • *Asthma* • *Elevated cholesterol* • *Claustrophobia* • *Epilepsy* • *Pregnancy* • *Heart attack* • *Stroke* • *Aneurysm* • *Open or bleeding lesions near or including the mouth* • *Seizure* • *Head injury* • *Diseases of the arteries* • *Diseases of the lungs* • *Frequent headaches* • *Heart palpitations* • *Chest pain* • *Dizzy spells* • *Shortness of breath* • *Painful joints* • *Blood clots* • *Smoking* *The purpose of this research project is to validate the results obtained from a new space suit energy expenditure measuring system against those from the standard open-circuit method.*
What will I be asked to do?	*The procedures involve two sessions, during which you will be asked to perform 30 minutes of exercise on a treadmill. Each 30 minute session will be broken up into three blocks at increasing speeds of 3 mph (20 minutes per mile), 4 mph (15 minutes per mile), and 5 mph (12 minutes per mile). The experimental session will take place at the Space Systems Lab at the University of Maryland, College Park. There you will be asked to perform treadmill exercise while wearing a helmet assembly connected to an air system with constant air circulation at a rate of 6 scfm. The helmet will provide constant two-way communication with the investigator. The control session will take place at the Human Performance Laboratory in the Biological Engineering Department at the University of Maryland, College Park. There you will perform the exact same treadmill exercise while wearing a Hans Rudolph™ Oro-Nasal mask, which will be connected to a system that analyzes exhaled air. The intake air is ambient. Each of these sessions will take about 1 hour. You will wear a Polar™ heart rate monitor during both of these sessions and your resting heart rate will be measured at the beginning of each session and monitored throughout. You will also fill out a short questionnaire about basic personal information, medical history, your exercise profile, and your feedback on the experiment.*

What about confidentiality?	*We will do our best to keep your personal information confidential. To help protect your confidentiality: (1) your name will not be included on the collected data; (2) a code will be placed on the collected data; (3) through the use of an identification key, the researchers will be able to link your data to your identity; (4) only the researchers will have access to the identification key; and (5) all data will be password-protected. If we write a report or article about this research project, your identity will be protected to the maximum extent possible.* *Your information may be shared with representatives of the University of Maryland, College Park or governmental authorities if you or someone else is in danger or if we are required to do so by law.*
What are the risks of this research?	*There may be some risks from participating in this research study. As with all exercise, you may experience fatigue. Both the helmet and the Hans Rudolph™ Oro-Nasal mask may cause some minimal discomfort during wear because of fit or additional mass.* *There is a slight possibility of over-pressure in the helmet which could lead to a lung overexpansion injury such as edema or pulmonary embolism. A higher pressure inside the helmet than ambient air could force some air into the bloodstream, blocking the flow of blood. Once an air bubble has entered the blood stream of the lungs, it can travel to the heart, brain and other parts of the body. If the air bubble happens to be blocking the flow of blood at the lungs, it is called a pulmonary embolism. Edema is the swelling of tissue due to accumulated fluid, which could be caused by the pressure differential. However, these are unlikely because the helmet assembly is not sealed in. Pressure testing has been performed and showed no pressure differential between the inside of the experimental helmet assembly and ambient air. You will be breathing ambient (not compressed) air.* *There is also a slight risk of a cardiovascular event due to the elevated physical workload of treadmill exercise. This risk is not unlike to that of any cardiovascular activity and the subjects have been selected for lack of additional risk factors.*
What are the benefits of this research?	*This research is not designed to help you personally, but the results may help the investigator learn more about possible unobtrusive methods for measuring astronaut energy expenditure in a space suit during extravehicular activity (EVA). We hope that, in the future, other people might benefit from this study through improved understanding of astronaut EVA workload without affecting the tasks they travel to space to perform.*
Do I have to be in this research? May I stop participating at any time?	*Your participation in this research is completely voluntary. You may choose not to take part at all. If you decide to participate in this research, you may stop participating at any time. If you decide not to participate in this study or if you stop participating at any time, you will not be penalized or lose any benefits to which you otherwise qualify.*

Initials _____ Date _____

Is any medical treatment available if I am injured?	*The University of Maryland does not provide any medical, hospitalization or other insurance for participants in this research study, nor will the University of Maryland provide any medical treatment or compensation for any injury sustained as a result of participation in this research study, except as required by law.*	
What if I have questions?	*This research is being conducted by Dr. David Akin and Agnieszka Kościelniak of the Department of Aerospace Engineering at the University of Maryland, College Park. If you have any questions about the research study itself, please contact:* **Dr. David Akin** **University of Maryland** **Building 382 Room 2100D** **College Park, MD 20742** **(e-mail) dakin@ssl.umd.edu** **(telephone) 301-405-1138** *or* **Agnieszka Kościelniak** **University of Maryland** **Building 382 Room 1100C** **College Park, MD 20742** **(e-mail) notaggy@umd.edu** **(telephone) 301-405-7353** *If you have questions about your rights as a research subject or wish to report a research-related injury, please contact:* **Institutional Review Board Office** **University of Maryland** **College Park, MD 20742** **(e-mail) irb@deans.umd.edu** **(telephone) 301-405-0678** *This research has been reviewed according to the University of Maryland, College Park IRB procedures for research involving human subjects.*	
Statement of Age of Subject and Consent	*Your signature indicates that:* • *you are at least 18 years of age;* • *the research has been explained to you;* • *your questions have been fully answered; and* • *you freely and voluntarily choose to participate in this research project.*	
Signature and Date	**NAME OF SUBJECT**	
	SIGNATURE OF SUBJECT	
	DATE	

IRB APPROVED
VALID UNTIL
NOV 09 2007
UNIVERSITY OF MARYLAND
COLLEGE PARK

B.5 Subject Questionnaire

Space Suit Energy Expenditure Measuring System Validation Study

Subject Questionnaire

Basic Information:

Sex: _____ Age: _____ Weight: _____ Height: _____

Medical History: (circle appropriate response)

Do you have any of the following conditions?

High blood pressure	yes	no
Heart murmur	yes	no
Emphysema	yes	no
Diabetes	yes	no
Asthma	yes	no
Elevated Cholesterol or Triglycerides	yes	no
Claustrophobia	yes	no
Epilepsy	yes	no
Pregnancy	yes	no
Open or bleeding lesions near or including the mouth	yes	no

Have you had any of the following?

Heart attack	yes	no
Stroke	yes	no
Aneurysm	yes	no
Seizure	yes	no
Head injury	yes	no
Diseases of the arteries	yes	no
Diseases of the lungs	yes	no

Have you ever experienced any of the following?

Frequent headaches	yes	no
Heart palpitations	yes	no
Chest pain w/exercise	yes	no
Dizzy spells	yes	no
Shortness of breath	yes	no
Painful joints	yes	no
Blood clots	yes	no

Do you use tobacco products?	yes	no

Are you taking any medications which might have adverse side affects as a result of low to medium intensity exercise?

_____

Do you have any other past or present health issues that may interfere with your ability to perform low to medium intensity treadmill exercise?

_____

Exercise Profile: (circle best answer)

How often do you exercise?

0-1 times a week
2-4 times a week
5-7 times a week

What is the typical duration of exercise?

N/A
Under 30 minutes
30 minutes to 1 hour
1-2 hours
more than 2 hours

What type of exercise is it? _____

How long have you been doing this exercise at this frequency and duration?

_____

Do you normally use a heart rate monitor while exercising? If so, how did the heart rates during this exercise compare to your usual routine?

_____

Have you ever had a VO2 max test? VO2 max is the highest rate at which oxygen can be taken up and utilized by a person during exercise. It can be increased with training and is often used as a measure of fitness. If so, when was the test administered and what is your VO2 max?

_____

Response to Experiment: (check appropriate box: 1 not at all, 5 very)

Question	**1**	**2**	**3**	**4**	**5**
Was the experimental session* strenuous?					
Was the apparatus worn during the experimental session comfortable?					
Did the apparatus worn during the experimental session make the work more strenuous?					
Was the control session** strenuous?					
Was the apparatus worn during the control session comfortable?					
Did the apparatus worn during the control session make the work more strenuous?					
Was the workload during the experimental and control sessions similar?					
Was the heart rate monitor comfortable?					
Did the heart rate monitor make the work more strenuous?					

* experimental session took place at the Space Systems Lab with the helmet assembly
** control session took place at the Human Performance Lab with the Oro-Nasal mask

Additional Comments:

B.6 IRB Approval

UNIVERSITY OF MARYLAND
INSTITUTIONAL REVIEW BOARD

2100 Blair Lee Building
College Park, Maryland 20742-5121
301.405.4212 TEL 301.314.1475 FAX
irb@deans.umd.edu
www.umresearch.umd.edu/IRB

November 27, 2006

MEMORANDUM

Application Approval Notification

To:	Dr. David L. Akin Agnieszka Koscielniak Department of Aerospace Engineering
From:	Roslyn Edson, M.S., CIP, RE IRB Manager University of Maryland, College Park
Re:	**IRB Protocol Number:** 06-0486 **Project Title:** "Space Suit Energy Expenditure Measuring System Validation Study"
Approval Date:	November 9, 2006
Expiration Date:	November 9, 2007
Application Type:	Initial
Research Type:	Nonexempt
Type of Review:	Full Board **Degree of Risk:** No greater than minimal

The University of Maryland, College Park Institutional Review Board (IRB) approved your IRB application. Please reference the above-cited IRB application number in any future communications with our office regarding this research. The research was approved in accordance with the University's IRB policies and procedures and 45 CFR 46, the Federal Policy for the Protection of Human Subjects.

Recruitment/Consent: For research requiring written informed consent, the IRB-approved and stamped informed consent document is enclosed. The IRB approval expiration date has been stamped on the informed consent document. Please keep copies of the consent forms used for this research for three years after the completion of the research.

Continuing Review: If you want to either continue to collect data from human subjects or to analyze private, identifiable data collected from human subjects after the expiration date for this approval, you must submit a renewal application to the IRB Office at least 30 days before the approval expiration date.

Modifications: Any changes to the approved protocol must be approved by the IRB before the change is implemented, except when a change is necessary to eliminate apparent immediate hazards to the subjects. If you would like to modify the approved protocol, please submit an addendum request to the IRB Office. The instructions for submitting an addendum are posted at:
http://www.umresearch.umd.edu/IRB/Irb_Addendum%20Protocol.htm.

(Continued)

Unanticipated Problems Involving Risks: You must promptly report any unanticipated problems involving risks to subjects or others to the IRB Manager at 301-405-0678 or **redson@umresearch.umd.edu.**

Student Researchers: Unless otherwise requested, this IRB approval document was sent to the Principal Investigator (PI). The PI should pass on the approval document or a copy to the student researchers. This IRB approval document may be a requirement for student researchers applying for graduation. The IRB may not be able to provide copies of the approval documents if several years have passed since the date of the original approval.

Additional Information: Please contact the IRB Office at 301-405-4212 if you have any IRB-related questions or concerns.

B.7 Protocol Modification Request

MEMORANDUM

TO:	Roslyn Edson, IRB Manager
FROM:	Dr. David Akin, Principal Investigator, Dept. of Aerospace Eng. Agnieszka Kościelniak, Student Investigator, Dept. of Aerospace Eng.
DATE:	March 5, 2007
PROJECT TITLE:	Space Suit Energy Expenditure Measuring System Validation Study
IRB NUMBER:	06-0486
SUBJECT:	Protocol Modification

The following are three modifications made to the protocol of this study and submitted for IRB approval. A modified consent form is also included.

1. The three speeds during the exercise sessions have been reduced from 3.0 mph, 4.0 mph, and 5.0 mph to 3.0 mph, 3.7 mph, and 4.4 mph. These new speeds include a slow, medium, and fast walking speed. The slowest speed requires a workload noticeably above resting values. The highest was selected as the human walk-run gait transition speed for the shortest subject using an inverted pendulum mechanical model. Running is no longer a component of this study. Before the start of each walking session, each subject will be asked to sit quietly for 8 minutes while wearing the session-appropriate equipment for a measurement of resting metabolic rate. This change was made to maintain the workloads during this study at a similar level to those experienced by astronauts during extravehicular activity. Running consumes significantly more energy than any reasonable workload on orbit. This protocol modification reduces heart rate and workload of the subjects and therefore the associated risks are lower.

2. During the control sessions, which include exercise with a standard oxygen consumption measuring system, the subjects will be asked to wear a modified construction hard hat. A bag of small lead weights has been firmly attached to the outside of an adjustable hard hat, which bring the total mass to about 5 pounds. The purpose of this additional piece of equipment is to simulate the weight of the experimental helmet assembly during the control session for similar workloads in both sessions. The inside of this helmet will be disinfected after each subject by wiping with 70% isopropyl alcohol. This modification does not present any additional risk to the subjects. This helmet is pictured below.

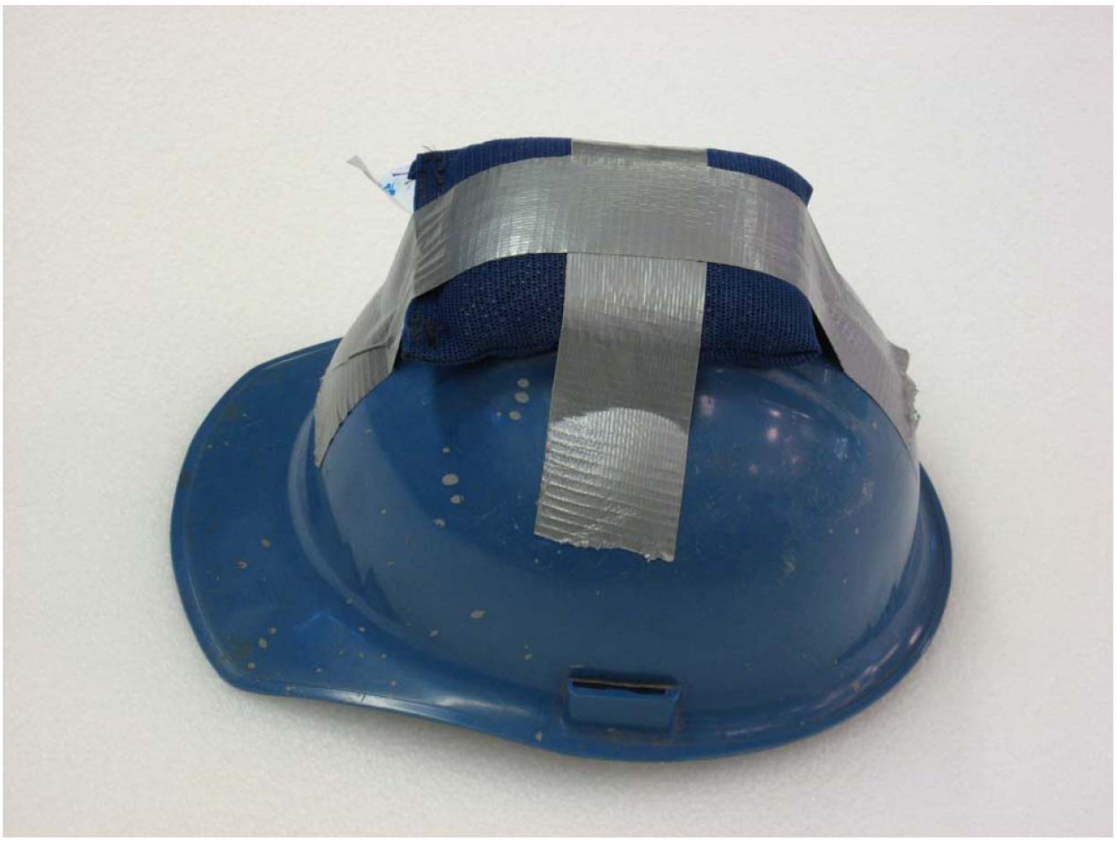

3. Due to equipment malfunctions at the Human Performance Laboratory at the Department of Biological Resources Engineering, the control sessions will now be performed at the Exercise Physiology Laboratory in the Kinesiology Department at the University of Maryland, College Park. This is only a change in location and does not affect the protocol or change the risk to subjects.

B.8 Protocol Modification Approval

UNIVERSITY OF MARYLAND
INSTITUTIONAL REVIEW BOARD

2100 Blair Lee Building
College Park, Maryland 20742-5121
301.405.4212 TEL 301.314.1475 FAX
irb@deans.umd.edu
www.umresearch.umd.edu/IRB

March 15, 2007

MEMORANDUM

Addendum Approval Notification

To:	Dr. David L. Akin Agnieszka Koscielniak Department of Aerospace Engineering
From:	Roslyn Edson, M.S., CIP, IRB Manager University of Maryland, College Park
Re:	**IRB Application Number:** 06-0486 **Project Title:** "Space Suit Energy Expenditure Measuring System Validation Study"
Approval Date Of Addendum:	March 12, 2007
Expiration Date of IRB Project Approval:	November 9, 2007
Application Type:	*Addendum/Modification; Approval of request, submitted to the IRB Office on 5 March 2007, to: (1) reduce the speed of the exercise sessions, 2) have subjects wear a hard hat during the control sessions, and (3) conduct the control sessions at the Exercise Physiology Laboratory in the Kinesiology Department.*
Type of Review of Addendum:	Expedited
Type of Research:	Non-exempt

The University of Maryland, College Park Institutional Review Board (IRB) Office approved your IRB application. The research was approved in accordance with the University's IRB policies and procedures and 45 CFR 46, the Federal Policy for the Protection of Human Subjects. Please reference the above-cited IRB application number in any future communications with our office regarding this research.

Recruitment/Consent: For research requiring written informed consent, the IRB-approved and stamped informed consent document is enclosed. The IRB approval expiration date has been stamped on the informed consent document. Please keep copies of the consent forms used for this research for three years after the completion of the research.

Continuing Review: If you want to continue to collect data from human subjects or to analyze private, identifiable data collected from human subjects, after the expiration date for this approval (indicated above), you must submit a renewal application to the IRB Office at least 30 days before the approval expiration date. ***(continued)***

Modifications: Any changes to the approved protocol must be approved by the IRB before the change is implemented, except when a change is necessary to eliminate an apparent immediate hazard to the subjects. If you would like to modify an approved protocol, please submit an addendum request to the IRB Office. The instructions for submitting an addendum are posted at: **http://www.umresearch.umd.edu/IRB/irb_Addendum%20Protocol.htm**.

Unanticipated Problems Involving Risks: You must promptly report any unanticipated problems involving risks to subjects or others to the IRB Manager at 301-405-0678 or **redson@umresearch.umd.edu**.

Student Researchers: Unless otherwise requested, this IRB approval document was sent to the Principal Investigator (PI). The PI should pass on the approval document or a copy to the student researchers. This IRB approval document may be a requirement for student researchers applying for graduation. The IRB may not be able to provide copies of the approval documents if several years have passed since the date of the original approval.

Additional Information: Please contact the IRB Office at 301-405-4212 if you have any IRB-related questions or concerns.

Appendix C : MATLAB CODE

C.1 Experimental Data Analysis Code

```
close all; clear all; clc; format compact;

%IMPORT THE TEXT PARAMETERS
%import the file parameters.txt from the correct folder
parameters = xlsread('M8parameters.xls');
%separate this data into appropriate variables
HRdata = parameters(1); %1 if HR data taken, 0 otherwise
makeplot = parameters(2); %1 if you want to plot, 0 otherwise
sex = parameters(3); %female = 1, male = 2
wt_lb = parameters(4); %subject weight in pounds
flow_scfm = parameters(5); %final flow reading in scfm, used in v5 & before
sit_start = parameters(6); %time (sec) when sitting data starts
sit_end = parameters(7); %time (sec) when sitting data ends
s3_0mph = parameters(8); %time (sec) when 3.0 mph starts
s3_7mph = parameters(9); %time (sec) when 3.7 mph starts
s4_4mph = parameters(10); %time (sec) when 4.4 mph starts
end_walk = parameters(11); %time (sec) test finished
HRclean = parameters(12); %hand cleaned = 1, matlab cleaned = 2
O2calib_before = parameters(13); %O2 calibration voltage before
O2calib_after = parameters(14); %O2 calibration voltage after
CO2calib_before = parameters(15); %CO2 calibration voltage before
CO2calib_after = parameters(16); %CO2 calibration voltage after
RH0 = parameters(17); %RH at rest extrapolated from hobo and CO2 data
RH1 = parameters(18); %RH at 3.0 mph from hobo data
RH2 = parameters(19); %RH at 3.7 mph from hobo data
RH3 = parameters(20); %RH at 4.4 mph extrapolated from hobo and CO2 data
scfm1 = parameters(21); %first flow rate (scfm)
scfm2 = parameters(22); %second flow rate (scfm)
scfm3 = parameters(23); %third flow rate (scfm)
scfm4 = parameters(24); %fourth flow rate (scfm)
flowtime1 = parameters(25); %time start first flow rate (scfm)
flowtime2 = parameters(26); %time start second flow rate (scfm)
flowtime3 = parameters(27); %time start third flow rate (scfm)
flowtime4 = parameters(28); %time start fourth flow rate (scfm)
age = parameters(29); %subject age at time of test
HRrest = parameters(30); %resting heart rate of subject
clear parameters flow_scfm

%IMPORT THE TEXT DATA
%first column is O2 voltages
%second column is CO2 voltages
%third column is HR voltages
%fourth column is time in seconds
RawVoltages = importdata('M8_MHcleandata.txt');

%DEVELOP RELATIVE HUMIDITY PROFILE
%based on assumed values of 10%, 20%, 30% and 45% and transition times
RH = RH0*ones(length(RawVoltages),1);
%only develop RH profile for workloads that took place
```

```
if s3_0mph > 0
    RH(s3_0mph*100:length(RH)) = RH1*ones(length(RH) - s3_0mph*100 + 1,1);
    if (s3_0mph + 180)*100 < length(RH)
        for x = 0:18000
            RH(s3_0mph*100 + x) = ...
                (RH0 - ((RH1-RH0)/18000)*s3_0mph*100) + ...
                ((RH1-RH0)/18000)*(s3_0mph*100 + x);
        end;
    end;
    clear x
end;
if s3_7mph > 0
    RH(s3_7mph*100:length(RH)) = RH2*ones(length(RH) - s3_7mph*100 + 1,1);
    if (s3_7mph + 180)*100 < length(RH)
        for x = 0:18000
            RH(s3_7mph*100 + x) = ...
                (RH1 - ((RH2-RH1)/18000)*s3_7mph*100) + ...
                ((RH2-RH1)/18000)*(s3_7mph*100 + x);
        end;
    end;
    clear x
end;
if s4_4mph > 0
    RH(s4_4mph*100:length(RH)) = RH3*ones(length(RH) - s4_4mph*100 + 1,1);
    if (s4_4mph + 180)*100 < length(RH)
        for x = 0:18000
            RH(s4_4mph*100 + x) = ...
                (RH2 - ((RH3-RH2)/18000)*s4_4mph*100) + ...
                ((RH3-RH2)/18000)*(s4_4mph*100 + x);
        end;
    end;
    clear x
end;

%AIR DATA
%make vector of flow values in scfm
%parameters matrix can store up to 4 values
%only used if flow was changed during session
flow_scfm = ones(floor(length(RawVoltages)/100), 1); %initialize
flow_scfm = scfm1*flow_scfm; %replace all ones with 1st value
if scfm2 > 0
    flow_scfm(flowtime2:length(flow_scfm),1) = ...
        scfm2*ones(length(flow_scfm) - flowtime2 + 1,1);
end;
if scfm3 > 0
    flow_scfm(flowtime3:length(flow_scfm),1) = ...
        scfm3*ones(length(flow_scfm) - flowtime3 + 1,1);
end;
if scfm4 > 0
    flow_scfm(flowtime4:length(flow_scfm),1) = ...
        scfm4*ones(length(flow_scfm) - flowtime4 + 1,1);
end;
flow_lpm = flow_scfm*28.3; %liters per minute

%OXYGEN DATA
%the calibration factor for oxygen from raw voltage varies with time
```

```
%it is equal to %O2max/volt_max
% %O2max varies with humidity
%volt_max is a linear function of estimated sensor drift

%equation for O2max is linear, extrapolated from vernier calibration data,
%R^2 = 1
O2max = -0.008*RH + 20.9;
%create O2max matrix with 1 data point per second
c = 0;
O2max_short = zeros(floor(length(RawVoltages)/100),1);
for n = 1:length(RawVoltages)
    if mod(n,100) == 0
        c = c + 1;
        O2max_short(c) = O2max(n);
    end;
end;
clear c n
%Vmax is a linear function of average voltages found during the before and
%after calibrations
Vmax = (O2calib_after - O2calib_before)/RawVoltages(:,4) + O2calib_before;
%convert raw voltage to %O2
O2 = (O2max./Vmax').*RawVoltages(:,1);

%average each second of data for smoother curve
O2count = 0;
O2tally = 0;
for x = 1:length(O2)
    O2tally = O2tally + O2(x);
    if x>0 & mod(x,100) == 0
        O2count = O2count + 1;
        O2_avg(O2count,:) = [RawVoltages(x,4)-.5 O2tally/100];
        O2tally = 0;
    end
end;
clear x O2tally O2count
if makeplot == 1
    %plot initial and smoothed data
    figure(1); grid on; hold on; box on;
    plot(RawVoltages(:,4),O2)
    plot(O2_avg(:,1),O2_avg(:,2),'r','LineWidth',1.5)
    xlabel('time (seconds)'); ylabel('% O_2'); title('O_2');
    legend('raw data','smoothed data','Location','SouthWest')
    %plot vertical lines at speed transition times
    plot([sit_start sit_start],[min(O2_avg(:,2)) max(O2_avg(:,2))],'g');
    plot([sit_end sit_end],[min(O2_avg(:,2)) max(O2_avg(:,2))],'g');
    if s3_0mph > 0
        plot([s3_0mph s3_0mph],[min(O2_avg(:,2)) max(O2_avg(:,2))],'g');
    end;
    if s3_7mph > 0
        plot([s3_7mph s3_7mph],[min(O2_avg(:,2)) max(O2_avg(:,2))],'g');
    end;
    if s4_4mph > 0
        plot([s4_4mph s4_4mph],[min(O2_avg(:,2)) max(O2_avg(:,2))],'g');
    end;
    if end_walk > 0
        plot([end_walk end_walk],[min(O2_avg(:,2)) max(O2_avg(:,2))],'g');
```

```
    end;
end;

%CARBON DIOXIDE DATA
%convert raw voltage to %CO2
CO2 = 0.6*RawVoltages(:,2);
%average each second of data for smoother curve
CO2count = 0;
CO2tally = 0;
for x = 1:length(CO2)
    CO2tally = CO2tally + CO2(x);
    if x>0 & mod(x,100) == 0
        CO2count = CO2count + 1;
        CO2_avg(CO2count,:) = [RawVoltages(x,4)-.5 CO2tally/100];
        CO2tally = 0;
    end
end;
clear x CO2tally CO2count
%get percent CO2 in cascade air from before and after calibrations
%(CO2 sensor is pre-calibrated by manufacturer)
% extrapolated line from before and after
CO2air = 0.6*(CO2calib_before + ...
    (CO2calib_after - CO2calib_before)/max(CO2_avg(:,1)).*CO2_avg(:,1));
if makeplot == 1
    %plot initial and smoothed data
    figure(2); grid on; hold on; box on;
    plot(RawVoltages(:,4),CO2)
    plot(CO2_avg(:,1),CO2_avg(:,2),'r','LineWidth',1.5)
    xlabel('time (seconds)'); ylabel('% CO_2'); title('CO_2');
    legend('raw data','smoothed data','Location','SouthEast')
    %plot vertical lines at transitions between speeds
    plot([sit_start sit_start],[min(CO2_avg(:,2)) max(CO2_avg(:,2))],'g');
    plot([sit_end sit_end],[min(CO2_avg(:,2)) max(CO2_avg(:,2))],'g');
    if s3_0mph > 0
        plot([s3_0mph s3_0mph],[min(CO2_avg(:,2)) max(CO2_avg(:,2))],'g');
    end;
    if s3_7mph > 0
        plot([s3_7mph s3_7mph],[min(CO2_avg(:,2)) max(CO2_avg(:,2))],'g');
    end;
    if s4_4mph > 0
        plot([s4_4mph s4_4mph],[min(CO2_avg(:,2)) max(CO2_avg(:,2))],'g');
    end;
    if end_walk > 0
        plot([end_walk end_walk],[min(CO2_avg(:,2)) max(CO2_avg(:,2))],'g');
    end;
end;

if HRdata == 1
    %HEART RATE DATA
    threshold = 1.5;
    %calculate Heart Rate
    count = 1;
    bpm_count = 0;
    HRb = zeros(1,length(RawVoltages));
    if RawVoltages(1,3) > threshold
        HRb(1,1) = 1;
```

```
end;
for h = 2:length(RawVoltages)
    if RawVoltages(h,3) > threshold
        HRb(1,h) = 1;
        if HRb(1,h-1) == 0
            beats(1,count) = RawVoltages(h,4);
            if count > 1
                if (beats(count) - beats(count-1)) < .9
                    bpm(count) = 60/(beats(count) - beats(count-1));
                else
                    %if beats are missing (more than 0.9 s between beats),
                    %make them nan, won't plot
                    bpm(count) = nan;
                end;
            end;
            count = count + 1;
        end;
    end;
    if RawVoltages(h,4) > 15 & mod(RawVoltages(h,4),5) == 0
        bpm_count = bpm_count + 1;
        stop = RawVoltages(h,4)-15;
        y = count - 1;
        nan_count = 0;
        while beats(y) > stop
            if isnan(bpm(y))
                %if there is data missing in the past 15 s
                nan_count = 1;
            end;
            y = y-1;
        end;
        if nan_count == 0
            if (y + 1) > length(beats)
                %this is if there are no beats in the past 15 s
                bpm6(bpm_count,:) = [RawVoltages(h,4)-7.5 nan];
            else
                bpm6(bpm_count,:) = [RawVoltages(h,4)-7.5 ...
                    (count-2-y)*60/(beats(count-1)-beats(y+1))];
            end;
        elseif nan_count == 1
            %this is if there is missing data in the past 15 s
            bpm6(bpm_count,:) = [RawVoltages(h,4)-7.5 nan];
        end;
        clear nan_count
    end;
end;
%find averages of HR for last 5 min of each speed
cr = 0; c1 = 0; c2 = 0; c3 = 0;
for b = 1:length(beats)
    if beats(b) > sit_start & beats(b) <= sit_end
        cr = cr + 1;
    elseif beats(b) > (s3_7mph - 300) & beats(b) <= s3_7mph
        c1 = c1 + 1;
    elseif beats(b) > (s4_4mph - 300) & beats(b) <= s4_4mph
        c2 = c2 + 1;
    elseif beats(b) > (end_walk - 300) & beats(b) <= end_walk
        c3 = c3 +1;
```

```
    end;
end;
HR_rest = cr/((sit_end-sit_start)/60)
%display heart rates for last 5 min of each speed
if s3_7mph > 0
    HR_3_0mph = c1/5
end;
if s4_4mph > 0
    HR_3_7mph = c2/5
end;
if end_walk > 0
    HR_4_4mph = c3/5
end;
if makeplot == 1
    %plot heart rate
    figure(3); grid on; hold on; box on;
    plot(beats(1,2:length(beats)),bpm(1,2:length(beats)),'b')
    plot(bpm6(:,1),bpm6(:,2),'r','LineWidth',1.5)
    xlabel('time (seconds)'); ylabel('heart rate (bpm)'); title('Heart Rate');
    legend('beat to beat', '15 second averages','Location','SouthEast')
    %plot vertical lines at transitions between speeds
    plot([sit_start sit_start],[min(bpm6(:,2)) max(bpm6(:,2))],'g');
    plot([sit_end sit_end],[min(bpm6(:,2)) max(bpm6(:,2))],'g');
    if s3_0mph > 0
        plot([s3_0mph s3_0mph],[min(bpm6(:,2)) max(bpm6(:,2))],'g');
    end
    if s3_7mph > 0
        plot([s3_7mph s3_7mph],[min(bpm6(:,2)) max(bpm6(:,2))],'g');
    end;
    if s4_4mph > 0
        plot([s4_4mph s4_4mph],[min(bpm6(:,2)) max(bpm6(:,2))],'g');
    end;
    if end_walk > 0
        plot([end_walk end_walk],[min(bpm6(:,2)) max(bpm6(:,2))],'g');
    end;
    plot([(sit_start + 1) sit_end], [HR_rest HR_rest],'m', 'LineWidth',3);
    if s3_7mph > 0
        plot([(s3_7mph - 300) s3_7mph], [HR_3_0mph HR_3_0mph],'m', 'LineWidth',3);
    end;
    if s4_4mph > 0
        plot([(s4_4mph - 300) s4_4mph], [HR_3_7mph HR_3_7mph],'m', 'LineWidth',3);
    end;
    if end_walk > 0
        plot([(end_walk - 300) end_walk], [HR_4_4mph HR_4_4mph],'m', 'LineWidth',3);
    end;
end;
clear h stop y bpm_count count HRb b cr c1 c2 c3
%get metabolic workload from heart rate using equations in Johnson
%find VO2max in L/min
if sex == 1 %female
    VO2max = 2.6 - 0.01*age;
elseif sex == 2 %male
    VO2max = 4.2 - 0.03*age;
end;
HRmax = 220 - age; %find max heart rate
%find VO2
```

```
    VO2fromHR = VO2max*(bpm6(:,2) - HRrest)/(HRmax - HRrest); %L/min
    MRfromHR = VO2fromHR*60*5; %metabolic rate in kcal/hr, using 5 kcal/L O2
    %find average metabolic workload for last 5 min of each speed from HR
    MR_HR_rest = 60*5*VO2max*(HR_rest - HRrest)/(HRmax - HRrest)
    if s3_7mph > 0
        MR_HR_3_0mph = 60*5*VO2max*(HR_3_0mph - HRrest)/(HRmax - HRrest)
    end;
    if  s4_4mph > 0
        MR_HR_3_7mph = 60*5*VO2max*(HR_3_7mph - HRrest)/(HRmax - HRrest)
    end;
    if end_walk > 0
        MR_HR_4_4mph = 60*5*VO2max*(HR_4_4mph - HRrest)/(HRmax - HRrest)
    end;
end;

if makeplot == 1
    %plot all three at once
    figure(4);
    subplot(3,1,1);grid on; hold on; box on;
    plot(O2_avg(:,1),O2_avg(:,2))
    plot(O2_avg(:,1),O2max_short,'r')
    ylabel('% O_2')
    plot([sit_start sit_start],[min(O2_avg(:,2)) max(O2_avg(:,2))],'g');
    plot([sit_end sit_end],[min(O2_avg(:,2)) max(O2_avg(:,2))],'g');
    if s3_0mph > 0
        plot([s3_0mph s3_0mph],[min(O2_avg(:,2)) max(O2_avg(:,2))],'g');
    end;
    if s3_7mph > 0
        plot([s3_7mph s3_7mph],[min(O2_avg(:,2)) max(O2_avg(:,2))],'g');
    end;
    if s4_4mph > 0
        plot([s4_4mph s4_4mph],[min(O2_avg(:,2)) max(O2_avg(:,2))],'g');
    end;
    if end_walk > 0
        plot([end_walk end_walk],[min(O2_avg(:,2)) max(O2_avg(:,2))],'g');
    end;
    subplot(3,1,2);grid on; hold on; box on;
    plot(CO2_avg(:,1),CO2_avg(:,2))
    plot(CO2_avg(:,1),CO2air,'r')
    ylabel('% CO_2')
    plot([sit_start sit_start],[min(CO2air) max(CO2_avg(:,2))],'g');
    plot([sit_end sit_end],[min(CO2air) max(CO2_avg(:,2))],'g');
    if s3_0mph > 0
        plot([s3_0mph s3_0mph],[min(CO2air) max(CO2_avg(:,2))],'g');
    end;
    if s3_7mph > 0
        plot([s3_7mph s3_7mph],[min(CO2air) max(CO2_avg(:,2))],'g');
    end;
    if s4_4mph > 0
        plot([s4_4mph s4_4mph],[min(CO2air) max(CO2_avg(:,2))],'g');
    end;
    if end_walk > 0
        plot([end_walk end_walk],[min(CO2air) max(CO2_avg(:,2))],'g');
    end;
    if HRdata == 1
        subplot(3,1,3);grid on; hold on; box on;
```

```
        plot(bpm6(:,1),bpm6(:,2))
        xlabel('time (seconds)')
        ylabel('heart rate (bpm)')
        plot([sit_start sit_start],[min(bpm6(:,2)) max(bpm6(:,2))],'g');
        plot([sit_end sit_end],[min(bpm6(:,2)) max(bpm6(:,2))],'g');
        if s3_0mph > 0
            plot([s3_0mph s3_0mph],[min(bpm6(:,2)) max(bpm6(:,2))],'g');
        end;
        if s3_7mph > 0
            plot([s3_7mph s3_7mph],[min(bpm6(:,2)) max(bpm6(:,2))],'g');
        end;
        if s4_4mph > 0
            plot([s4_4mph s4_4mph],[min(bpm6(:,2)) max(bpm6(:,2))],'g');
        end;
        if end_walk > 0
            plot([end_walk end_walk],[min(bpm6(:,2)) max(bpm6(:,2))],'g');
        end;
    end;
end;

%%%%%%%%%%
%FIND VO2

%difference between oxygen in outlet air with and without human respiration
perc_change_O2 = (O2max_short - O2_avg(:,2))/100;
VO2 = perc_change_O2.*flow_lpm;
clear perc_change_O2

%FIND TOTAL METABOLIC RATE FROM O2
TMR_O2_kcph = VO2*5*60; %Johnson pg. 11: 5000 kcal/1 L O2
%find averages of metabolic rate from O2 for last 5 min of each speed
MR_O2_rest = mean(TMR_O2_kcph((sit_start + 1):sit_end))
if s3_7mph > 0
    MR_O2_3_0mph = mean(TMR_O2_kcph((s3_7mph - 300):s3_7mph))
end;
if s4_4mph > 0
    MR_O2_3_7mph = mean(TMR_O2_kcph((s4_4mph - 300):s4_4mph))
end;
if end_walk > 0
    MR_O2_4_4mph = mean(TMR_O2_kcph((end_walk - 300):end_walk))
end;

%FIND BMR
wt_kg = wt_lb/2.205;
%use Schoffield pg. 17, adults 18-30
if sex == 1
    BMR_mjpd = 0.062*wt_kg + 2.036; %mJ/24hr
elseif sex == 2
    BMR_mjpd = 0.063*wt_kg + 2.896; %mJ/24hr
end;
BMR_kcph = BMR_mjpd*239.006/24 %kilocalories per hour

%FIND VCO2
perc_change_CO2 = (CO2air - CO2_avg(:,2))/100;
VCO2 = perc_change_CO2.*flow_lpm;
clear perc_change_CO2
```

```
%FIND TOTAL METABOLIC RATE FROM CO2
RQ = 1; %assume
VO2_rq = -VCO2/RQ;
TMR_CO2_kcph = VO2_rq*5*60; %Johnson pg. 11: 5000 kcal/1 L O2
%find averages of metabolic rate from O2 for last 5 min of each speed
MR_CO2_rest = mean(TMR_CO2_kcph((sit_start + 1):sit_end))
if s3_7mph > 0
   MR_CO2_3_0mph = mean(TMR_CO2_kcph((s3_7mph - 300):s3_7mph))
end;
if s4_4mph > 0
   MR_CO2_3_7mph = mean(TMR_CO2_kcph((s4_4mph - 300):s4_4mph))
end;
if end_walk > 0
   MR_CO2_4_4mph = mean(TMR_CO2_kcph((end_walk - 300):end_walk))
end;

%FIND METS
TMR_O2_mets = TMR_O2_kcph/BMR_kcph;
TMR_CO2_mets = TMR_CO2_kcph/BMR_kcph;
if makeplot == 1
   figure(5); grid on; hold on; box on;
   plot(O2_avg(:,1),TMR_O2_mets,'b');
   plot(CO2_avg(:,1),TMR_CO2_mets,'r');
   xlabel('time (seconds)'); ylabel('Total Metabolic Rate (mets)');
   legend('from O_2 sensor','from CO_2 sensor','Location','SouthEast')
   %plot vertical line at transitions between speeds
   plot([sit_start sit_start],[min(TMR_CO2_mets) max(TMR_CO2_mets)],'g');
   plot([sit_end sit_end],[min(TMR_CO2_mets) max(TMR_CO2_mets)],'g');
   if s3_0mph > 0
      plot([s3_0mph s3_0mph],[min(TMR_CO2_mets) max(TMR_CO2_mets)],'g');
   end;
   if s3_7mph > 0
      plot([s3_7mph s3_7mph],[min(TMR_CO2_mets) max(TMR_CO2_mets)],'g');
   end;
   if s4_4mph > 0
      plot([s4_4mph s4_4mph],[min(TMR_CO2_mets) max(TMR_CO2_mets)],'g');
   end;
   if end_walk > 0
      plot([end_walk end_walk],[min(TMR_CO2_mets) max(TMR_CO2_mets)],'g');
   end;
end;

%PLOT METABOLIC RATE IN KILOCALORIES PER HOUR
if makeplot == 1
   figure(6); grid on; hold on; box on;
   plot(O2_avg(:,1),TMR_O2_kcph,'b');
   plot(CO2_avg(:,1),TMR_CO2_kcph,'r');
   plot(bpm6(:,1),MRfromHR,'g')
   plot(O2_avg(:,1),BMR_kcph*ones(length(O2_avg),1),'k')
   plot([sit_start sit_start],[min(TMR_O2_kcph) max(TMR_O2_kcph)],'g');
   plot([sit_end sit_end],[min(TMR_O2_kcph) max(TMR_O2_kcph)],'g');
   if s3_0mph > 0
      plot([s3_0mph s3_0mph],[min(TMR_O2_kcph) max(TMR_O2_kcph)],'g');
   end;
   if s3_7mph > 0
```

```
        plot([s3_7mph s3_7mph],[min(TMR_O2_kcph) max(TMR_O2_kcph)],'g');
    end;
    if s4_4mph > 0
        plot([s4_4mph s4_4mph],[min(TMR_O2_kcph) max(TMR_O2_kcph)],'g');
    end;
    if end_walk > 0
        plot([end_walk end_walk],[min(TMR_O2_kcph) max(TMR_O2_kcph)],'g');
    end;
    plot([(sit_start + 1) sit_end], [MR_O2_rest MR_O2_rest],'c');
    plot([(sit_start + 1) sit_end], [MR_CO2_rest MR_CO2_rest],'m');
    plot([(sit_start + 1) sit_end], [MR_HR_rest MR_HR_rest],'g');
    if s3_7mph > 0
        plot([(s3_7mph - 300) s3_7mph], [MR_O2_3_0mph MR_O2_3_0mph],'c');
        plot([(s3_7mph - 300) s3_7mph], [MR_CO2_3_0mph MR_CO2_3_0mph],'m');
        plot([(s3_7mph - 300) s3_7mph], [MR_HR_3_0mph MR_HR_3_0mph],'g');
    end;
    if s4_4mph > 0
        plot([(s4_4mph - 300) s4_4mph], [MR_O2_3_7mph MR_O2_3_7mph],'c');
        plot([(s4_4mph - 300) s4_4mph], [MR_CO2_3_7mph MR_CO2_3_7mph],'m');
        plot([(s4_4mph - 300) s4_4mph], [MR_HR_3_7mph MR_HR_3_7mph],'g');
    end;
    if end_walk > 0
        plot([(end_walk - 300) end_walk], [MR_O2_4_4mph MR_O2_4_4mph],'c');
        plot([(end_walk - 300) end_walk], [MR_CO2_4_4mph MR_CO2_4_4mph],'m');
        plot([(end_walk - 300) end_walk], [MR_HR_4_4mph MR_HR_4_4mph],'g');
    end;
    xlabel('time (seconds)'); ylabel('Total Metabolic Rate (kcph)');
    legend('from O_2 sensor','from CO_2 sensor','from HR sensor','BMR','Location','NorthWest')
end;

%RESPIRATORY EXCHANGE RATIO
rer = -VCO2./VO2;

%plot VO2, VCO2, and RER
if makeplot == 1
    figure(7);
    subplot(3,1,1);grid on; hold on; box on;
    plot(O2_avg(:,1),VO2);
    ylabel('VO_2 (L/min)');
    plot([sit_start sit_start],[min(VO2) max(VO2)],'g');
    plot([sit_end sit_end],[min(VO2) max(VO2)],'g');
    if s3_0mph > 0
        plot([s3_0mph s3_0mph],[min(VO2) max(VO2)],'g');
    end;
    if s3_7mph > 0
        plot([s3_7mph s3_7mph],[min(VO2) max(VO2)],'g');
    end;
    if s4_4mph > 0
        plot([s4_4mph s4_4mph],[min(VO2) max(VO2)],'g');
    end;
    if end_walk > 0
        plot([end_walk end_walk],[min(VO2) max(VO2)],'g');
    end;
    subplot(3,1,2);grid on; hold on; box on;
    plot(CO2_avg(:,1),-VCO2);
    ylabel('VCO_2 (L/min)');
```

```
    plot([sit_start sit_start],[min(-VCO2) max(-VCO2)],'g');
    plot([sit_end sit_end],[min(-VCO2) max(-VCO2)],'g');
    if s3_0mph > 0
        plot([s3_0mph s3_0mph],[min(-VCO2) max(-VCO2)],'g');
    end;
    if s3_7mph > 0
        plot([s3_7mph s3_7mph],[min(-VCO2) max(-VCO2)],'g');
    end;
    if s4_4mph > 0
        plot([s4_4mph s4_4mph],[min(-VCO2) max(-VCO2)],'g');
    end;
    if end_walk > 0
        plot([end_walk end_walk],[min(-VCO2) max(-VCO2)],'g');
    end;
    subplot(3,1,3);grid on; hold on; box on;
    plot(O2_avg(:,1),rer);
    xlabel('time (seconds)')
    ylabel('RER')
    plot([sit_start sit_start],[min(rer) max(rer)],'g');
    plot([sit_end sit_end],[min(rer) max(rer)],'g');
    if s3_0mph > 0
        plot([s3_0mph s3_0mph],[min(rer) max(rer)],'g');
    end;
    if s3_7mph > 0
        plot([s3_7mph s3_7mph],[min(rer) max(rer)],'g');
    end;
    if s4_4mph > 0
        plot([s4_4mph s4_4mph],[min(rer) max(rer)],'g');
    end;
    if end_walk > 0
        plot([end_walk end_walk],[min(rer) max(rer)],'g');
    end;
end;
%write all results to excel file for easy analysis
xlswrite('results.xls',MR_O2_rest,1,'B2')
xlswrite('results.xls',MR_CO2_rest,1,'C2')
xlswrite('results.xls',MR_HR_rest,1,'D2')
xlswrite('results.xls',HR_rest,1,'G2')
if s3_7mph > 0
    xlswrite('results.xls',MR_O2_3_0mph,1,'B3')
    xlswrite('results.xls',MR_CO2_3_0mph,1,'C3')
    xlswrite('results.xls',MR_HR_3_0mph,1,'D3')
    xlswrite('results.xls',HR_3_0mph,1,'G3')
end;
if s4_4mph > 0
    xlswrite('results.xls',MR_O2_3_7mph,1,'B4')
    xlswrite('results.xls',MR_CO2_3_7mph,1,'C4')
    xlswrite('results.xls',MR_HR_3_7mph,1,'D4')
    xlswrite('results.xls',HR_3_7mph,1,'G4')
end;
if end_walk > 0
    xlswrite('results.xls',MR_O2_4_4mph,1,'B5')
    xlswrite('results.xls',MR_CO2_4_4mph,1,'C5')
    xlswrite('results.xls',MR_HR_4_4mph,1,'D5')
    xlswrite('results.xls',HR_4_4mph,1,'G5')
end;
```

```
figure(8)
%pretty version of plot 6
hold on; box on; grid on;
plot(O2_avg(:,1),TMR_O2_kcph,':r','LineWidth',1.5)
plot(CO2_avg(:,1),TMR_CO2_kcph,'--b','LineWidth',1.5)
plot(bpm6(:,1),MRfromHR,'g','LineWidth',1)
xlabel('time (sec)','FontSize',14)
ylabel('metabolic rate (kcal/hr)','FontSize',14)
legend('from O_2 sensor','from CO_2 sensor','from heart rate
sensor','FontSize',14,'Location','SouthEast')
set(gca,'FontSize',12)
plot([(sit_start + 1) sit_end], [MR_O2_rest MR_O2_rest],'k','LineWidth',1);
plot([(sit_start + 1) sit_end], [MR_CO2_rest MR_CO2_rest],'k','LineWidth',1);
plot([(sit_start + 1) sit_end], [MR_HR_rest MR_HR_rest],'k','LineWidth',1);
if s3_7mph > 0
   plot([(s3_7mph - 300) s3_7mph], [MR_O2_3_0mph MR_O2_3_0mph],'k','LineWidth',1);
   plot([(s3_7mph - 300) s3_7mph], [MR_CO2_3_0mph MR_CO2_3_0mph],'k','LineWidth',1);
   plot([(s3_7mph - 300) s3_7mph], [MR_HR_3_0mph MR_HR_3_0mph],'k','LineWidth',1);
end;
if s4_4mph > 0
   plot([(s4_4mph - 300) s4_4mph], [MR_O2_3_7mph MR_O2_3_7mph],'k','LineWidth',1);
   plot([(s4_4mph - 300) s4_4mph], [MR_CO2_3_7mph MR_CO2_3_7mph],'k','LineWidth',1);
   plot([(s4_4mph - 300) s4_4mph], [MR_HR_3_7mph MR_HR_3_7mph],'k','LineWidth',1);
end;
if end_walk > 0
   plot([(end_walk - 300) end_walk], [MR_O2_4_4mph MR_O2_4_4mph],'k','LineWidth',1);
   plot([(end_walk - 300) end_walk], [MR_CO2_4_4mph MR_CO2_4_4mph],'k','LineWidth',1);
   plot([(end_walk - 300) end_walk], [MR_HR_4_4mph MR_HR_4_4mph],'k','LineWidth',1);
end;
saveas(8,'prettyplot.emf')

%PANDOLF
load = 6/2.2; %helmet mass in kg
speeds_mph = [0; 3; 3.7; 4.4];
speeds_mps = speeds_mph*1609/3600;
grade = 0.01; % 1% grade
tf = 1; %terrain factor (1 for treadmill)
Pandolf_W = 1.5*wt_kg + 2*(wt_kg+load)*(load/wt_kg)^2 + ...
   tf*(wt_kg+load)*(1.5*speeds_mps.^2 + 0.35*speeds_mps*grade);
Pandolf_kcph = Pandolf_W*3600/4184
xlswrite('results.xls',Pandolf_kcph,1,'E2:E5')
```

C.2 Input Parameters Sample

1	HRdata	1 if HR data taken, 0 otherwise
1	makeplot	1 if you want to plot, 0 otherwise
2	sex	1 = female, 2 = male
156	wt_lb	subject weight in lb
0	flow_scfm	air flow in scfm
0	sit_start	time when sitting data starts in seconds
300	sit_end	time when sitting data ends in seconds, start getting on treadmill
360	s3_0mph	time 3.0 mph starts in seconds
966	s3_7mph	time 3.7 mph starts in seconds
1569	s4_4mph	time 4.4 mph starts in seconds
2160	end_walk	time test finished in seconds
2	HRclean	1 if hand cleaned, 2 if matlab cleaned
2.8965	O2calib_before	O2 calibration before voltage
2.9469	O2calib_after	O2 calibration after voltage
0.042	CO2calib_before	CO2 calibration before voltage
0.036	CO2calib_after	CO2 calibration after voltage
10	RH0	RH at rest extrapolated from hobo and CO2 data
20	RH1	RH at 3.0 mph from hobo data
30	RH2	RH at 3.7 mph from hobo data
45	RH3	RH at 4.4 mph extrapolated from hobo and CO2 data
6.4	scfm1	first flow rate (scfm)
-1	scfm2	second flow rate (scfm): -1 if no more change
-1	scfm3	third flow rate (scfm): -1 if no more change
-1	scfm4	fourth flow rate (scfm): -1 if no more change
0	flowtime1	time start first flow rate (s): should be 0
-1	flowtime2	time start second flow rate (s): -1 if no more change
-1	flowtime3	time start third flow rate (s): -1 if no more change
-1	flowtime4	time start fourth flow rate (s): -1 if no more change
26	age	subject age at time of test
82.2	HRrest	resting heart rate

C.3 Gas Sensor Calibration Code

```
% calibrate O2 sensor by bypassing the helmet and recording just cascade
% air before and after each run
% average these short calibration runs to get one value
close all; clear all; clc; format compact;

%get data
x = importdata('M8 calib before.txt');
xx = x.data;
beforeO2 = xx(:,1);
beforeCO2 = xx(:,2);
y = importdata('M8 calib after.txt');
yy = y.data;
afterO2 = yy(:,1);
afterCO2 = yy(:,2);
clear x xx y yy

%average each second of before data for smoother curve
O2count = 0; CO2count = 0;
O2tally = 0; CO2tally = 0;
for xb = 1:length(beforeO2)
    O2tally = O2tally + beforeO2(xb);
    CO2tally = CO2tally + beforeCO2(xb);
    if xb>0 & mod(xb,100) == 0
        O2count = O2count + 1;
        CO2count = CO2count + 1;
        before_smoothO2(O2count) = [O2tally/100];
        before_smoothCO2(CO2count) = [CO2tally/100];
        O2tally = 0; CO2tally = 0;
    end
end;
clear xb O2tally O2count CO2tally CO2count

%average each second of after data for smoother curve
O2count = 0; CO2count = 0;
O2tally = 0; CO2tally = 0;
for xa = 1:length(afterO2)
    O2tally = O2tally + afterO2(xa);
    CO2tally = CO2tally + afterCO2(xa);
    if xa>0 & mod(xa,100) == 0
        O2count = O2count + 1;
        CO2count = CO2count + 1;
        after_smoothO2(O2count) = [O2tally/100];
        after_smoothCO2(CO2count) = [CO2tally/100];
        O2tally = 0; CO2tally = 0;
    end
end;
clear xa O2tally O2count CO2tally CO2count

%average data
before_avgO2 = mean(beforeO2)
before_avgCO2 = mean(beforeCO2)
after_avgO2 = mean(afterO2)
```

```
after_avgCO2 = mean(afterCO2)


%plot everything for O2
figure(1); grid on; box on; hold on;
plot(before_smoothO2,'b');
plot(before_avgO2*ones(length(before_smoothO2),1),'b.')
plot(after_smoothO2,'r');
plot(after_avgO2*ones(length(after_smoothO2),1),'r.')
legend('before data','before average','after data','after average',...
    'Location','NorthWest')
xlabel('time (seconds)'); ylabel('voltage'); title('O_2');

%plot everything for CO2
figure(2); grid on; box on; hold on;
plot(before_smoothCO2,'b');
plot(before_avgCO2*ones(length(before_smoothCO2),1),'b.')
plot(after_smoothCO2,'r');
plot(after_avgCO2*ones(length(after_smoothCO2),1),'r.')
legend('before data','before average','after data','after average',...
    'Location','NorthWest')
xlabel('time (seconds)'); ylabel('voltage'); title('CO_2');
```

C.4 Heart Rate Data Filtering Code

```
%clean interference out of HR data
close all; clear all; clc; format compact;

%IMPORT THE TEXT DATA
%% first column is O2 voltages
%% second column is CO2 voltages
%% third column is HR voltages
x = importdata('M8 data.txt');
RawVoltages = x.data;
clear x

%add fourth column to Raw Voltages with time in seconds
RawVoltages(:,4) = zeros(length(RawVoltages),1);
for n = 1:length(RawVoltages)
   RawVoltages(n,4) = n/100;
end;
clear n

%HEART RATE DATA
threshold = 1.5;

%clean HR data
for cd = 1:length(RawVoltages)
   if RawVoltages(cd,3) > threshold
      cHR = 1;
      high = 1;
      while high == 1
         if RawVoltages((cd + cHR),3) < threshold
            high = 0;
         else cHR = cHR + 1;
         end;
      end;
      if cd < 250000
         if cHR < 1
            while cHR ~= 0
               RawVoltages((cd + cHR - 1),3) = 0;
               cHR = cHR - 1;
            end;
         end;
      else
         if cHR < 5
            while cHR ~= 0
               RawVoltages((cd + cHR - 1),3) = 0;
               cHR = cHR - 1;
            end;
         end;
      end;
   end;
end;

%calculate Heart Rate
count = 1;
```

```
bpm_count = 0;
HRb = zeros(1,length(RawVoltages));
if RawVoltages(1,3) > threshold
   HRb(1,1) = 1;
end;
for h = 2:length(RawVoltages)
   if RawVoltages(h,3) > threshold
      HRb(1,h) = 1;
      if HRb(1,h-1) == 0
         beats(1,count) = RawVoltages(h,4);
         if count > 1
            bpm(count) = 60/(beats(count) - beats(count-1));
         end;
         count = count + 1;
      end;
   end;
end;

figure(3); grid on; hold on; box on;
plot(beats(1,2:length(beats)),bpm(1,2:length(beats)),'b')
xlabel('time (seconds)'); ylabel('heart rate (bpm)'); title('Heart Rate');
legend('beat to beat', '15 second averages','Location','SouthEast')

clear h stop y bpm_count count HRb beats

%csvwrite('Mcleandata.txt',RawVoltages)
save Mcleandata.txt RawVoltages -ASCII
NewVoltages = importdata('Mcleandata.txt');
```

C.5 Sample Unprocessed Raw Voltage Data from NI-DAQmx

```
NI VI Logger
Created: 4/6/2007 11:59:12.764 AM Eastern Daylight Time
Number of scans: 216262
Scan rate: 0.01 seconds

Row,Time,O2(Voltage),CO2(Voltage),HR(Voltage)
1,11:18:26.125 AM,2.91704,0.471493,1.16245
2,11:18:26.135 AM,2.91704,0.471493,1.16245
3,11:18:26.145 AM,2.91704,0.471493,1.16245
4,11:18:26.155 AM,2.91704,0.471493,1.17264
5,11:18:26.165 AM,2.91704,0.471493,1.16245
6,11:18:26.175 AM,2.91704,0.471493,1.16245
7,11:18:26.185 AM,2.91704,0.471493,1.17264
8,11:18:26.195 AM,2.91704,0.471493,1.17264
9,11:18:26.205 AM,2.91704,0.471493,1.17264
10,11:18:26.215 AM,2.91704,0.471493,1.16245
11,11:18:26.225 AM,2.91704,0.471493,1.17264
12,11:18:26.235 AM,2.91704,0.471493,1.17264
13,11:18:26.245 AM,2.91704,0.471493,1.16245
14,11:18:26.255 AM,2.92724,0.471493,1.17264
15,11:18:26.265 AM,2.91704,0.471493,1.17264
16,11:18:26.275 AM,2.91704,0.471493,1.16245
17,11:18:26.285 AM,2.91704,0.461299,1.17264
18,11:18:26.295 AM,2.91704,0.471493,1.17264
19,11:18:26.305 AM,2.91704,0.471493,1.17264
20,11:18:26.315 AM,2.91704,0.471493,1.17264
…
```

C.6 Sample Processed Raw Voltage Data

O_2 Voltage	CO_2 Voltage	HR Voltage	Time (s)
2.9170400e+000	4.7149300e-001	1.1624500e+000	1.0000000e-002
2.9170400e+000	4.7149300e-001	1.1624500e+000	2.0000000e-002
2.9170400e+000	4.7149300e-001	1.1624500e+000	3.0000000e-002
2.9170400e+000	4.7149300e-001	1.1726400e+000	4.0000000e-002
2.9170400e+000	4.7149300e-001	1.1624500e+000	5.0000000e-002
2.9170400e+000	4.7149300e-001	1.1624500e+000	6.0000000e-002
2.9170400e+000	4.7149300e-001	1.1726400e+000	7.0000000e-002
2.9170400e+000	4.7149300e-001	1.1726400e+000	8.0000000e-002
2.9170400e+000	4.7149300e-001	1.1726400e+000	9.0000000e-002
2.9170400e+000	4.7149300e-001	1.1624500e+000	1.0000000e-001
2.9170400e+000	4.7149300e-001	1.1726400e+000	1.1000000e-001
2.9170400e+000	4.7149300e-001	1.1726400e+000	1.2000000e-001
2.9170400e+000	4.7149300e-001	1.1624500e+000	1.3000000e-001
2.9272400e+000	4.7149300e-001	1.1726400e+000	1.4000000e-001
2.9170400e+000	4.7149300e-001	1.1726400e+000	1.5000000e-001
2.9170400e+000	4.7149300e-001	1.1624500e+000	1.6000000e-001
2.9170400e+000	4.6129900e-001	1.1726400e+000	1.7000000e-001
2.9170400e+000	4.7149300e-001	1.1726400e+000	1.8000000e-001
2.9170400e+000	4.7149300e-001	1.1726400e+000	1.9000000e-001
2.9170400e+000	4.7149300e-001	1.1726400e+000	2.0000000e-001
…			

Appendix D: RESULTS

D.1 Session Outcomes and Subject Comments

Subject	*Experimental Session Results*	*Control Session Results*
F1	• session completed with treadmill 1 • subject mentioned slight sore throat • subject accidentally pulled out safety key and stopped treadmill 2 minutes into fast speed, restarted immediately and completed full 10 minutes at fast speed afterward • subject periodically took a few running steps to keep up with fast speed	• control session completed • subject switched to jog about 6 minutes into the fast speed • subject said that the workloads were similar but the control session weighted helmet does not rest on the shoulders like the experimental helmet assembly
F2	• subject chose to terminate session during fast speed • subject periodically took a few running steps to keep up with fast speed • treadmill 1 was used	• subject did not take part in a control session
F3	• completed session with treadmill 1	• control session completed • subject said the control session was easier
F4	• treadmill 1 malfunctioned during medium speed during the first attempt • session was repeated for a full data set with treadmill 3	• control session completed • initially had some trouble fitting oronasal mask because subject's face was shorter (nose to chin) than the mask, tightening strap seemed to eliminate leaking
M1	• completed session with treadmill 1	• control session completed
M2	• completed session with treadmill 1	• control session completed • hose popped out from of mask about 1 minute into slow speed, was pushed back in almost immediately • subject said the headgear from both sessions had similar weight but the experimental helmet assembly forced your neck and back posture more
M3	• completed session with treadmill 1 • helmet sitting on shoulders caused pressure points, subject shrugged shoulders throughout session to relieve these points	• control session completed • data inexplicably dropped to 0 about 5 min into rest period and then came back, these points were excluded • subject said the experimental session was harder because of motion constraint

M4	• treadmill 1 malfunctioned during fast speed • subject mentioned the helmet assembly forced his head down and therefore his glasses slid off • session was repeated for a full data set with treadmill 3 • subject had to stop to retie shoe 4 minutes into medium speed, restarted session at the beginning of medium speed	• control session completed • hose started coming out of mask about 1 minute into slow walk, was pushed back in • accidentally only walked at slow speed for 9 minutes and all other speeds occurred a minute too early, last 5 minutes taken into account after a transition that was only 4 minutes • subject said the control session didn't force his head down in a particular position as much as the experimental session
M5	• treadmill 1 malfunctioned during slow speed • session was not repeated	• subject did not take part in control session
M6	• completed session with treadmill 2 • subject complained the walking belt was shorter than his stride length at fast speed and made the walk awkward • repeated session with treadmill 3	• control session completed
M7	• completed session with treadmill 2 • repeated session with treadmill 3 • subject could not sustain fast speed with walking gait and switched to a run during both sessions • subject accidentally pulled off safety stop 1.5 minutes into the fast speed, the session was restarted at the beginning of the fast speed	• control session completed • hose fell out from mask about 2.5 minutes into the slow walk, was replaced right away, caused dip in data, not part of averaged data • subject started running instead of walking 3 minutes into fast speed • subject says the control session was more comfortable because ambient air was not as dry as cascade air
M8	• session completed with treadmill 3	• control session completed • subject said control session was harder because it was more difficult to exhale into the smaller space of the hose rather than the large helmet volume

D.2 All Metabolic Rates and Heart Rates

All metabolic rates are given in kcal/hr and heart rates are given in beats per minute

	MR from O_2	MR from CO_2	MR from HR	MR from Pandolf	MR from Control	HR from Exp. Ses.	HR from Con. Ses.
F1							
rest	48	77	0	81	69	62	81
slow	484	322	243	233	304	108	116
medium	679	469	389	312	421	136	148
fast	966	709	616	407	630	179	181
F3							
rest	-124	55	57	77	65	81	70
slow	87	229	194	223	246	105	98
medium	375	307	309	299	331	125	117
fast	602	435	498	390	486	159	146
F4							
rest	182	74	3	77	58	67	68
slow	391	320	237	223	244	110	100
medium	490	438	396	299	341	140	128
fast	1001	753	637	390	568	185	171
M1							
rest	54	133	7	108	82	67	74
slow	566	510	398	308	333	116	106
medium	716	660	544	412	446	134	125
fast	991	918	820	538	652	168	157
M2							
rest	-97	98	0	101	85	67	77
slow	295	351	209	288	308	93	93
medium	525	482	320	386	390	107	103
fast	719	631	488	504	491	127	120
M3							
rest	274	88	27	103	80	82	80
slow	620	355	352	295	316	119	110
medium	787	483	556	395	406	141	123
fast	1004	680	917	516	645	182	161
M4							
rest	7	88	88	79	65	81	94
slow	582	420	428	226	296	122	119
medium	794	531	600	303	377	142	136
fast	1070	797	826	396	553	170	165
M6							
rest	354	121	11	97	87	71	92
slow	758	379	326	279	326	109	125
medium	787	502	476	373	425	127	140
fast	989	725	772	487	609	163	170

M7							
rest	-56	84	0	81	67	75	80
slow	312	414	446	233	284	126	117
medium	471	553	718	312	366	158	138
fast	882	843	959	407	594	186	174
M8							
rest	-122	126	24	91	115	85	102
slow	406	357	284	262	309	113	111
medium	624	477	507	351	394	137	125
fast	809	631	740	459	552	163	151

D.3 Experimental Data Plotted

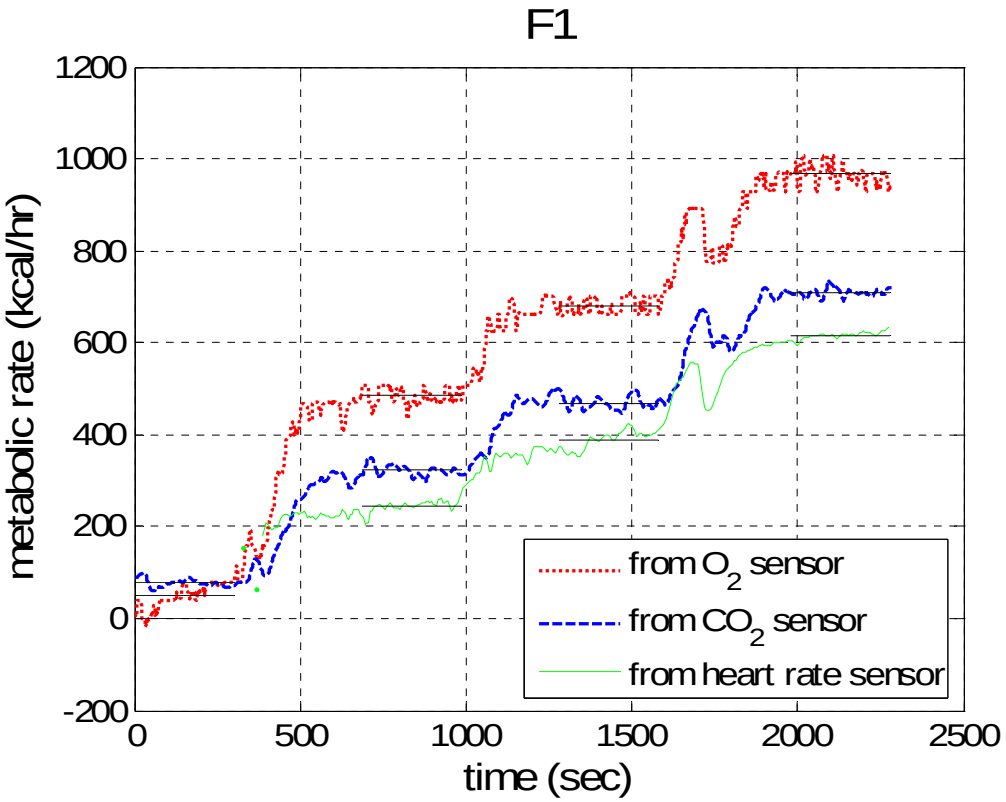

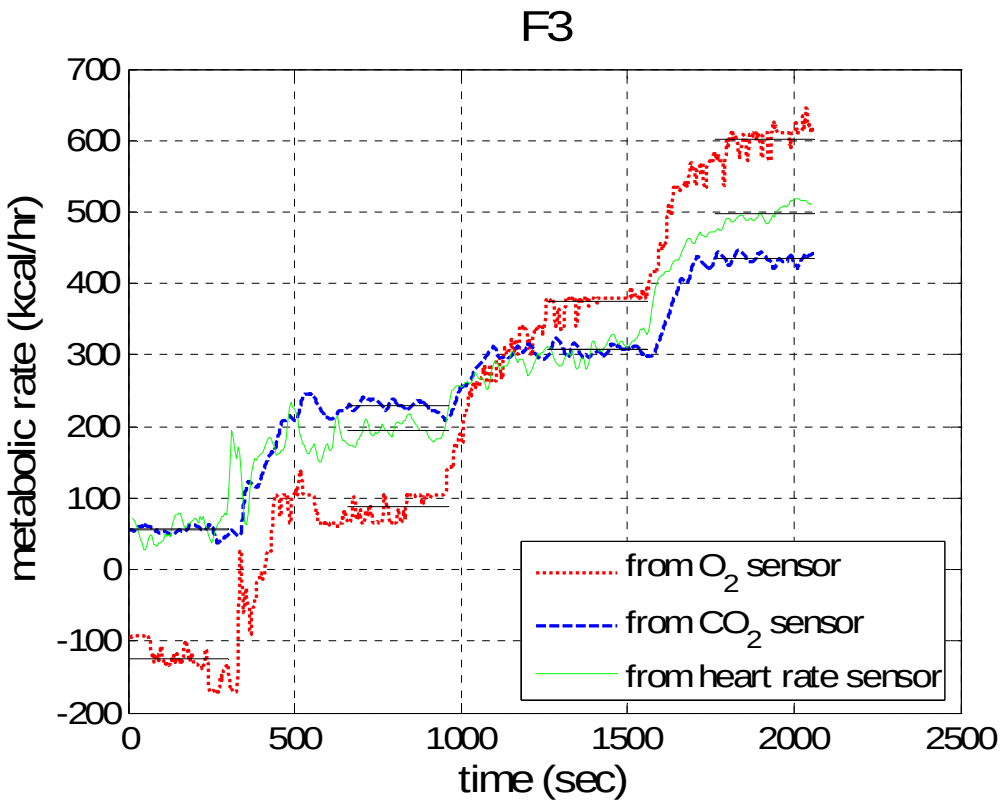
F3
700
600
500
400
300
200
100
0
-100
-200
metabolic rate (kcal/hr)
0
500
1000
1500
2000
2500
time (sec)
from O2 sensor
from CO2 sensor
from heart rate sensor

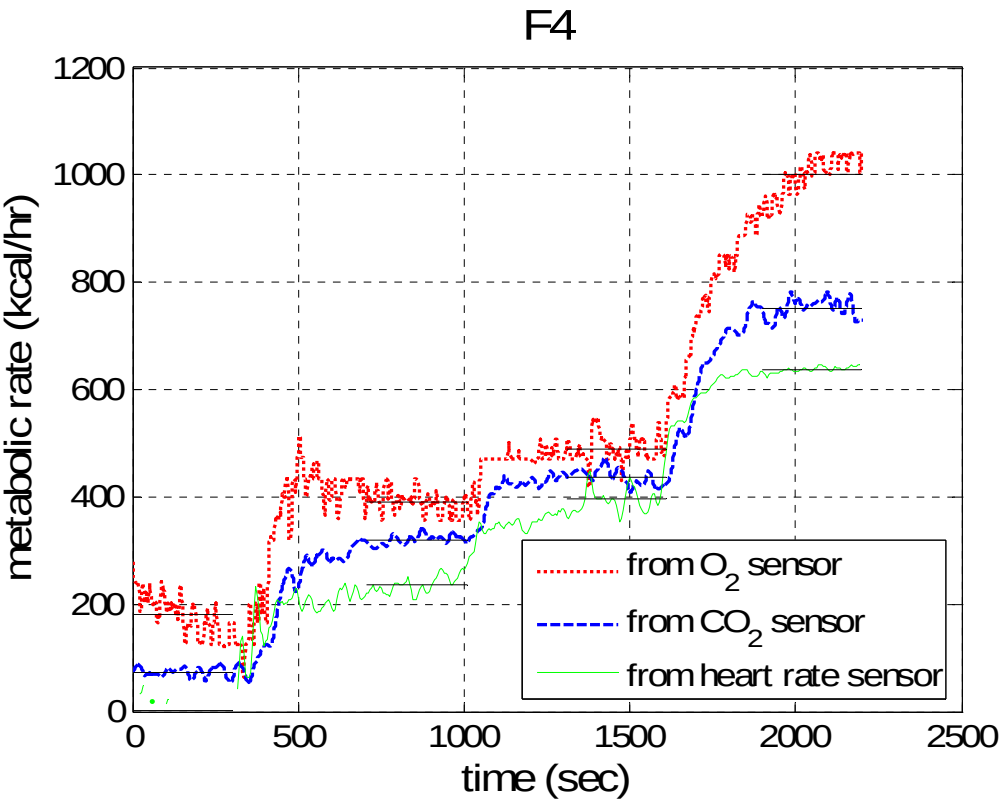
F4
1200
1000
800
600
400
200
0
metabolic rate (kcal/hr)
0
500
1000
1500
2000
2500
time (sec)
from O2 sensor
from CO2 sensor
from heart rate sensor

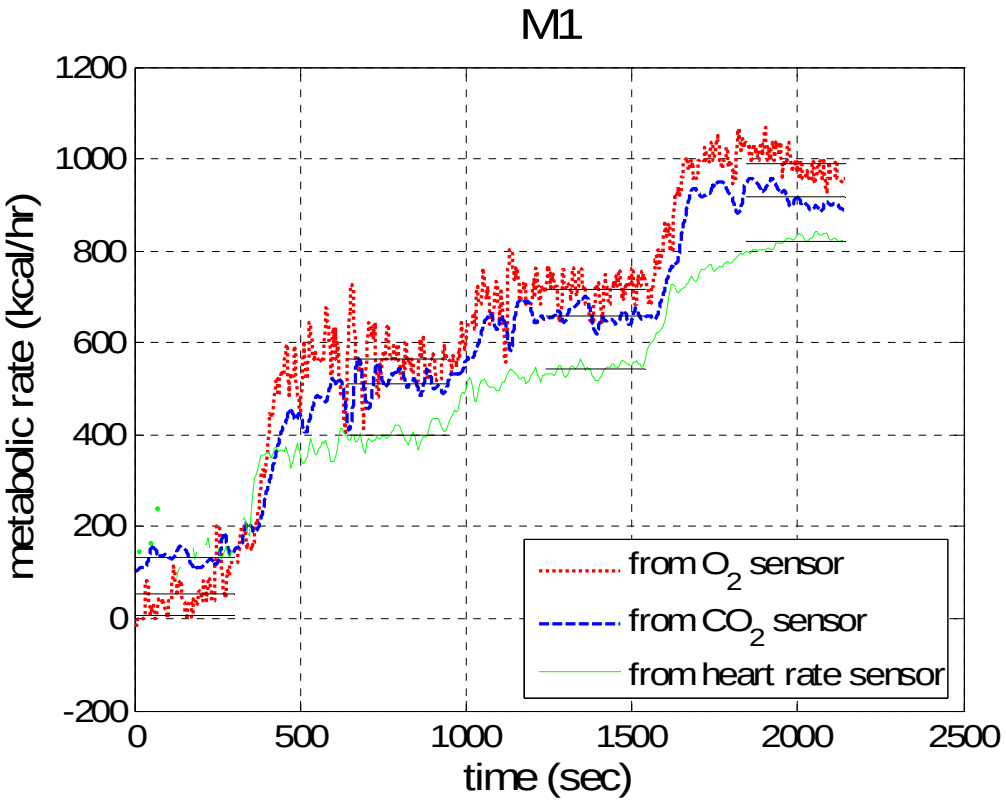
M1
metabolic rate (kcal/hr)
time (sec)
from O_2 sensor
from CO_2 sensor
from heart rate sensor

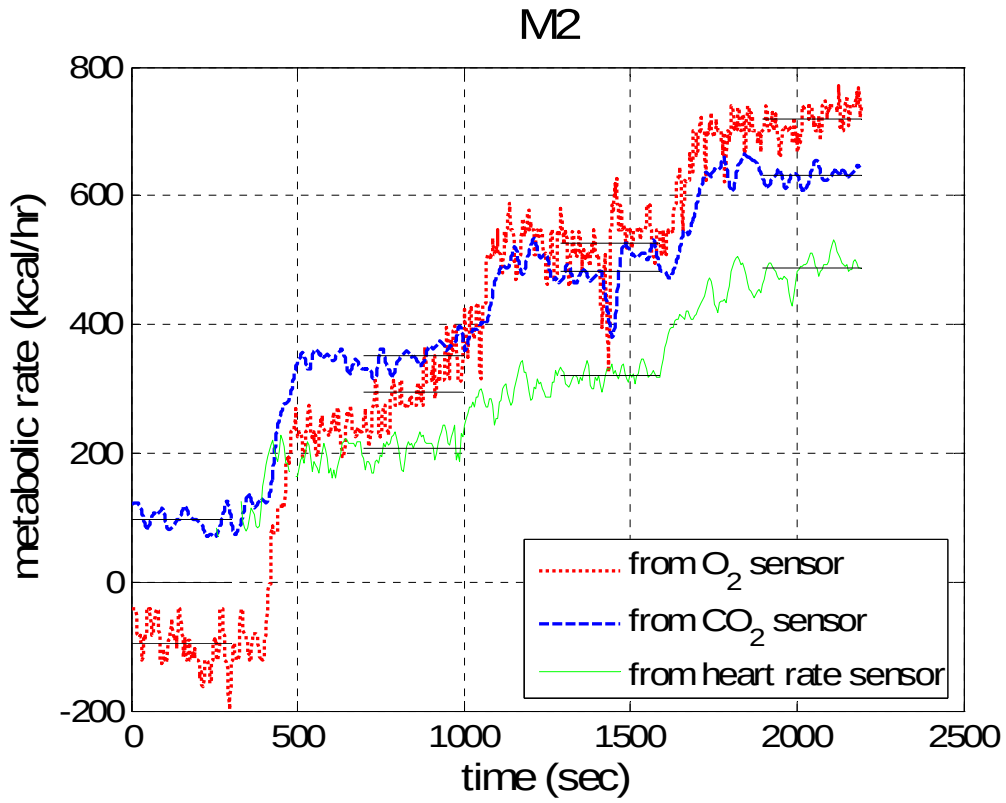
M2
metabolic rate (kcal/hr)
time (sec)
from O_2 sensor
from CO_2 sensor
from heart rate sensor

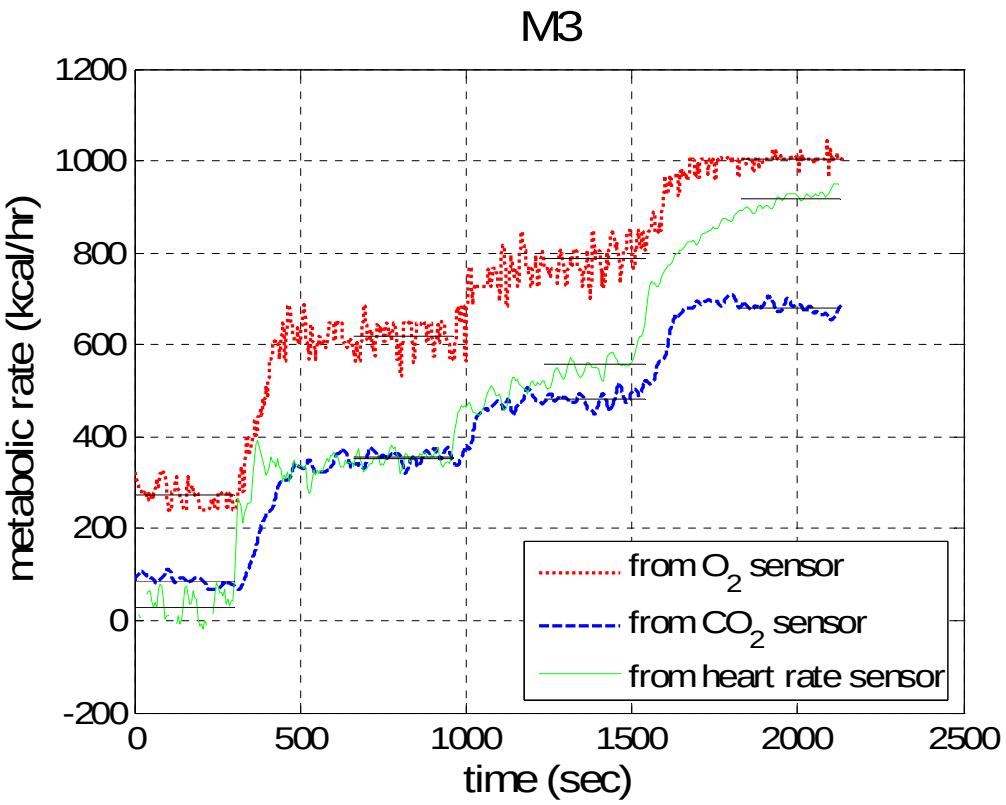
M3
metabolic rate (kcal/hr)
time (sec)
from O2 sensor
from CO2 sensor
from heart rate sensor
1200
1000
800
600
400
200
0
-200
0
500
1000
1500
2000
2500

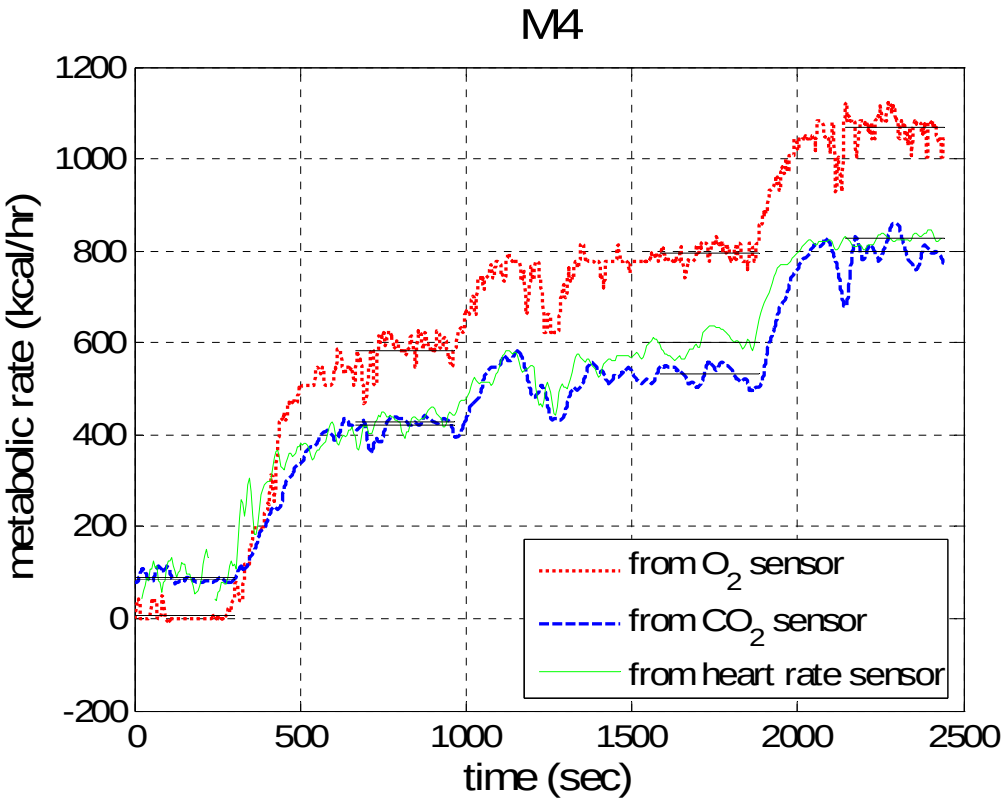
M4
metabolic rate (kcal/hr)
time (sec)
from O2 sensor
from CO2 sensor
from heart rate sensor
1200
1000
800
600
400
200
0
-200
0
500
1000
1500
2000
2500

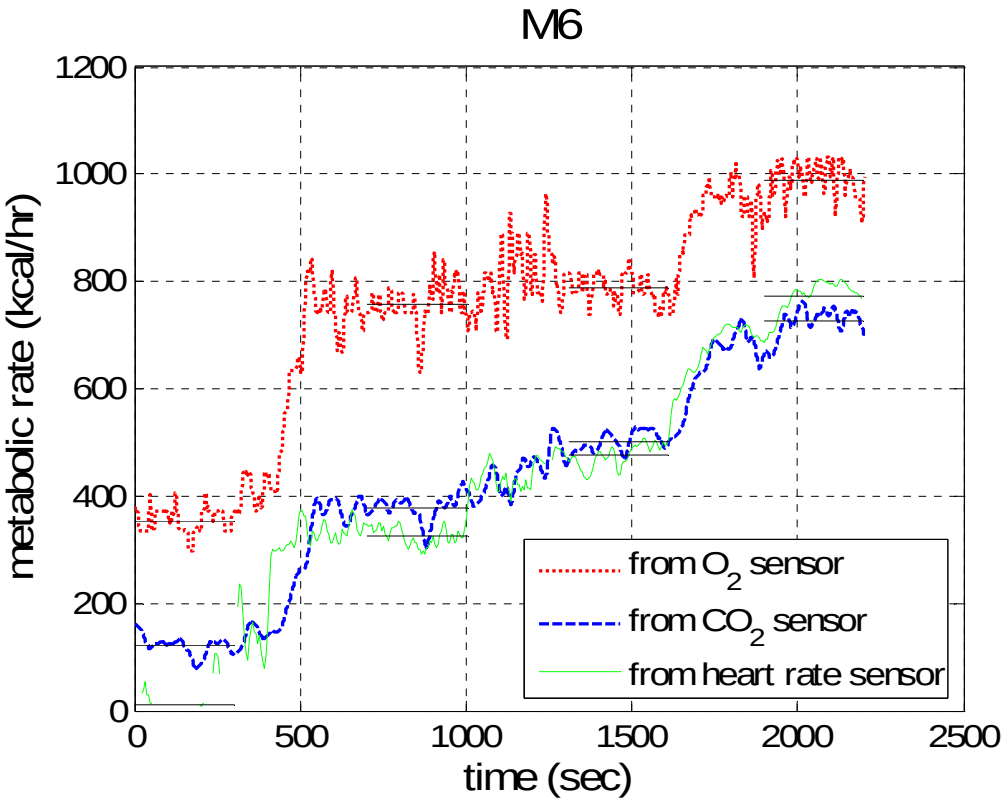
M6
metabolic rate (kcal/hr)
time (sec)
from O_2 sensor
from CO_2 sensor
from heart rate sensor
0
200
400
600
800
1000
1200
0
500
1000
1500
2000
2500

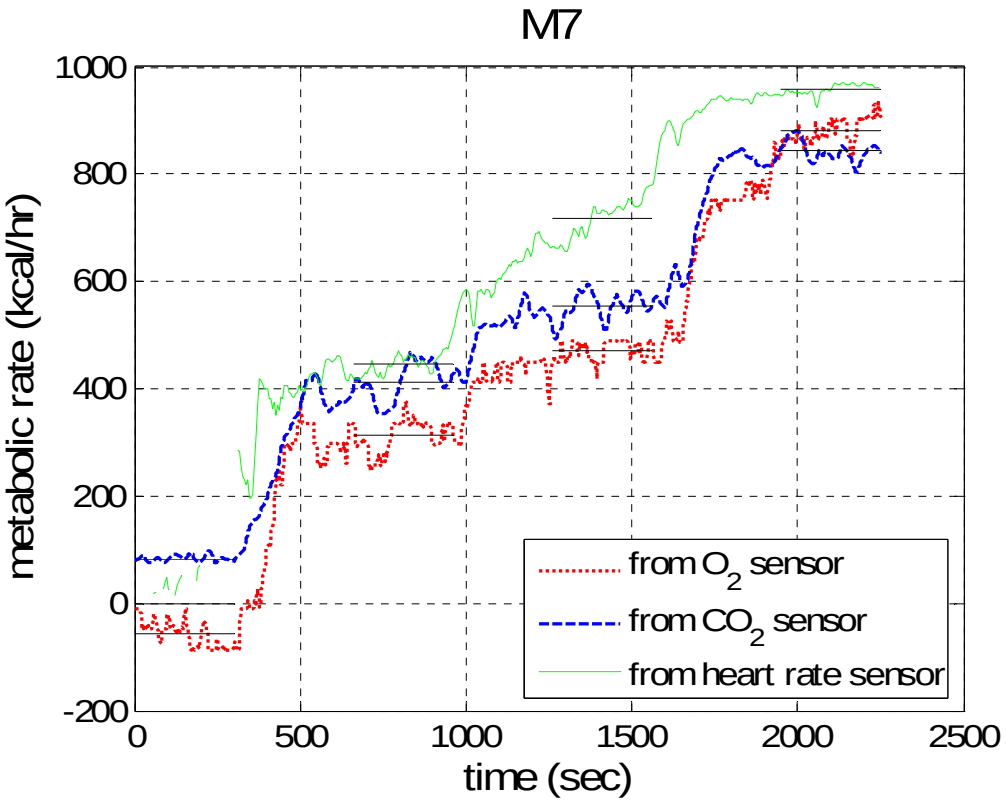
M7
metabolic rate (kcal/hr)
time (sec)
from O_2 sensor
from CO_2 sensor
from heart rate sensor
-200
0
200
400
600
800
1000
0
500
1000
1500
2000
2500

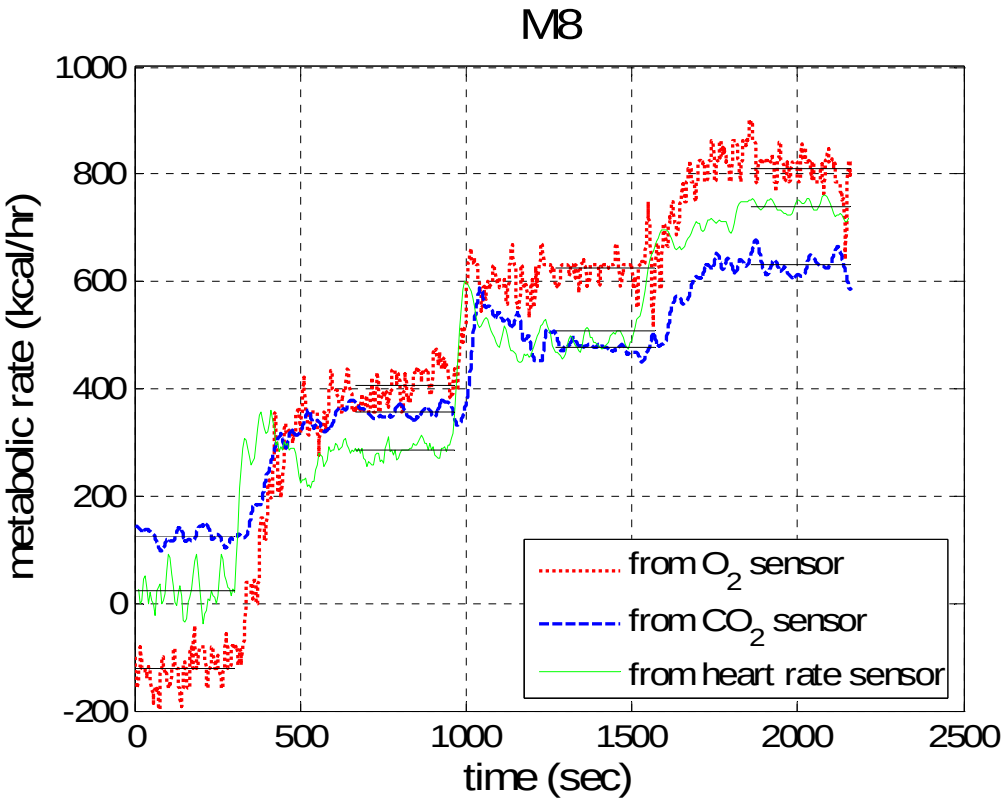
M8
1000
800
600
400
200
0
-200
0
500
1000
1500
2000
2500
metabolic rate (kcal/hr)
time (sec)
from O2 sensor
from CO2 sensor
from heart rate sensor

D.4 RER Plots from Experimental Sessions

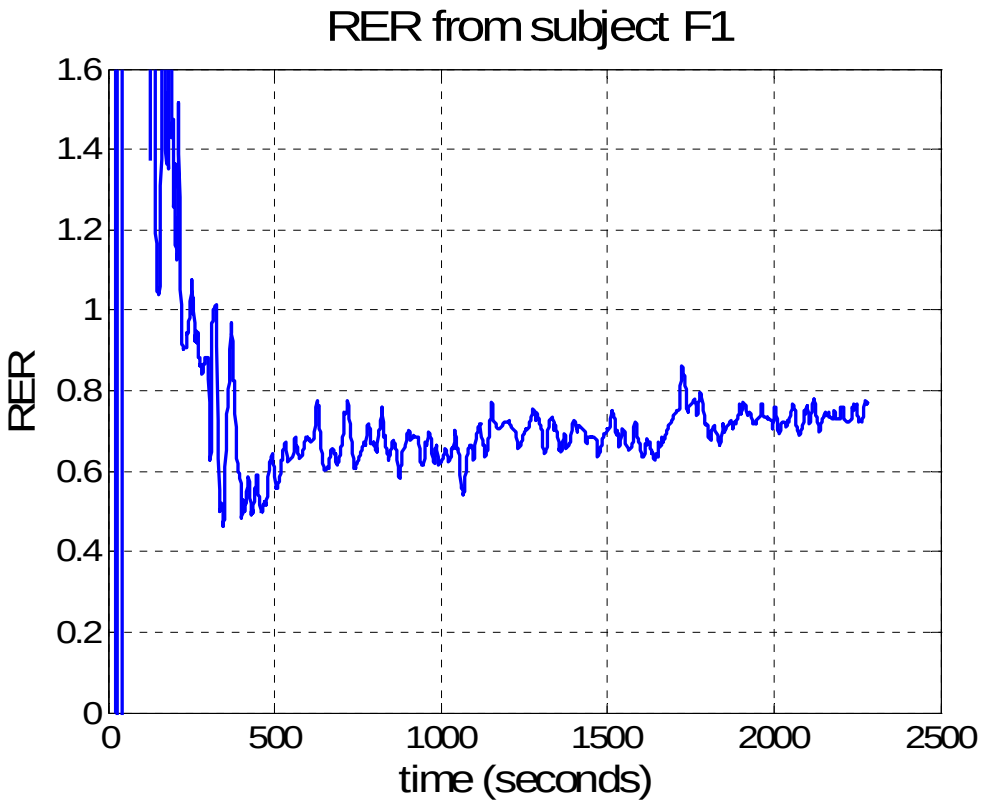

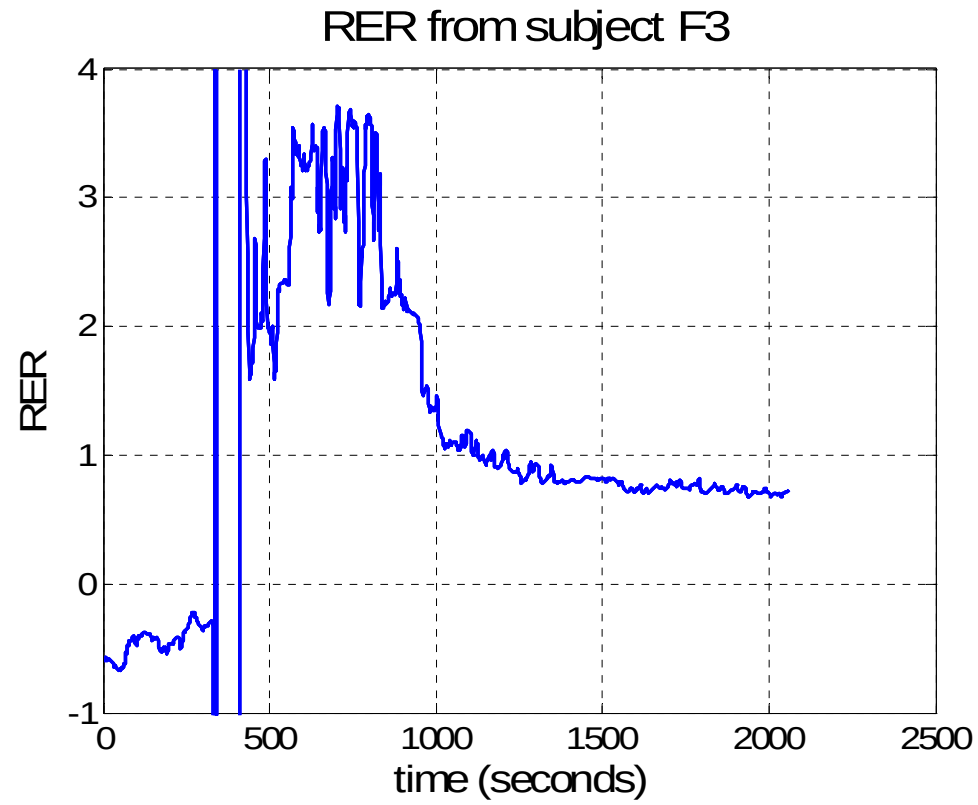
RER from subject F3
RER
time (seconds)
4
3
2
1
0
-1
0
500
1000
1500
2000
2500

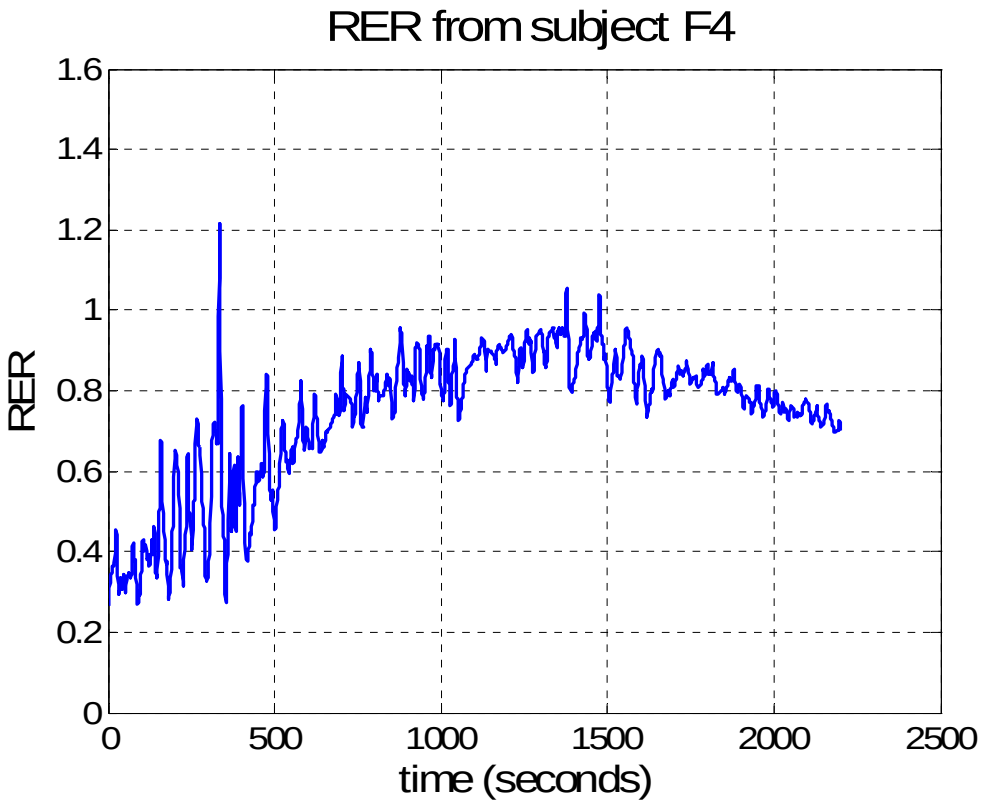
RER from subject F4
RER
time (seconds)
1.6
1.4
1.2
1
0.8
0.6
0.4
0.2
0
0
500
1000
1500
2000
2500

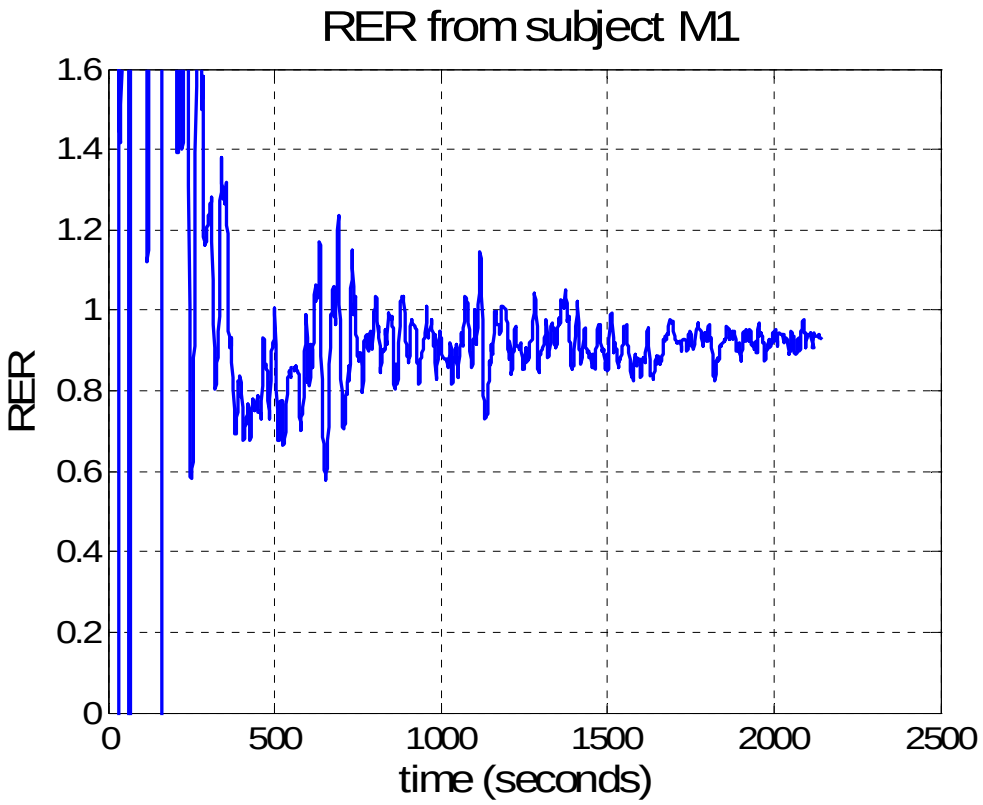
RER from subject M1
RER
time (seconds)
1.6
1.4
1.2
1
0.8
0.6
0.4
0.2
0
0
500
1000
1500
2000
2500

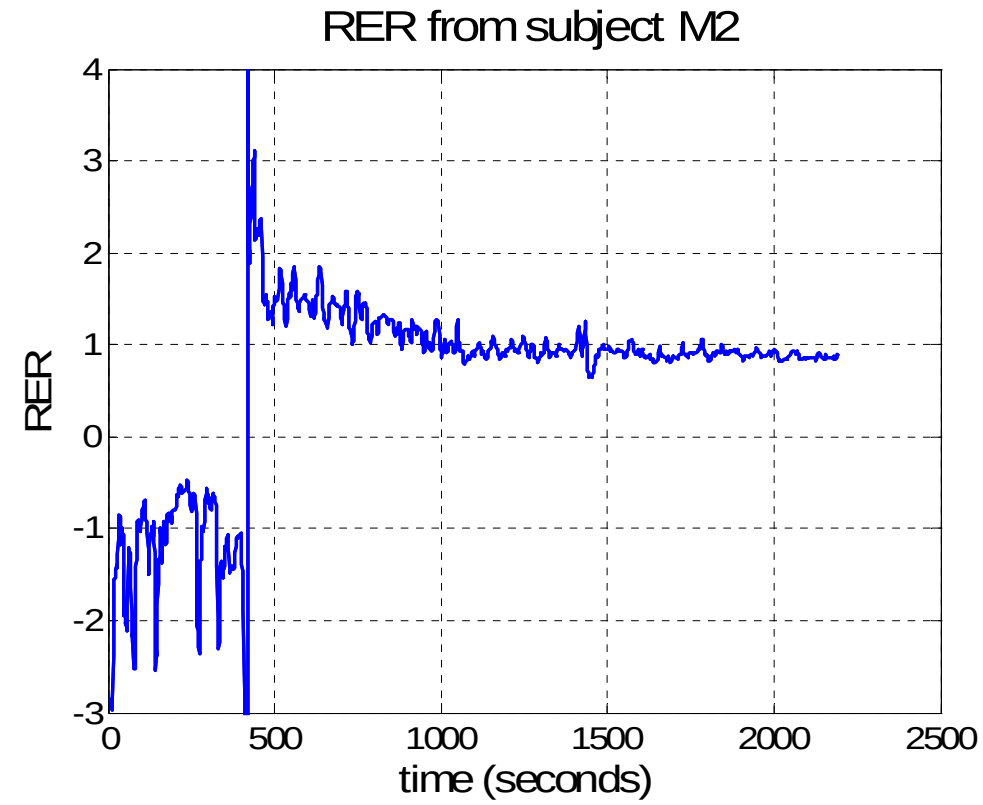
RER from subject M2
RER
time (seconds)
4
3
2
1
0
-1
-2
-3
0
500
1000
1500
2000
2500

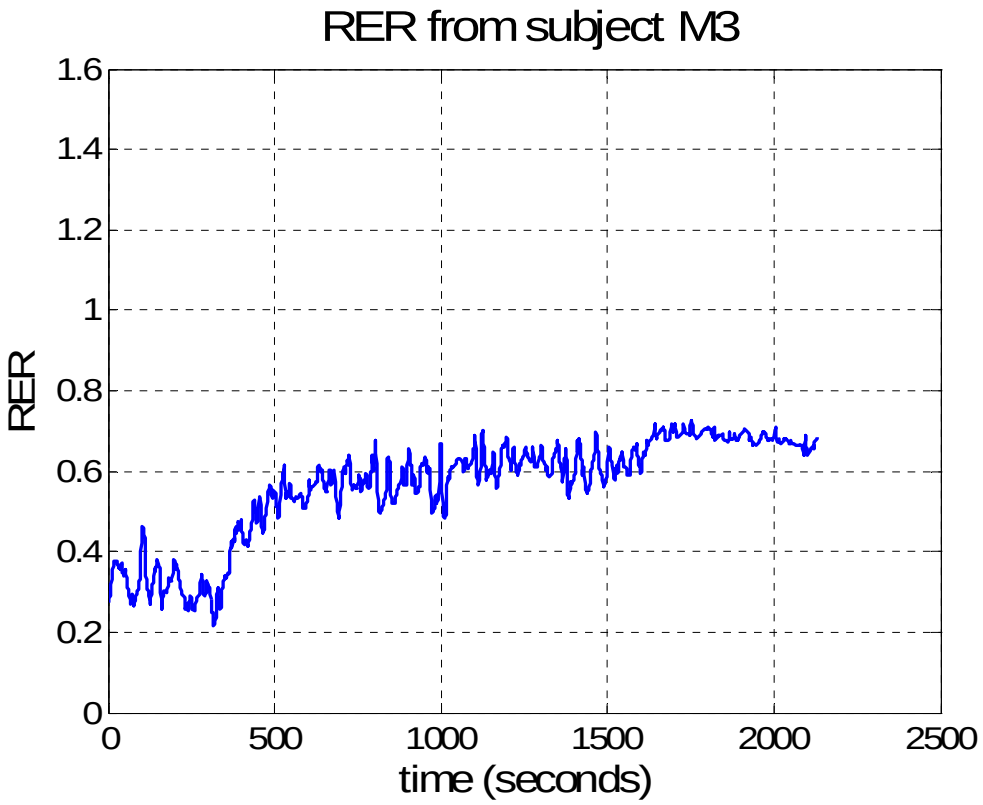
RER from subject M3
RER
time (seconds)
0
0.2
0.4
0.6
0.8
1
1.2
1.4
1.6
0
500
1000
1500
2000
2500

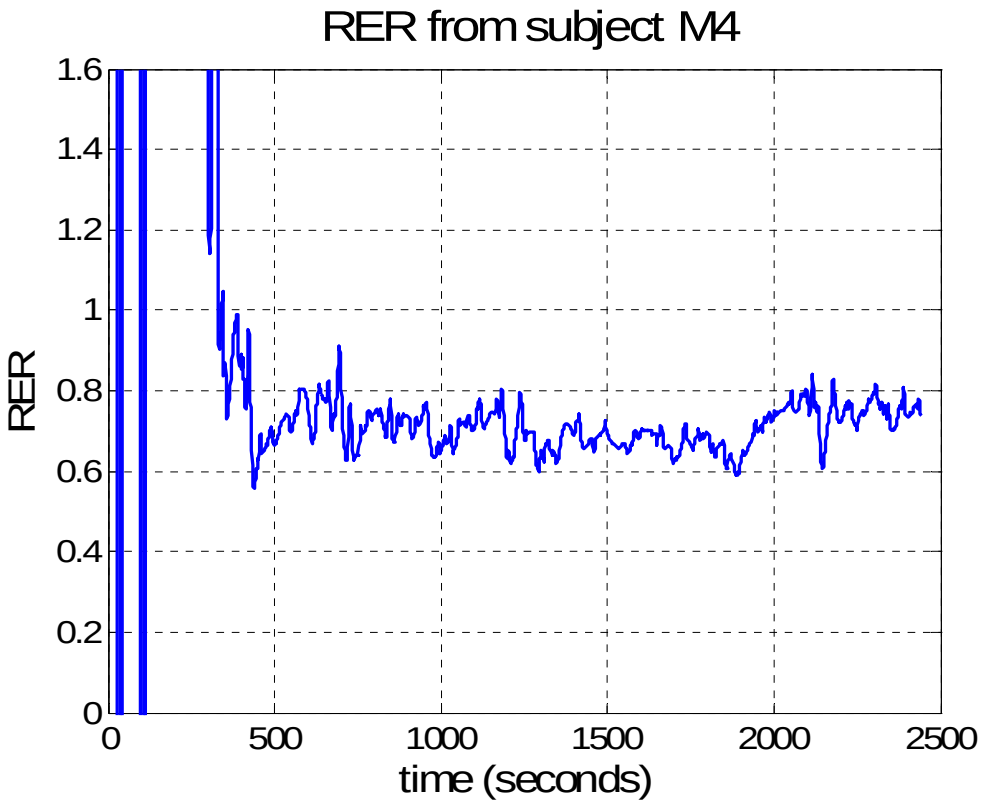
RER from subject M4
RER
time (seconds)
0
0.2
0.4
0.6
0.8
1
1.2
1.4
1.6
0
500
1000
1500
2000
2500

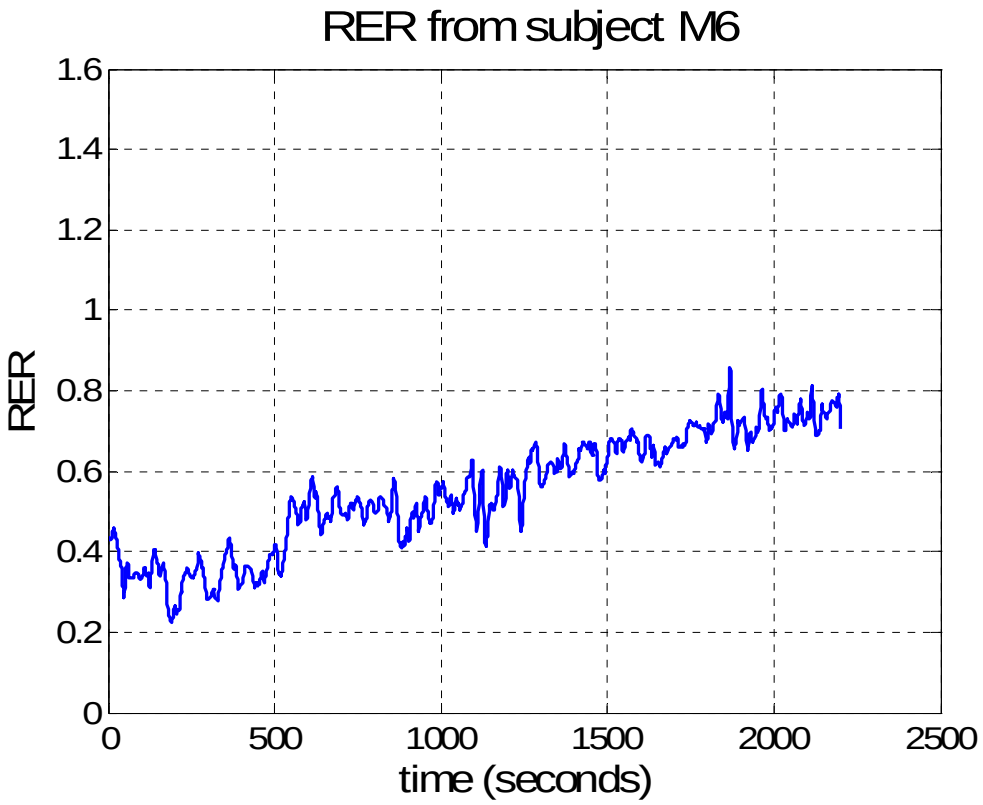
RER from subject M6
RER
time (seconds)
1.6
1.4
1.2
1
0.8
0.6
0.4
0.2
0
0
500
1000
1500
2000
2500

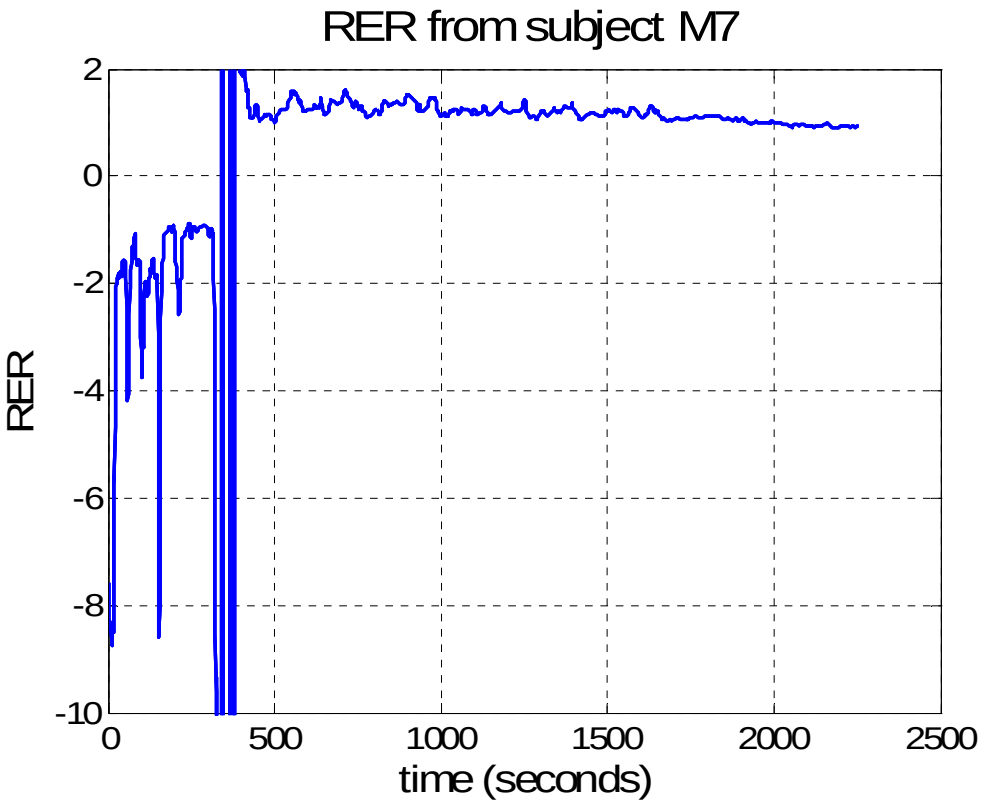
RER from subject M7
RER
time (seconds)
2
0
-2
-4
-6
-8
-10
0
500
1000
1500
2000
2500

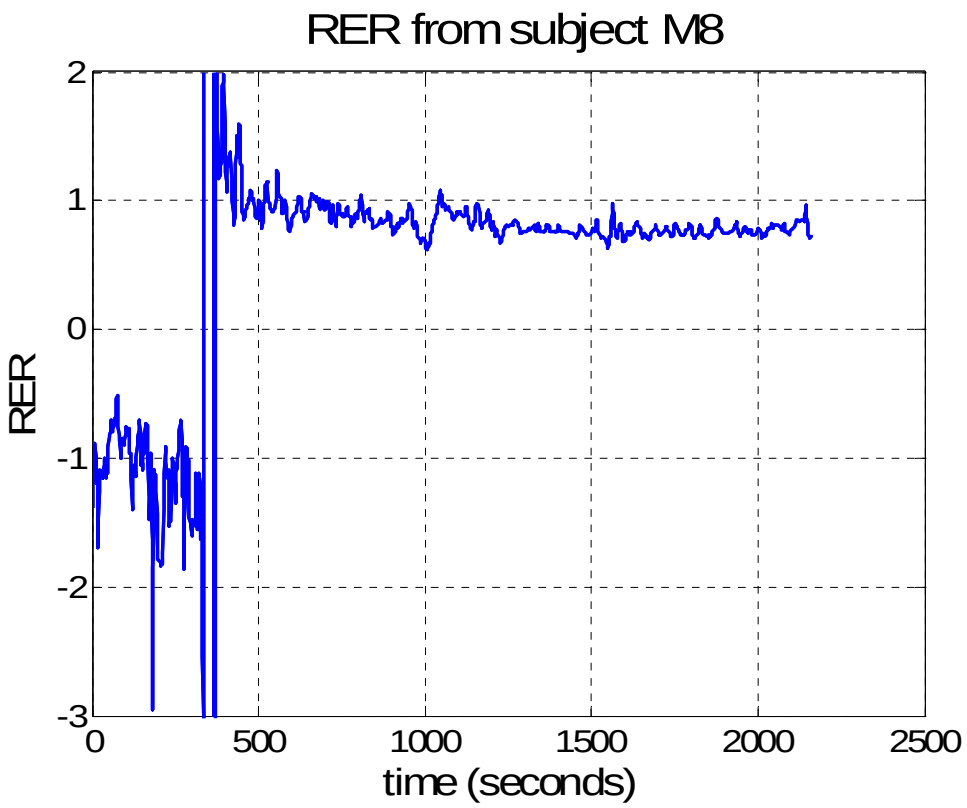
RER from subject M8
RER
time (seconds)
2
1
0
-1
-2
-3
0
500
1000
1500
2000
2500

D.5 Control Data Plotted

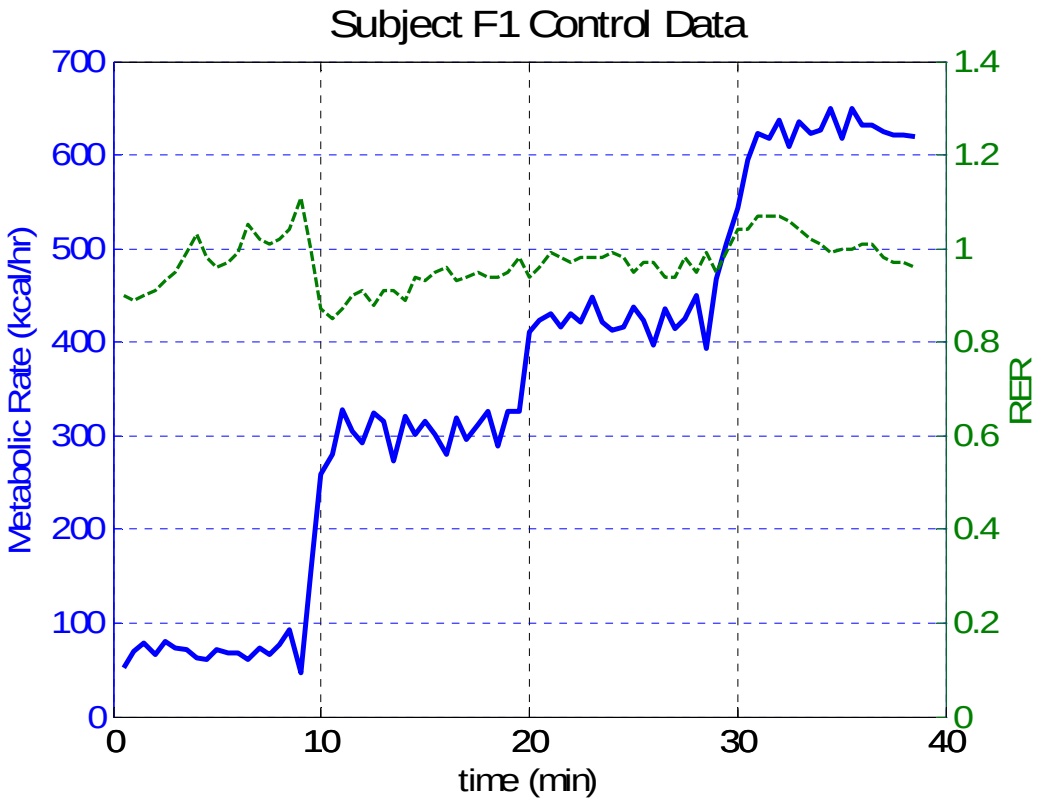

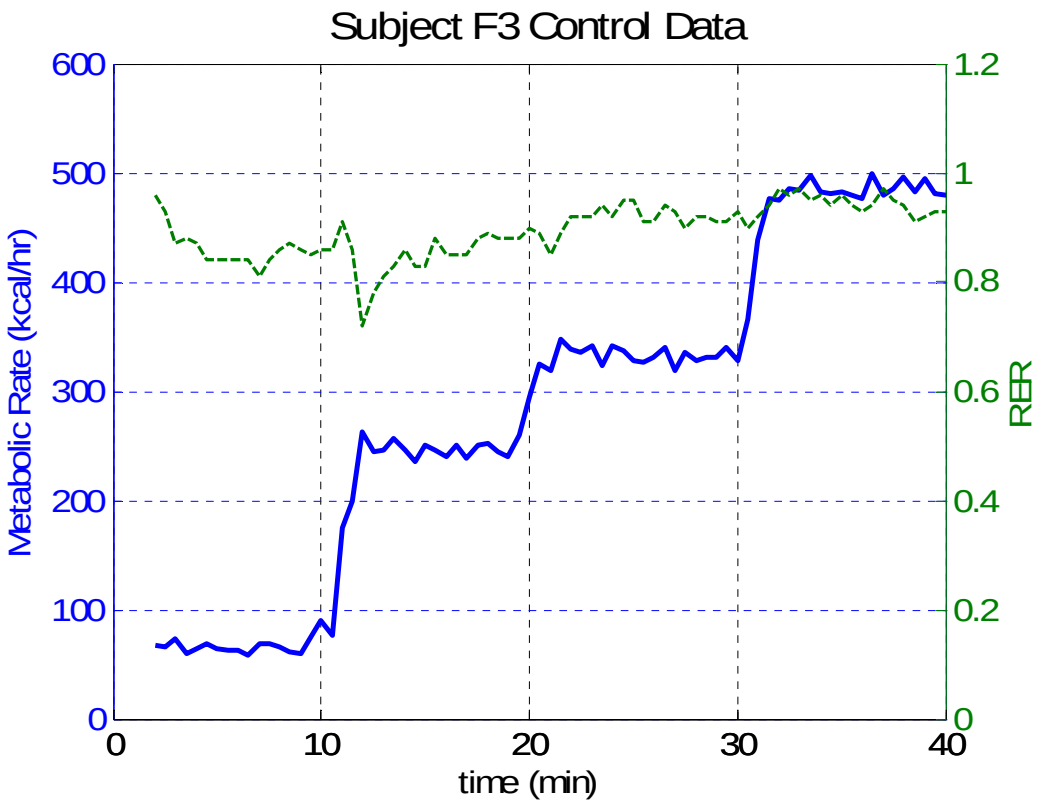
Subject F3 Control Data
Metabolic Rate (kcal/hr)
RER
time (min)
0
100
200
300
400
500
600
0
0.2
0.4
0.6
0.8
1
1.2
0
10
20
30
40

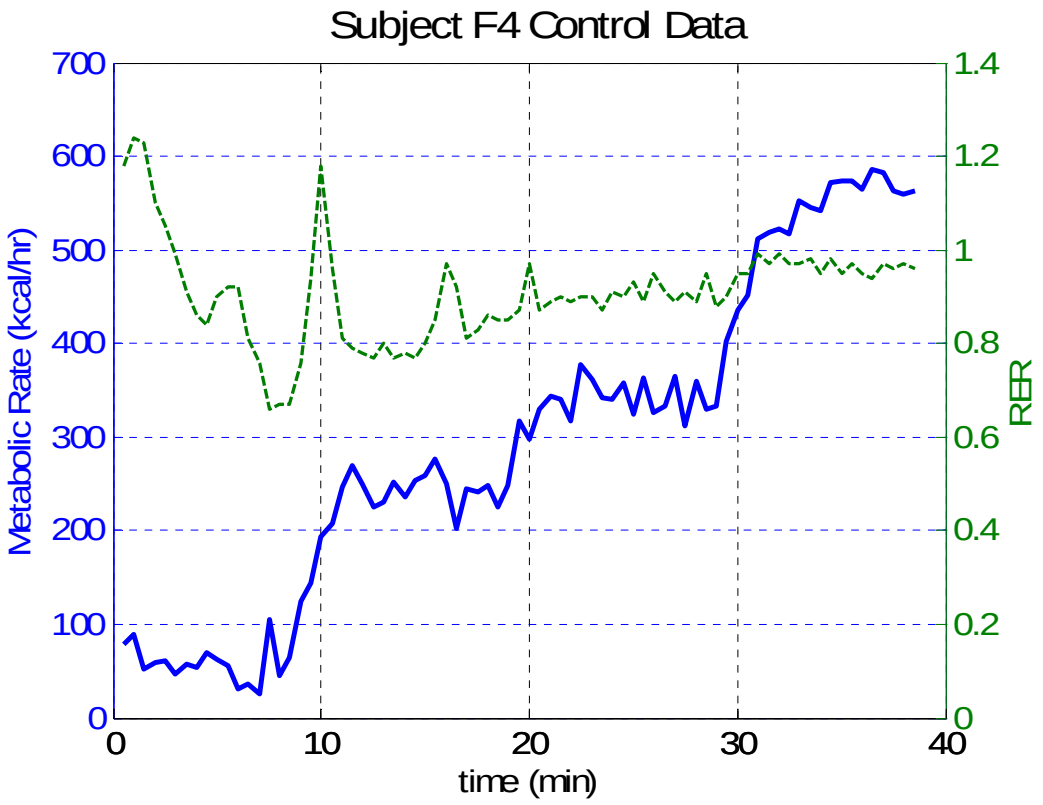
Subject F4 Control Data
Metabolic Rate (kcal/hr)
RER
time (min)
0
100
200
300
400
500
600
700
0
0.2
0.4
0.6
0.8
1
1.2
1.4
0
10
20
30
40

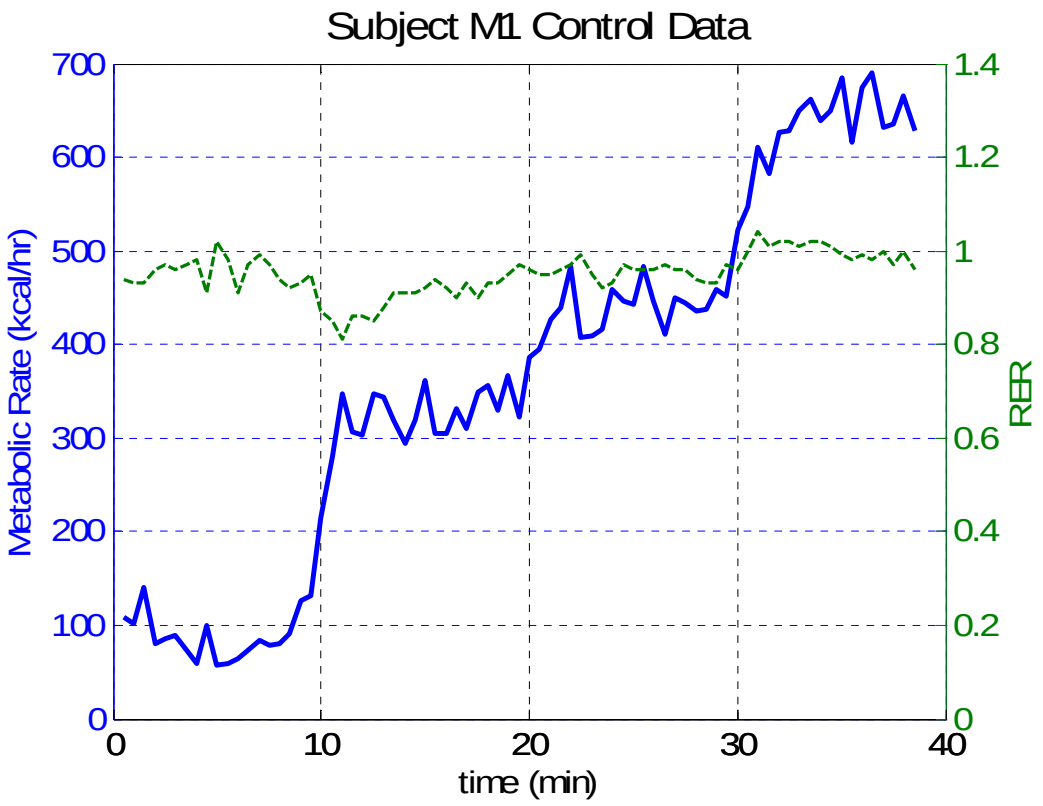
Subject M1 Control Data
Metabolic Rate (kcal/hr)
RER
time (min)
0
100
200
300
400
500
600
700
0
0.2
0.4
0.6
0.8
1
1.2
1.4
0
10
20
30
40

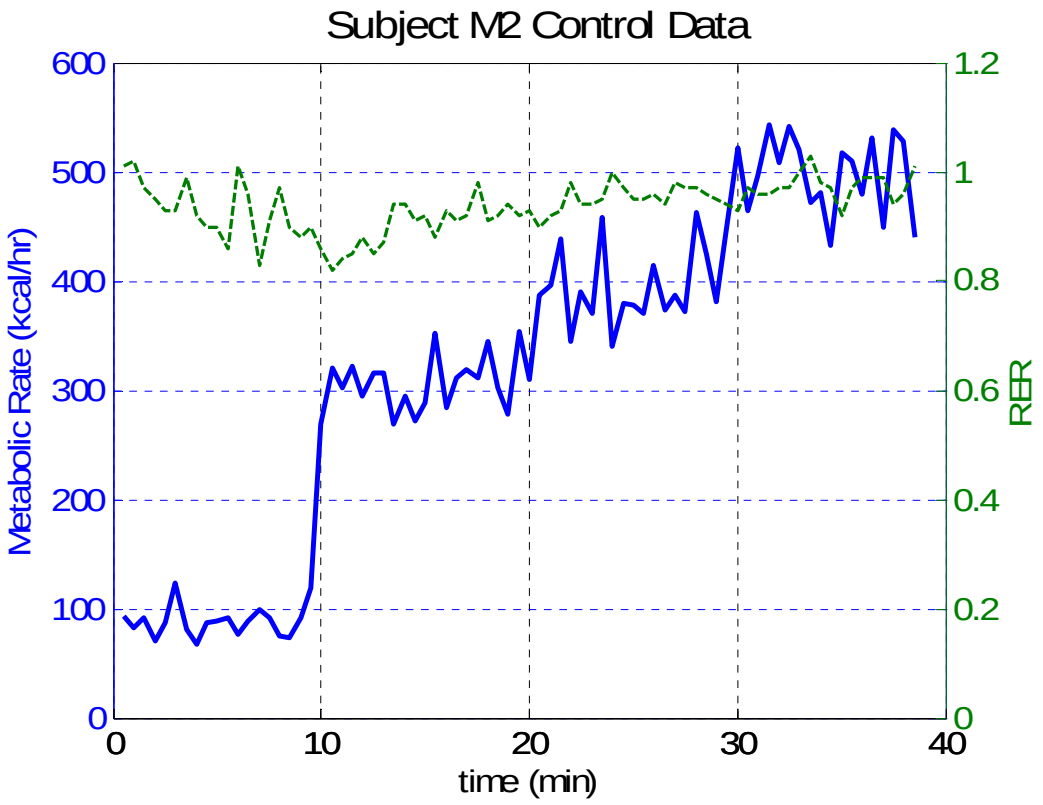
Subject M2 Control Data
Metabolic Rate (kcal/hr)
RER
time (min)
0
100
200
300
400
500
600
0
0.2
0.4
0.6
0.8
1
1.2
0
10
20
30
40

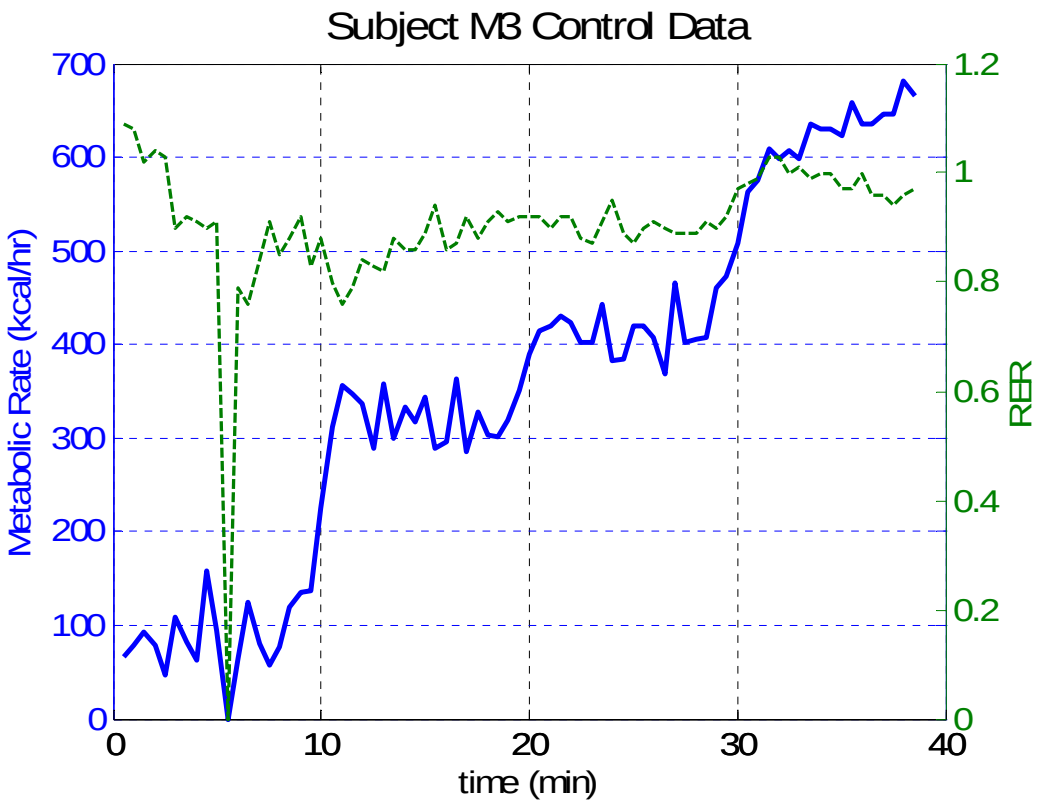
Subject M3 Control Data
Metabolic Rate (kcal/hr)
RER
time (min)
0
100
200
300
400
500
600
700
0
0.2
0.4
0.6
0.8
1
1.2
0
10
20
30
40

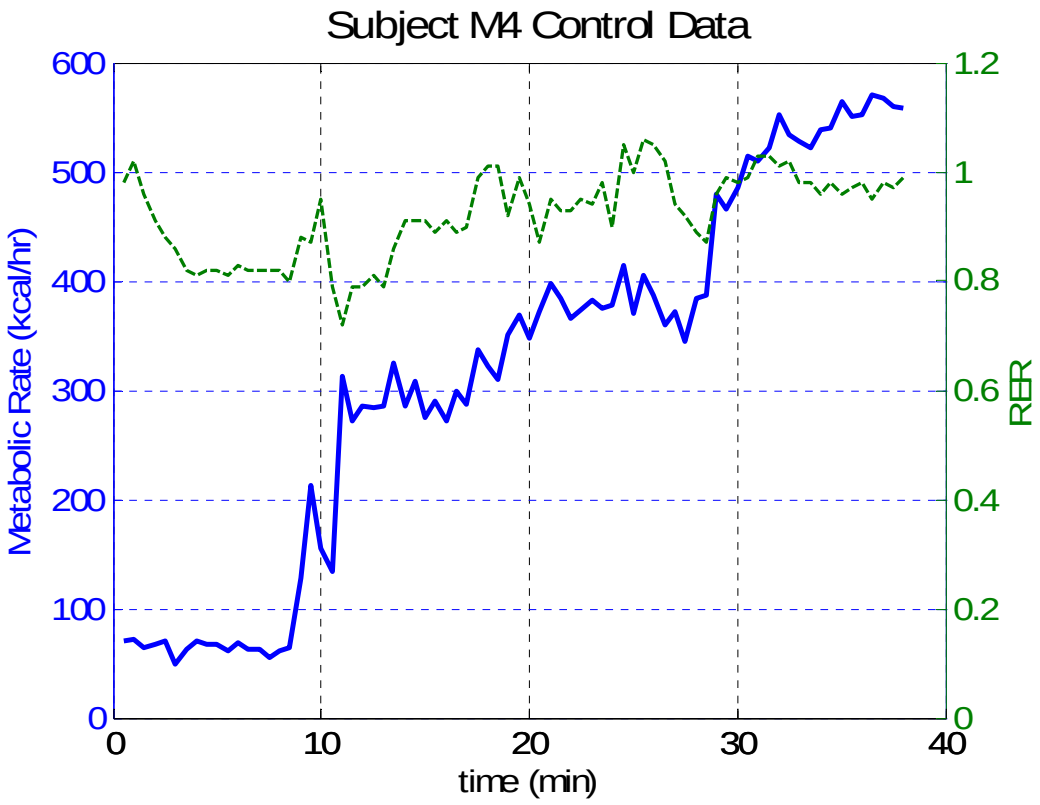
Subject M4 Control Data
Metabolic Rate (kcal/hr)
RER
time (min)
0
100
200
300
400
500
600
0
0.2
0.4
0.6
0.8
1
1.2
0
10
20
30
40

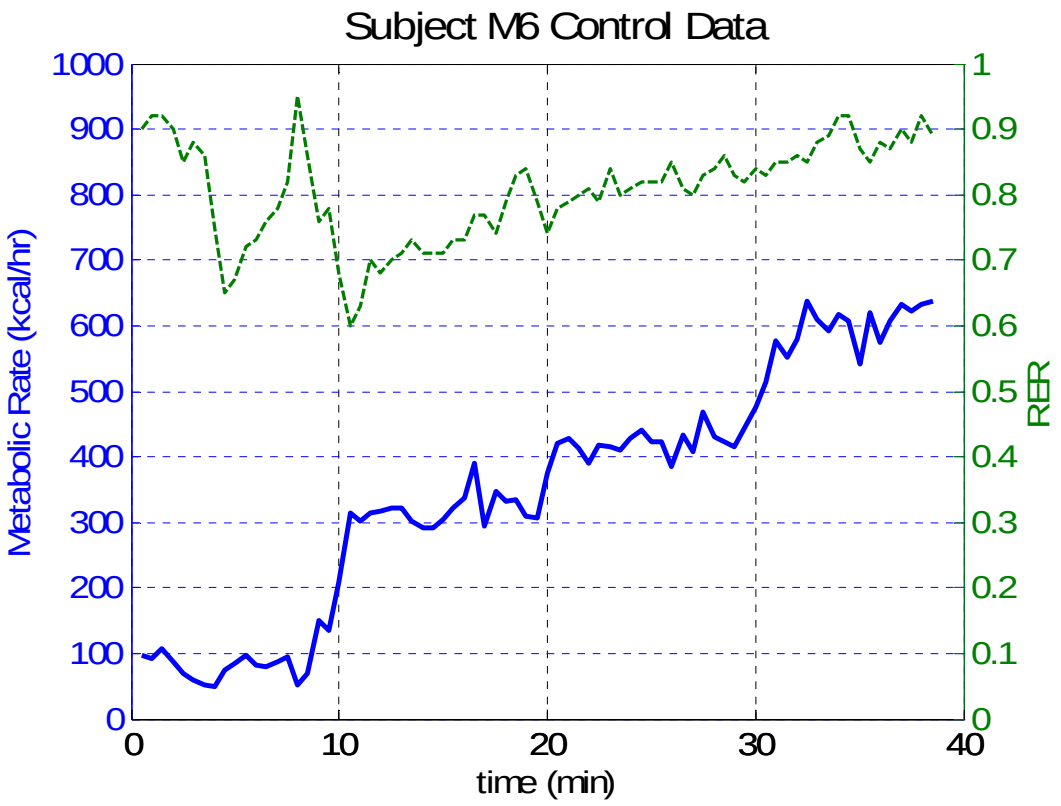
Subject M6 Control Data
Metabolic Rate (kcal/hr)
RER
time (min)
0
100
200
300
400
500
600
700
800
900
1000
0.1
0.2
0.3
0.4
0.5
0.6
0.7
0.8
0.9
1
0
10
20
30
40

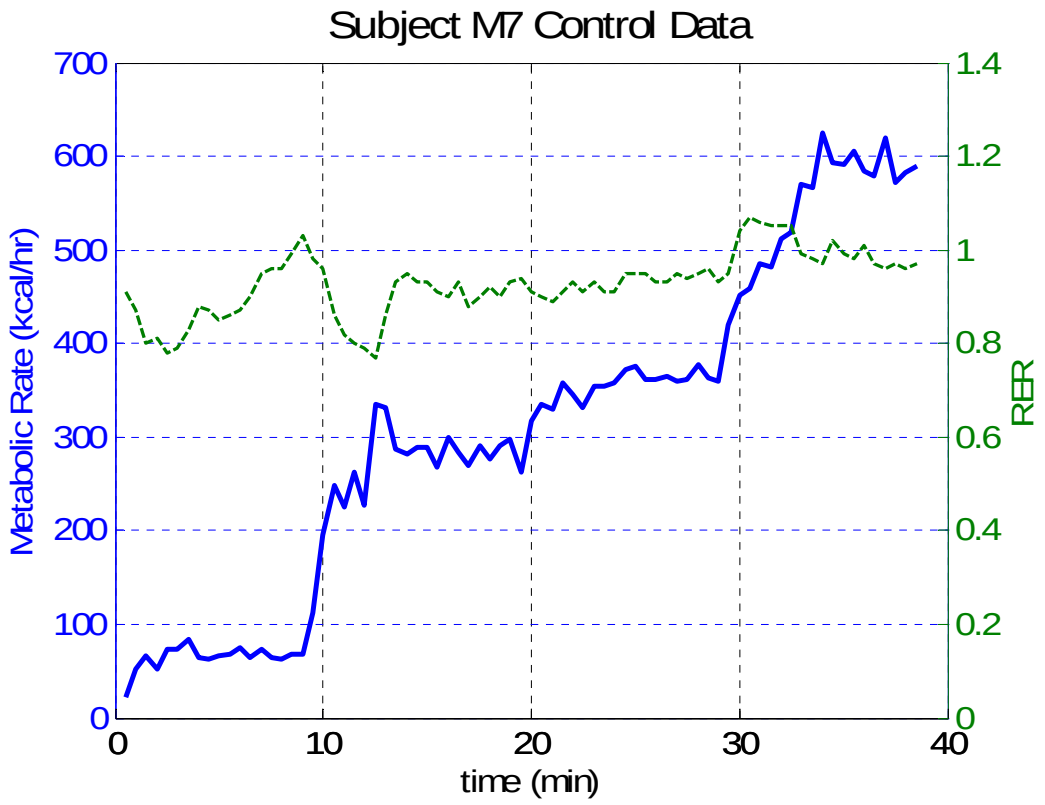
Subject M7 Control Data
Metabolic Rate (kcal/hr)
RER
time (min)
0
100
200
300
400
500
600
700
0.2
0.4
0.6
0.8
1
1.2
1.4
0
10
20
30
40

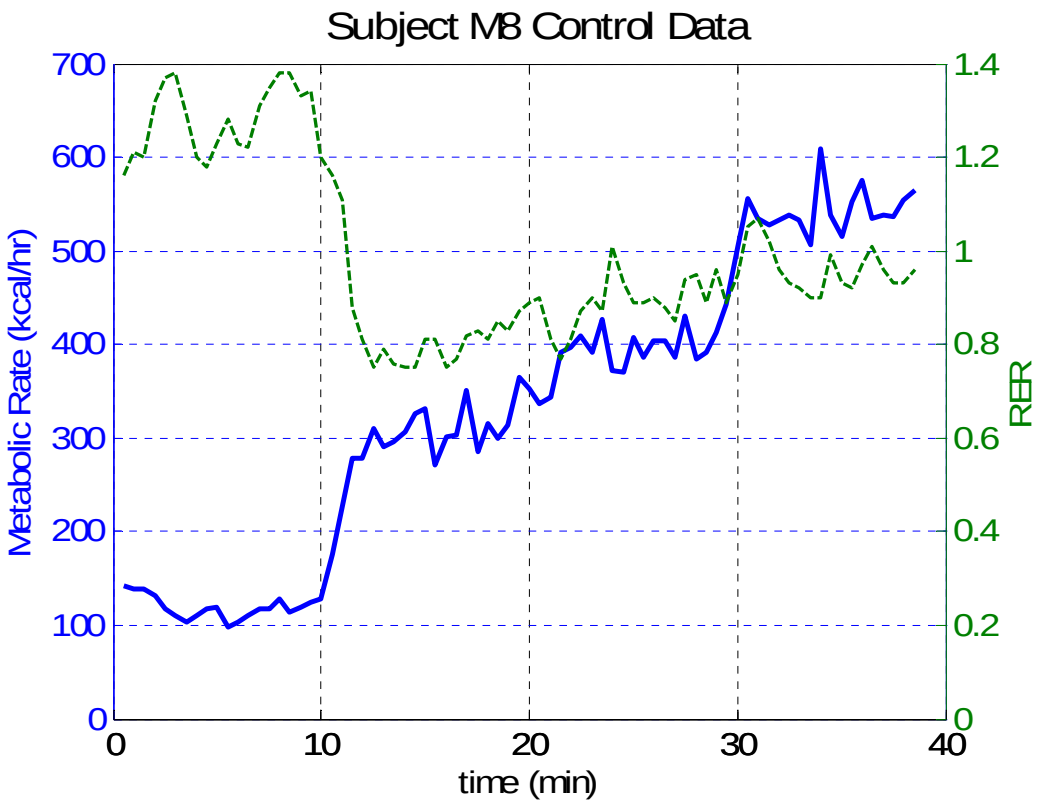
Subject M8 Control Data
Metabolic Rate (kcal/hr)
RER
time (min)
0
100
200
300
400
500
600
700
0
0.2
0.4
0.6
0.8
1
1.2
1.4
0
10
20
30
40

Bibliography

[1] Powers, S.K., Howley, E.T., Exercise Physiology: Theory and Application to Fitness and Performance. 4th Ed. E-text release 2.0. McGraw-Hill, ISBN 0-07-245011-8, 2001.

[2] Montoye, H.J., Kemper, H.C.G., Saris, W.H.M., Washburn, R.A., Measuring Physical Activity and Energy Expenditure. Human Kinetics, ISBN 0-87322-500-7, Champaign, IL, 1996.

[3] Manier, L., Johnson, T., Nair, S.S., Miles, J.B. "A Review of Muscular Efficiency Studies for Different Exercises", Paper No. 2001-01-2264, International Conference on Environmental Systems, Orlando, FL, 2001.

[4] Johnson, A.T., Biomechanics and Exercise Physiology. Out of print. Accessed at http://www.bre.umd.edu/johnbiom.htm in Jan. 2007.

[5] Åstrand, P.O., Rodahl, K., Textbook of Work Physiology, McGraw-Hill Book Company, New York, NY, 1970.

[6] Kinney, J.M., "The Application of Indirect Calorimetry to Clinical Studies," *Assessment of Energy Metabolism in Health and Disease,* Ross Laboratories, Columbus, OH, 1980.

[7] Cowell, S.A., Stocks, J.M., Evans, D.G., Simonson, S.R., Greenleaf, J.E., "The Exercise and Environmental Physiology of Extravehicular Activity," *Aviation, Space, and Environmental Medicine,* Vol. 73, No. 1, pg. 54-67, 2002.

[8] Waligora, J.M., Horrigan, D.J., "Metabolic Cost of Extravehicular Activities," *Biomedical Results from Skylab,* Ch. 38, pg. 395-399, NASA, Houston, TX, 1977.

[9] Waligora, J.M., Horrigan, D.J., "Metabolism and Heat Dissipation During Apollo EVA Periods," *SP-368 Biomedical Results of Apollo,* Ch. 4, pg.115-128, NASA, Houston, TX, 1975.

[10] Barer, A.S. "EVA Medical Problems," *Acta Astronautica,* Vol. 23, pg. 187-193, 1991.

[11] Horrigan, D.J., "Metabolic Rate Control During Extravehicular Activity Simulations and Measurement Techniques During Actual EVAs," Paper No. 60, 8th Conference on Space Simulation, pg. 741-748, 1975.

[12] Michel, E.L., Rummel, J.A., Sawin, C.F., Buderer, M.C., Lem, J.D., "Results of Skylab Medical Experiment M171 Metabolic Activity," *Biomedical Results from Skylab,* Ch. 36, pg. 373-387, NASA, Houston, Texas, 1975.

[13] Waligora, J.M., Kumar, K.V., "Energy Utilization Rates During Shuttle Extravehicular Activities," *Acta Astronautica,* Vol. 36, Nos. 8-12, pg. 595-599, 1995.

[14] Thomas, G.A., Trevino, L.A., "Extravehicular Activity Metabolic Profile Development Based on Apollo, Skylab, and Shuttle Missions," Paper No. 972502, 27th International Conference on Environmental Systems, Lake Tahoe, NV, 1997.

[15] Stein, T.P., Leskiw, M.J., Schluter, M.D., Hoyt, R.W., Lane, H.W., Gretebeck, R.E., LeBlanc, A.D., "Energy Expenditure and Balance During Spaceflight on

the Space Shuttle," *American Journal of Physiology- Regulatory, Integrative and Comparative Physiology,* Vol. 276, Issue 6, 1999.
[16] Osipov Y.Y., Spichkov A.N., Filipenkov S.N., "Metabolic Assessments During Extra-Vehicular Activity," *Acta Astronautica,* Vol. 42, pg. 123-137, 1998.
[17] Katuntsev, V.P., Osipov, Y.Y., Barer, A.S., Gnoevaya, N.K., Tarasenkov, G.G., "The Main Results of EVA Medical Support on the MIR Space Station," *Acta Astronautica,* Vol. 54, pg. 577-583, 2004.
[18] The Mars Society, "Mars Desert Research Station Official Media Kit," accessed at http://www.marssociety.org/MDRS/media/mediakit.asp in March 2007.
[19] Dyson, K.S., Hughson, R.L., "Preliminary Study of the Physiological Demands of Mars Analogue Extravehicular Activity," Paper No. IAC-05-A1.P.02, International Astronautical Congress, Fukuoka, Japan, 2005.
[20] COSMED, "K4 b^2 Brochure", accessed at http://www.cosmed.it/products.cfm?p=1&fi=1&a=1&cat=1 in March 2007.
[21] Braden, J.R., Akin, D.L., "Development and Testing Update on the MX-2 Neutral Buoyancy Space Suit Analogue," Paper No. 04ICES-235, International Conference on Environmental Systems, Vancouver, B.C., Canada, 2004.
[22] Jacobs, S.E., Akin, D.L., Braden, J.R., "System Overview and Operations of the MX-2 Neutral Buoyancy Space Suit Analogue," 2006-01-2287, International Conference on Environmental Systems, Norfolk, VA, 2006.
[23] Braden, J.R. "Mars Suit" Space Systems Laboratory internal instructional video, Part 3, Scene 7, 2005.
[24] Webb Associates (ed.), "Anthropometric Source Book Volume II: A Handbook of Anthropometric Data," NASA Reference Publication 1024, NASA Scientific and Technical Information Office, 1978.
[25] National Instruments, "Low-Cost Multifunction DAQ for USB", NI-6008 Data Sheet accessed at http://sine.ni.com/nips/cds/view/p/lang/en/nid/14604 in March 2007.
[26] Vernier, "O_2 Gas Sensor," User Guide accessed at http://www.vernier.com/probes/o2-bta.html in March 2007.
[27] Vaisala, "GMM 220 Carbon Dioxide Modules for Harsh and Demanding OEM Applications," Technical information accessed at http://www.vaisala.com/businessareas/instruments/products/carbondioxide/gmm220 in June 2006.
[28] Vaisala, "Vaisala CARBOCAP® Sensor Technology for Stable Carbon Dioxide Measurement," Product brochure accessed at http://www.vaisala.com/businessareas/instruments/products/carbondioxide/gmm220 in March 2007.
[29] Vernier, "Hand-Grip Heart Rate Monitor," User Guide accessed at http://www.vernier.com/probes/hgh-bta.html in March 2007.
[30] Teledyne Hastings, "Model Nall Mass Flow Meters Instruction Manual," accessed at http://www.teledyne-hi.com/Manual/manuals.htm in March 2007.
[31] Teledyne Hastings, "Nall-Series Mass Flowmeters," accessed at http://www.teledyne-hi.com/products/p-flow.htm in March 2007.

[32] Viasys Healthcare, "Oxycon Pro®," accessed at http://www.jaeger-toennies.com/english/products/cardio-respiratory/cardiopulmonary-ex-testing/oxycon-pro/ox-pro.html in May 2007.

[33] Kram, R., Domingo, A., Ferris, D.P., "Effect of Reduced Gravity on the Preferred Walk-Run Transition Speed," *Journal of Experimental Biology,* Vol. 200, Number 4, pg. 821-826, The Company of Biologists LTD, Great Britain, 1997.

[34] Franklin, B.A. (ed.). ACSM's Guidelines for Exercise Testing and Prescription, 6th ed., American College of Sports Medicine, ISBN 0-683-30355-4, Philadelphia, PA, 2000.

[35] Pandolf, K.B., Givoni, B., Goldman, R.F., "Predicting Energy Expenditure with Loads While Standing or Walking Very Slowly," *Journal of Applied Physiology,* Vol. 43, Number 4, pg. 577-581, 1977.

[36] Hall, C., Figueroa, A., Fernhall, B., Kanaley, J.A., "Energy Expenditure of Walking and Running: Comparison with Prediction Equations," *Medicine and Science in Sports and Exercise,* Vol. 36, Number 12, pg. 2128-2134, 2004.

[37] Bigard, A.X., Guezennec, C.Y., "Evaluation of the Cosmed K2 Telemetry System During Exercise at Moderate Altitude," *Medicine and Science in Sports and Exercise,* Vol. 27, Number 9, pg. 1333-1338, 1995.

[38] Alpha Omega Instruments, "Oxygen Sensor Types," accessed at http://www.aoi-corp.com/additional_information/oxygen_sensor_types/ in May 2007.